ISSN 1097-8135

Life Science Journal

Acta Zhengzhou University Overseas Edition

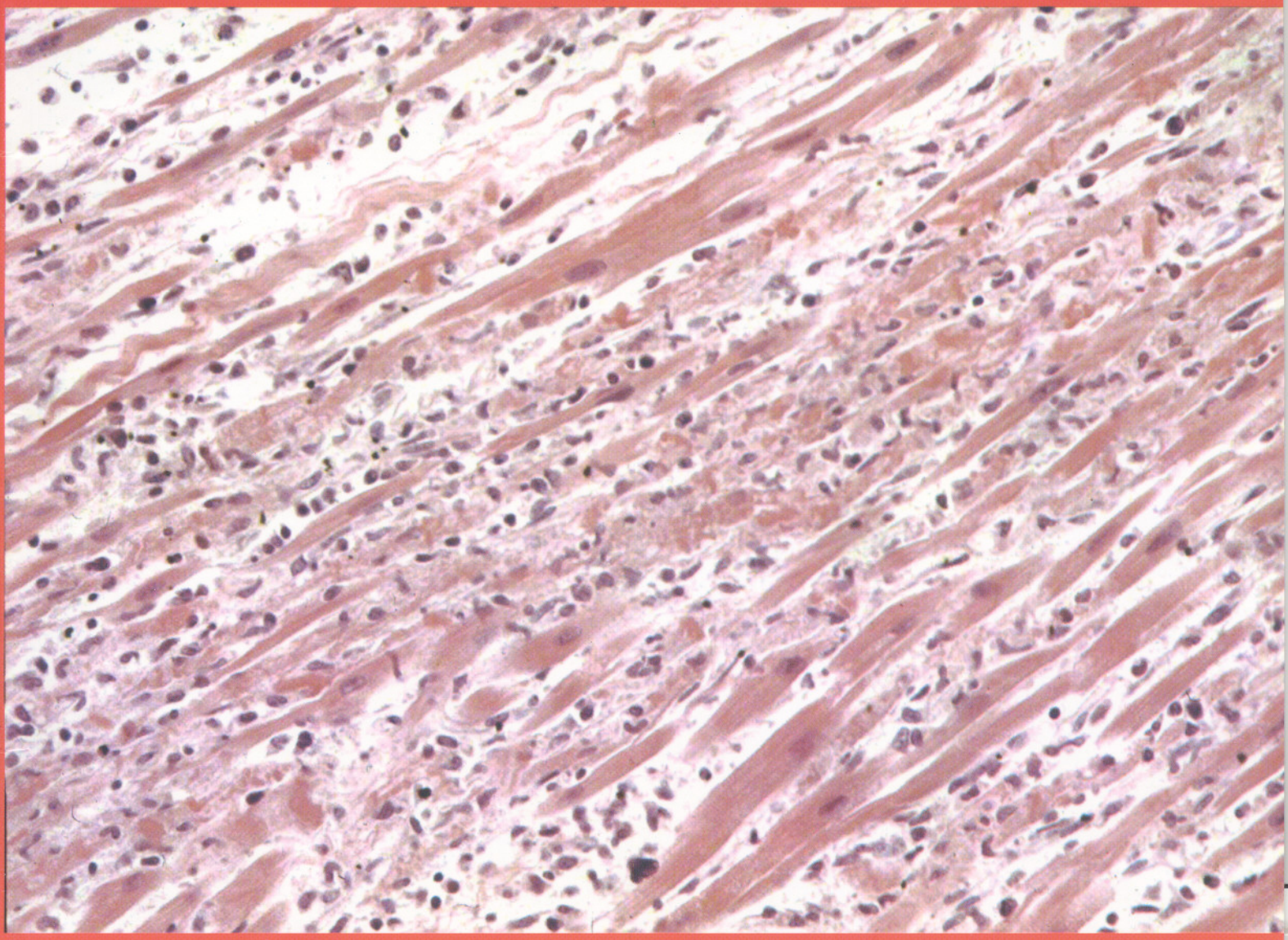

Volume 3 Number 4, December 2006

Life Science Journal

Volume 3 Number 4 December 2006

Life Science Journal

Acta Zhengzhou University Overseas Edition

Life Science Journal, the Acta Zhengzhou University Overseas Edition, is an international journal with the purpose to enhance our natural and scientific knowledge dissemination in the world under the free publication principle. The journal is calling for papers from all who are associated with Zhengzhou University – home and abroad. Any valuable papers or reports that are related to life science are welcome. Other academic articles that are less relevant but are of high quality will also be considered and published. Papers submitted could be reviews, objective descriptions, research reports, opinions/debates, news, letters, and other types of writings. All publications of *Life Science Journal* are under vigorous peer-review. Let's work together to disseminate our research results and our opinions.

CONTENTS

On the cover : Histologic examination of the left ventricular myocardium.

The figure showed the inflammation was severe and diffuse, going transmural from the endocardium to the epicardial surface, and the severe myodegeneration and myocytolysis. See *A Survey of Human Myocarditis Cases Diagnosed Using Alexa Immunofluorescence Dyes and Confocal Microscopy* by George E Sandusky *et al*, pages 37 - 41 in this issue.

Expression Patterns and Action Analysis of Genes Associated with the Responses to Ischemia, Hypoxia and Starvation during Rat Liver Regeneration

Cunshuan Xu[1], Fang Fang[1], Hongpeng Han[1], Xiaoguang Chen[2]

1. College of Life Science, Henan Normal University, Xinxiang, Henan 453007, China

2. Key Laboratory for Cell Differentiation Regulation, Xinxiang, Henan 453007, China

Abstract: Objective. The aim of this project was to study the responses to ischemia, hypoxia and starvation after partial hepatectomy (PH) at transcriptional level. **Methods.** The genes associated with the responses to ischemia, hypoxia and starvation were obtained by collecting the data of databases and referring to theses. Their expression changes in regenerating liver were checked by the Rat Genome 230 2.0 Array. **Results.** It was found that 120, 65 and 23 genes respectively associated to the responses to ischemia, hypoxia, starvation were associated with liver regeneration (LR). The initial and total expressing gene numbers occurring in initiation of LR (0.5 – 4 hours after PH), transition from G0 to G1 (4 – 6 hours after PH), cell proliferation (6 – 66 hours after PH), cell differentiation and structure-function reorganization (66 – 168 hours after PH) were 54, 11, 34, 3 and 54, 49, 70, 49 respectively, which illustrated that the genes were mainly triggered in the initial phase, and worked at different phases. According to their expression similarity, these genes were classified into 5 types including 63 only up-, 26 predominantly up-, 63 only down-, 16 predominantly down-, and 8 up/down-regulated genes, and the total times of their up- and down-regulated expression were 639 and 372, demonstrating that the expression of major genes was enhanced during LR, while the minority attenuated. According to the time relevance, they were classified into 14 groups, demonstrating that the cellular physiological and biochemical activities were staggered during LR. According to gene expression patterns, they were classified into 24 types, showing that the activities mentioned above were diverse and complicated during LR. **Conclusion.** The response to ischemia was mainly enhanced in the prophase, and hypoxia enhanced almost during the LR, while the response to starvation was nearly no change during LR, in which 176 genes associated with LR played an important role. [Life Science Journal. 2006;3(4):1 – 11] (ISSN: 1097 – 8135).

Keywords: partial hepatectomy; Rat Genome 230 2.0 Array; responses to ischemia, hypoxia and starvation; liver regeneration; gene

Abbreviations: GCOS: GeneChip operating software; LR: liver regeneration; NAP: normalization analysis program; PH: partial hepatectomy; SO: sham operation; SP: stress protein

1 Introduction

When the living things are stimulated by heat[1,2], cold[3], osmotic pressure change[4], water deprivation[5], drug[6], toxicant[7], oxidation[8], unfolded protein[9], pathogen infection[10, 11], fear[12], wounding[13], pain[14], hypoxia[15], ischemia[16], nutritional deficiency[17], hormonprivia[18], starvation[19] and so on, the relevant stress protein (SP) genes are activated to protect organisms against these harmful stimuli. The stress response to one stimulus can usually increase cell tolerance to another stimulus. It implies stress proteins induced by different stimuli have functional cross[20]. The remnant hepatocytes compensate the hepatectomized liver tissue by proliferation and the structure-function reconstruction after partial hepatectomy (PH)[21], which is called liver regeneration (LR)[22, 23]. According to the cellular physiological activities, the process is usually categorized into four stages[24] including initiation phase (0.5 – 4 hours after PH), transition from G0 to G1 (4 – 6 hours after PH), cell proliferation (6 – 66 hours after PH), cell differentiation and reorganization of the structure-function (66 – 168 hours after PH)[24]. According to time course, it is classified into four phases including forepart (0.5 – 4 hours after PH), prophase (6 – 12 hours after PH), metaphase (16 – 66 hours after PH), and anaphase (72 – 168 hours after PH)[22]. In addition, PH can induce body's responses to hurtful stimulus, such as ischemia, hypoxia and starvation, in which involve nearly 350 genes. These genes exist the interaction. It is almost impossible to clarify the action of genes associated with ischemia, hypoxia and starvation at transcriptional

level during LR unless high-throughput gene expression profiles[25, 26]. So we used the Rat Genome 230 2.0 Array[27,28] containing 207 genes associated with the response to ischemia, 96 genes to hypoxia and 38 genes to starvation to detect gene expression changes in LR after PH. 176 genes were found to be associated with LR[29]. And their expression characters, patterns and actions during LR were further analyzed.

2 Materials and Methods

2.1 Regenerating liver preparation

Healthy Sprague-Dawley rats weighing 200 – 250 g were obtained from the Animal Center of Henan Normal University. The rats were separated into two groups randomly, hepatectomized group and sham-operation (SO) group. Each group included 6 rats (male: female = 1:1). PH was performed according to Higgins and Anderson[21], by which the left and middle lobes of liver were removed. Rats were killed by cervical vertebra dislocation at 0.5, 1, 2, 4, 6, 8, 12, 24, 36, 54, 66, 72, 120, 144 and 168 hours after PH and the regenerating livers were observed at corresponding time point. The livers were rinsed three times in PBS at 4 ℃, then 100 – 200 mg livers from middle parts of right lobe of each group (total 1 – 2 g livers, 0.1 – 0.2 g × 6 samples, per group) were gathered and mixed together, then stored at −80 ℃. The SO group was the same as hepatectomized group except the liver lobes were unremoved. The laws of animal protection of China were enforced strictly.

2.2 RNA isolation and purification

Total RNA was isolated from frozen livers according to the manual of Trizol Reagent (Invitrogen Corporation, Carlsbad, California, USA)[30] and then purified base on the guide of RNeasy mini kit (Qiagen, Inc, Valencia, CA, USA)[31]. Total RNA samples were checked to exhibit a 2:1 ratio of 28S rRNA to 18S rRNA intensities by agarose electrophoresis (180 V, 0.5 hour). Total RNA concentration and purity were estimated by optical density measurements at 260/280 nm[32].

2.3 cDNA, cRNA synthesis and purification

1 – 8 μg total RNA as template was used for cDNA synthesis. cDNA purification was based on the way established by Affymetrix[27]. cRNA labeled with biotin was synthesized using cDNA as the template, and cDNA and cRNA were purified according to the purification procedure of GeneChip Analysis[27]. Measurement of cDNA, cRNA concentration and purity were the same as above.

2.4 cRNA fragmentation and microarray detection

15 μl (1 μg/μl) cRNA incubated with 5 × fragmentation buffer at 94 ℃ for 35 minutes was digested into 35 – 200 bp fragments. The hybridization buffer was added to the prehybridized Rat Genome 230 2.0 microarray produced by Affymetrix, then hybridization was carried out at 45 ℃ for 16 hours on a rotary mixer at 60 rpm. The microarray was washed and stained by GeneChip fluidics station 450 (Affymetrix Inc., Santa Clara, CA, USA). The chips were scanned by GeneChip Scan 3000 (Affymetrix Inc., Santa Clara, CA, USA), and the signal values of gene expression were observed[28].

2.5 Microarray data analysis

The normalized signal values, signal detections (P, A, M) and experiment/control (Ri) were obtained by quantifying and normalizing the signal values using GCOS (GeneChip operating software) 1.2[28].

2.6 Normalization of the microarray data

To minimize error from the microarray analysis, each analysis was performed three times. Results with a total ratio were maximal (R^m) and that the average of three housekeeping genes β-actin, hexokinase and glyseraldehyde-3-phosphate dehydrogenase approached 1.0 (R^h) were taken as a reference. The modified data were generated by applying a correction factor (R^m/R^h) multiplying the ratio of every gene in R^h at each time point. To remove spurious gene expression changes resulting from errors in the microarray analysis, the gene expression profiles at 0 – 4 hours, 6 – 12 hours and 12 – 24 hours after PH were reorganized by NAP software (normalization analysis program) according to the cell cycle progression of the regenerating hepatocytes. Data statistics and cluster analysis were done using GeneMath, GeneSpring, Microsoft Excel software[28, 33, 34].

2.7 Identification of genes associated with LR

Firstly, the nomenclature of three kinds of physiological responses mentioned above was adopted from the GENEONTOLOGY database (www.geneontology.org), and inputted into the databases at NCBI (www.ncbi.nlm.nih.gov) and RGD (rgd.mcw.edu) to identify the rat, mouse and human genes associated with the physiological responses. According to maps of biological pathways embodied by GENMAPP (www.genmapp.org), KEGG (www.genome.jp/kegg/pathway.html#amino) and BIOCARTA (www.biocarta.com/genes/index.asp), the genes associated with the biological process were collated. The results of this

analysis were codified, and compared with the results obtained for mouse and human searches in order to identify human and mouse genes which are different from those of rat. Comparing these genes with the analysis output of the Rat Genome 230 2.0 Array, those genes which showed a greater than twofold change in expression level observed as meaningful expression changes[29], were referred to as rat homologous or rat specific genes associated with the responses to ischemia, hypoxia and starvation under evaluation. Genes, which displayed reproducible results with three independent analyses with the chip and which showed a greater than twofold change in expression level in at least one time point during LR with significant difference ($0.01 \leqslant P < 0.05$) or extremely significant difference ($P \leqslant 0.01$) between PH and SO, were referred to as associated with LR.

3 Results

3.1 Expression changes of the genes associated with the response to ischemia, hypoxia and starvation during LR

According to the data of databases at NCBI, GENEMAP, KEGG BIOCARTA and RGD, the responses to ischemia, hypoxia and starvation involved 225, 117 and 41 genes respectively, in which 207, 96 and 38 genes were contained in the Rat Genome 230 2.0 Array separately. Among them, 176 genes revealed meaningful changes in expression at least at one time point after PH, showed significant or extremely significant differences in expression when comparing PH with SO, and were repeatable in three detections by Rat Genome 230 2.0 array. The results suggested that the genes were associated with LR. Up-regulation ranged from 2 to 257 times higher than the control, and down-regulation did 2 – 17 (Table 1). The analysis indicated that 63 genes were up-regulated, 63 genes down-, 50 genes up/down- during LR. Total up- and down-regulated genes were 639 and 372, respectively (Figure 1A). At the initiation stage of LR (0.5 – 4 hours after PH), 54 genes were up-regulated, 29 genes down-, 2 genes up/down-; at the transition phase from G0 to G1 (4 – 6 hours after PH), 49 genes were up-, 13 genes down-; at cell proliferation period (6 – 66 hours after PH), 70 genes were up-, 93 genes down-, 32 genes up/down-; at cell differentiation and reorganization of the structure-function stage (66 – 168 hours after PH), 49 genes were up-regulation, 56 genes down-, 9 genes up/down- (Figure 1B).

Table 1. Expression abundance of 176 ischemia, hypoxia and starvation response-associated genes during rat LR

Gene Abbr.	Accosiated to others	Fold difference	Gene Abbr.	Accosiated to others	Fold difference	Gene Abbr.	Accosiated to others	Fold difference	Gene Abbr.	Accosiated to others	Fold difference
1 Ischemia			Hspe1		0.2	*Tert	2	5.3,0.3	Mmp9	1	0.5,9.5
Adm	2	8.0	Icam1	2	3.0	*Tff3		0.3	Myc		19.7
Adora2a		0.5	Ikbkb		0.3	*Tgfb1	2,3	4.0	Nfkb1	1	0.4,2.3
Ager		0.4	Ikbkg		0.4	*Thbd		9.6	Nol3		2.6
AGT		5.0	Il1b		0.4	Tlr2		10.6	Nos3	1	0.3,2.1
Agtr1a		0.4	Il6		0.3,6.1	Tlr4		0.5	Npm1		0.5,2.8
Agtr2		0.4	Kcnk2		0.4	Tnf		3.2	Nr4a2		0.4,7.1
Akt1	2,3	4.0	Kcnk4		0.1,2.0	Tnfrsf10b		4.9	Pdlim1		0.5,3.2
Alox5		0.2,2.5	*Kdr		0.4,2.4	Tp53	2	2.9	Peg3		0.4
*Ang1		0.4,58.2	Lcn2		0.5,257.2	Txnip		2.9	Plau		0.4,3.0
Angpt1	2	0.2,9.2	Lgals3		5.7	Ucp3		2.2,0.5	Plaur		13.9
Angptl4	3	3.2	Mag		0.4,2.3	Ung		0.4	Prkaa1	3	7.5
Apoe		0.1	Mapk1	2	2.7	Vegfa	2	4.5,0.1	*Psen2	1	0.2
*Ascl1		0.1,2.2	Mapk8		0.5,19.7	Vhl	2	2.0	Ptgs1	1	3.4
Atm	2,3	0.3	Mapt		0.4	Zfp162		0.5	Ptgs2	1	0.1,2.1
Bcl2	2,3	0.3	Met		0.4,2.3	**2 Hypoxia**			Serpine1	1	16.7
BCL2L1	2	0.4,2.1	Mmp9	2	0.5,9.5	Ace		0.5	Sesn2		4.3
Bdkrb2		0.4	Mtap1a		0.5	Adm	1	8.0	Slc2a1		0.2
Bdnf		0.4,26	*Mtap2		0.4,3.6	Akt1	1,3	3.9	Slc2a4		0.1
Birc4		5.0	Mthfr		0.4,3.7	Angpt1	1	9.2,0.2	Sod2	1	5.6
Camk2a		0.5	Nedd9		0.5	App		6.4	Stat5a		0.2
*Casp12		0.4,2.6	Nes		0.2,4.6	Arnt2		6.8,0.4	Tert	1	0.3,5.3
Ccnd1		7.5	Nfkb1	2	0.4,2.3	Atm	1,3	0.3	Tgfb1	1,3	4.0
Chuk		0.3	Nos3	2	0.3,2.1	Atp1b1		6.7	Th		0.4
Cirbp	2	0.3	*Ntf3		0.1	Bcl2	1,3	0.3	Tp53	1	2.9
*Clu		3.0	P2rx7		0.4,2.5	Bcl2l1	1	2.1,0.4	Trib3		4.9
Cnr1		0.1	Parg		4.8	Birc2		2.8	Vegfa	1	0.1,4.5

Cts1		2.0	*Pcna		10.6	Bnip3		0.4	Vh1	1	2.0
Cybb		2.5	Pla2g2a		11.3	Camk2d		2.1	**3 Starvation**		
Daf1		0.2	Plat		0.4,4.9	Capn2		2.1	Aco1		0.5
Ddit3	2	0.5,2.7	Pln		0.3	Casp1		3.0	Akt1	1,2	3.9
Diablo		2.6	*Pon1		0.4	Casp9		0.5	Angptl4	1	3.2
E2f1		21.2	Pon2		0.5	Ccl2		128.0	Atm	1,2	0.3
Edn1	2	0.4,2.6	Prkaa2	3	0.2,5.3	*Cirbp	1	0.3	Bcl2	1,2	0.3
Eif2s1		2.4	*Prss15		2.4	Creb1		0.5	Casp8		10.6
Endog		4.6	Psen2	2	0.2	Cyp19a1		6.5,0.2	Cck		0.5
Epor		0.4	Pspn		0.3,2.1	Ddit3	1	2.7,0.5	Ccne1		18.5
F2		0.3	Pten		0.5	Ddit4		3.0,0.2	Fads1		0.1
F2rl2		0.2	Ptgs2	2	0.1,2.1	Drd2		8.6	Ghrl		4.0
F5		0.5	Ptk2		8.9	Edn1	1	2.6,0.4	Impact		0.4
Fgf2	2	0.5,2.1	Rela		0.5	Ednra		0.5	Mc4r		0.1
Fos	2	28.4	Serpine1	2	16.7	Egln1		4.4	Mcl1		4.3
Fut4		0.5,2.2	Sgk		6.5	Egr1		18.6	Mcts1		0.2
Fyn		0.5	Shc1		0.5	Fgf2	1	2.1,0.5	Ppara		0.3
Gfap		0.3,2.6	Shh		0.5,2.8	Fos	1	28.4	Ppargc1a		0.2,2.5
Grasp		2.8	Slc23a2		0.2	Hif3a		0.3	Prkaa1	2	7.5
Grin2a		2.4	Slc6a11		6.0	Hyou1		0.3	Prkaa2	1	0.2,5.3
Hdh		2.3	*Slc8a1		0.4,5.7	Icam1	1	3.0	Retn		0.2,2.2
Hgf		0.4	Slc8a3		0.2,2.2	Igf1r		0.4	Rpl11		6.5
Hrh3		0.2	Sod2	2	5.6	Itgb1		2.6	Slc38a3		5.3
Hspa1a		0.2	Sstr2		0.4,4.9	Jun		6.9	Tgfb1	1,2	4.0
Hspa1b		0.3,3.4	Stat4		0.4,4.0	Map2k1		9.1	Trim24		0.1
Hspb8		4.7	Tac1		0.2	Mapk1	1	2.7			

* Reported genes associated with LR; Associated to others: involved in other responses

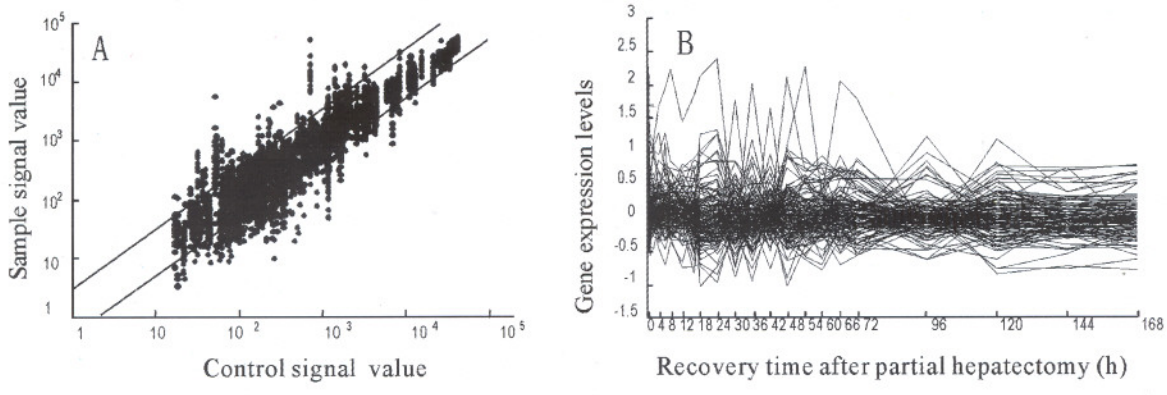

Figure 1. Expression frequency, abundance and changes of 176 ischemia, hypoxia and starvation response-associated genes during rat LR. Detection data of Rat Genome 230 2.0 Array were analyzed and graphed by Microsoft Excel. A. Gene expression frequency. The dots above bias indicated the genes up-regulated more than two folds, and total times of up-regulation were 639; those under bias indicated the genes down-regulated more than two folds, and that of down-regulation were 372; and the ones between biases no-sense alterative; B. Gene expression abundance and changes. 113 genes were 2 – 257 folds up-regulated, and 113 genes 2 – 17 folds down-regulated.

3.2 Initial expression time of the genes associated with the responses to ischemia, hypoxia and starvation during LR

At each time point of LR, the numbers of initial up-, down-regulated and total up-, down-regulated genes were in sequence both 21 and 7 at 0.5 hour; 13, 15 and 26, 19 at 1st hour; 12, 0 and 35, 3 at 2nd hour; 8, 7 and 42, 8 at 4th hour; 3, 3 and 37, 10 at 6th hour; 1, 2 and 35, 6 at 8th hour; 0, 5 and 32, 9 at 12th hour; 8, 8 and 30, 16 at 16th hour; 8, 14 and 37, 34 at 18th hour; 2, 2 and 38, 26 at 24th hour; 7, 6 and 24, 23 at 30th hour; 0, 4 and 28, 24 at 36th hour; 1, 1 and 27, 9 at 42nd hour; 2, 4 and 41, 31 at 48th hour; 0, 2 and 27, 19 at 54th hour; 1, 1 and 31, 14 at 60th hour; 1, 0 and 26, 18 at 66th hour; 0, 2 and 22, 20 at 72nd hour; 1, 3 and 19, 15 at 96th hour; 1, 1 and 27, 25 at 120th hour; 0, 0 and 20, 16 at 144th hour; 0, 0 and 16, 20 at 168th hour (Figure 2). Wholly, gene expression changes occurred during the whole LR, with the up- and down-regulation times 639 and 372, respectively.

The initially up-regulated genes were predominantly expressed in the forepart, and the down- in the prophase and metaphase, whereas there were only few initial expressions in the anaphase.

3.3 Expression similarity and time relevance of the genes associated with the responses to ischemia, hypoxia and starvation during LR

176 genes mentioned above during LR could be characterized based on their similarity in expression as following: only up-, predominantly up-, only down-, predominantly down-, and up-/down-regulated, involved in 63, 26, 63, 16 and 8 genes, respectively (Figure 3). They could also be classified based on time relevance to 14 groups including 0.5th hour and 168th hour, 1st and 2nd hour, 4th hour, 6th and 8th hour, 12th and 16th hour, 18th and 120th hour, 24th and 30th hour, 36th and 48th hour, 42nd hour, 54th hour, 60th and 66th hour, 72nd and 96th hour, 144th hour, in which the up- and down-regulated gene numbers were

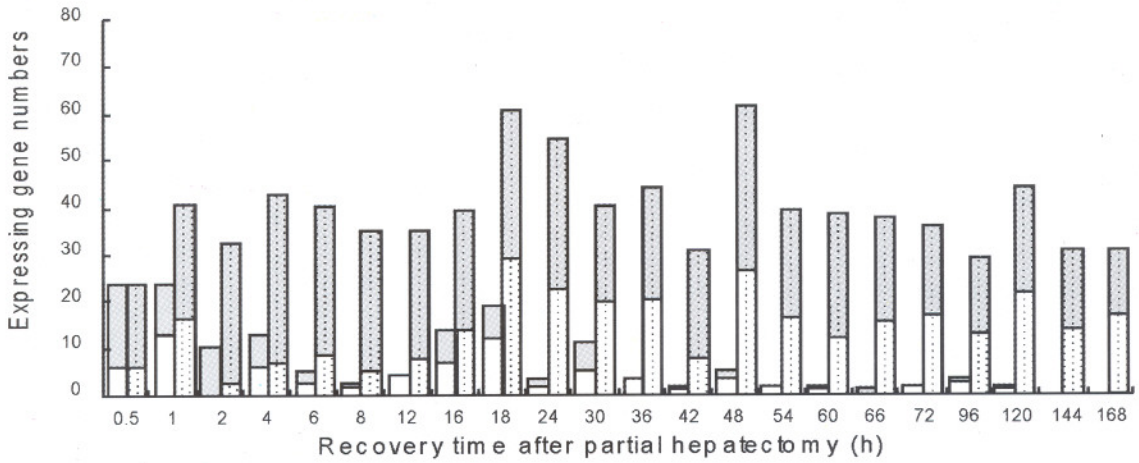

Figure 2. The initial and total expression profiles of 176 genes associated with the responses to ischemia, hypoxia and starvation at each time point of LR. Grey bars: Up-regulated genes; White bars: Down-regulated genes. Blank bars represent initially expressed genes, in which up-regulation genes are predominant in the forepart, and the down- in the prophase and metaphase, whereas only few in the anaphase. Dotted bars represent the totally expressed genes, in which some genes are up-regulation and others down-regulation during LR.

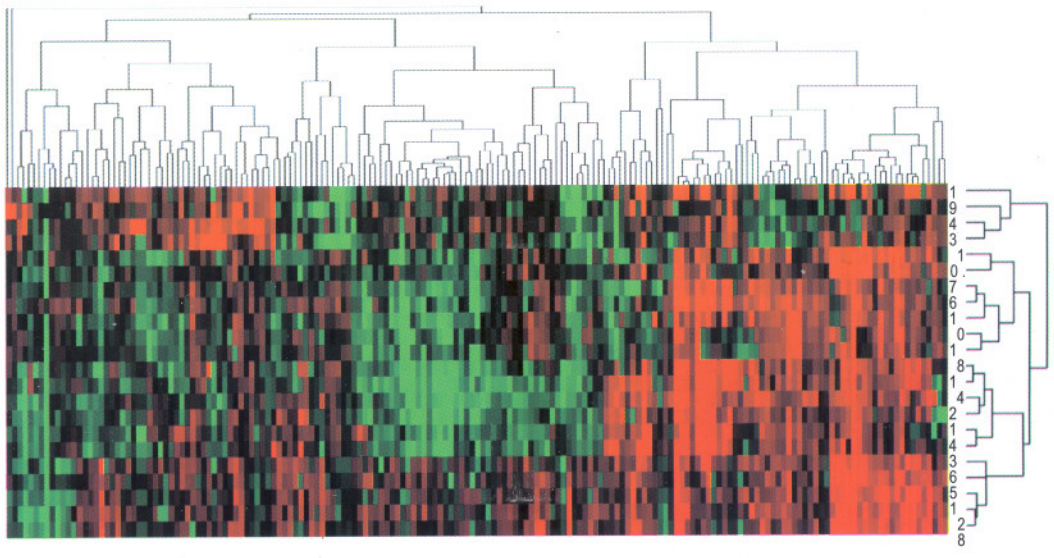

Figure 3. Expression similarity and time relevance cluster of 176 genes associated with the responses to ischemia, hypoxia and starvation during LR. Detection data of Rat Genome 230 2.0 Array were analyzed by H-clustering. Red represents up-regulation genes mainly associated with energy metabolism, vascular repair and apoptosis-promoting; Green represents down- ones mostly associated with anticoagulation; Black: No-sense in expression change. The upper and right trees respectively show expression similarity and time series cluster, by which the above genes were classified into 5 and 14 groups separately.

respectively 50th and 26th, 35th and 3rd, 79th and 18th, 35th and 6th hour, 32nd and 9th, 30th and 16th, 75th and 60th, 51th and 32nd, 69th and 55th, 58th and 33rd, 48th and 38th, 19th and 15th, 27th and 25th, 36th and 36th (Figure 3). The up-regulation genes were mainly associated with energy metabolism, vascular repair and apoptosis-promoting. The down- genes were mostly anticoagulation-associated genes.

3.4 Expression patterns of the genes associated with the responses to ischemia, hypoxia and starvation during LR

176 genes mentioned above during LR might be categorized according to the changes in expression into 24 types of patterns: (1) 11 genes up-regulated at one time point, i. e. 2nd, 6th, 16th, 30th, 42nd, 48th, 60th, 66th, 96th, 120th hour after PH (Figure 4A); (2) 9 genes up-regulated at two time points, i. e. 16th and 42nd hour, 16tg and 96th hour, 24th and 36th hour, 30th and 42nd hour, 30th and 96th hour, 48th and 120th hour (Figure 4B); (3) 2 genes up-regulated at three time points (Figure 4B); (4) 3 genes up-regulated at one phase, i. e. 1st－48th hour, 4th－8th hour, 16th－96th hour (Figure 4C); (5) 2 genes up-regulated at two phases (Figure 4C); (6) 3 genes up-regulated at one time point/one phase (Figure 4C); (7) 6 genes up-regulated at two time points/one phase (Figure 4D); (8) 8 genes up-regulated at one time point/two phases (Figure 4E); (9) 5 genes up-regulated at two time points/two phases (Figure 4D); (10) 4 genes up-regulated at three time points/two phases (Figure 4E); (11) 2 genes up-regulated at one time point/three phases (Figure 4F); (12) 2 genes up at two time points/ three phases (Figure 4F); (13) 3 genes up-regulated at multiple time points/ multiple phases (Figure 4G); (14) 24 genes down-regulated at one time point, i. e. 4, 6, 8, 12, 18, 30, 36, 42, 48, 54, 60, 72, 96 hours (Figure 4H); (15) 11 genes down-regulated at two points in time, i. e. 1 and 168 h, 1 and 72 h, 30 and 96 h, 16 and 30 h, 18 and 48 h, 30 and 48 h, 16 and 30 h, 18 and 54 h, 120 and 168 h, 36 and 48 hours , 48 and 60 hours (Figure 4I); (16) 7 genes down-regulated at three time points (Figure 4J); (17) 6 genes down-regulated at four time points (Figure 4K); (18) 2 genes down-regulated at one time point/one phase (Figure 4L); (19) 2 genes down-regulated at two time points/one phase (Figure 4L); (20) 4 genes down-regulated at two time points/two phases (Figure 4L); (21) 7 genes down at multiple time points/ multiple phases (Figure 4M); (22) 15 genes first up-regulated and then down-regulated (Figure 4N); (23) 8 genes first down-regulated and then up-regulated (Figure 4O); (24) 27 genes up/down mixed (Figure 4P).

4 Discussion

The responses to ischemia, hypoxia and starvation are instinctive reaction of self-regulation and adaptation of the organism. Lots of proteins are associated with them. In the response to ischemia, three proteins including adrenomedullin (ADM) inhibit ischemia[35]. Five proteins including icrotubule-associated protein 2 (MTAP2) prevent or repair ischemic damnification[36]. Three proteins including angiotensinogen serpin inhibitor clade A member 8 (AGT) regulate blood pressure[37]. Interleukin 6 (IL6) relates to maintaining blood balance[38]. Poly ADP-ribose glycohydrolase (PARG) resists the inflammation caused by ischemia/reperfusion[39]. Uncoupling protein 3 (UCP3) enhances the endurance of cells to local ischemia[40]. Lectin galactose binding soluble 3 (LGALS3) relates to hematopoiesis and regulation of haematocyte number[41]. Adrenergic receptor α 2a (ADRA2A) can restrain noradrenalin excretion[42]. Endothelin receptor type A (EDNRA) produces noradrenalin and hypertension Ⅱ[43]. Eight proteins including protein tyrosine kinase 2 (PTK2) relate to maintaining the normal function and development of blood vessel[44]. Paraoxonase 2 (PON2) can cause the disease of coronary artery through induction of atherosis[45]. 5, 10-methylenetetrahydrofolate reductase (MTHFR) inhibits coronary artery disease[46]. Adenosine monophosphate-activated protein kinase α2 catalytic subunit (PRKAA2) can sustain the supply and demand balance of the cell energy[47]. Tachykinin 1 (TAC1) inhibits the ischemic transmission of nervous excitement[48]. 70 kDa heat shock protein 1B (HSPA1B) participates in activities of cell resisting adversity[49]. E2F transcription factor 1 (E2F1) promotes cell growth by gene transcription and regulating signal conduction pathway[49]. Thrombomodulin (THBD) resists ischemia[50]. Lipocalin 2 (LCN2) restrains production of red cell[51]. Three proteins including angiopoietin 1 (ANGPT1) promote coagulation[52]. Four proteins including proliferating cell nuclear antigen (PCNA) protect the cell or tissue under ischemia[53]. Three proteins including histamine receptor H3 (HRH3) can prick up damage[54]. Seven proteins including diablo homolog (DIABLO) promote apoptosis[55]. Ataxia telangiectasia mutated homolog (ATM) induce apoptosis[56]. Baculoviral IAP repeat-containing 4 (BIRC4) and 70kDa heat shock protein 1A (HSPA1A) suppress apopto-

sis[57]. Serine or cysteine peptidase inhibitor clade E member 1 (Serpine 1) restrains the function of hepatocyte growth factor[58]. Five proteins including FBJ murine osteosarcoma viral oncogene homolog (FOS) maintain nerve function[59]. Three proteins including intercellular adhesion molecule 1 (Icam1) accelerates inflammatory response[60]. Solute carrier family 8 member 1 (SLC8A1) hastens transportation of Ca^{2+}[61]. Serum glucocorticoid regulated kinase (SGK) modulates the balance of Na^{+} *in vivo*[62]. Phospholamban (PLN) depresses the activity of Ca^{2+} ATPase[63]. The meaningful expression profiles of these genes are same or similar at some point while different at others, indicating that they may co-regulate response to ischemia. Among them, *fos* was up- at 0.5th－30th, 42nd－48th and 120th hour after PH, and reached a peak at 0.5th hour that was 28.4 folds of control, which was consistent with the results reported by Kawaguchi K *et al*[64]. *adm* nearly up- in all LR phase, and reached a peak at 48th and 54th hour that was 8 folds of control. *agt* was up- at 1st－24th and 144th hour after PH, and reached a peak at 8th hour that was 5 folds of control. *ptk2* was up- for many periods of time after PH, and reached a peak at 66th hour that was 8.9 folds of control. *angpt1* was up- at 12th－24th, 36th and 48th－60th hour after PH, and reached a peak at 48th hour that was 9.2 folds of control. *lcn2* was nearly up- for all the LR, and reached a peak at 24th hour that is 257.2 folds of control. *e2f1* was up- at 18th－30th, 54th－72nd and 120th hour after PH, and reached a peak at 24th hour that was 21.2 folds of control. *serpine1* was up- at 1st－48th hour after PH, and reached a peak at 6th hour that was 16.7 folds of control. It is speculated that the genes mentioned above genes play crucial roles in ischemia response during LR.

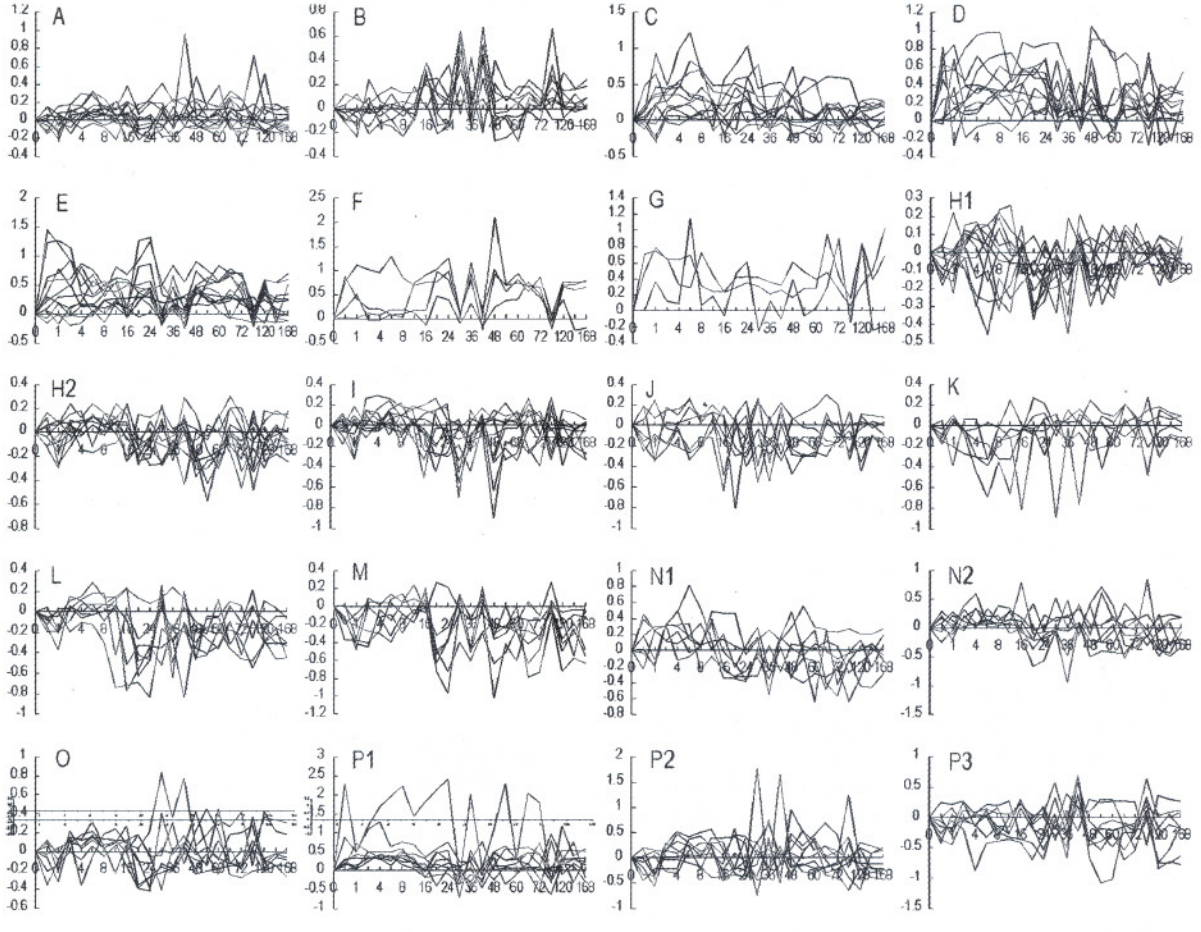

Figure 4. Twenty-five expression patterns of 176 genes associated with the responses to ischemia, hypoxia and starvation during LR. Expression patterns were obtained by the analysis of detection data of Rat Genome 230 2.0 array with Microsoft Excel. A－G: 63 up-regulation genes; H－M: 63 down-regulated genes; N－P: 50 up/down-regulated genes. X-axis represents recovery time after PH (h); Y-axis shows logarithm ratio of the signal values of genes at each time point to control.

Among the proteins associated with response to hypoxia, four proteins including DNA-damage-inducible transcript 4 (DDIT4) resist anoxic injury[65]. EGL nine homolog 1 (EGLN1) participates hypoxia stress[66]. Thymoma viral proto-oncogene 1 (AKT1) can raise the activities of AMP kinase to keep the heart's normal functions[66]. Five proteins including tribbles homolog 3 (TRIB3) can accelerate apoptosis under hypoxia[67]. Aryl hydrocarbon receptor nuclear translocator 2 (ARNT2) takes part in the removal of dioxins in vivo produced under hypoxia[68]. Angiotensin I converting enzyme 1 (ACE1) stimulates vasoconstriction[69]. cAMP responsive element binding protein 1 (CREB1) restrains nerve excitation[70]. Dopamine receptor 2 (DRD2) relates to spirit anxiety[71]. Four proteins including amyloid beta precursor protein (APP) play the role in nerve protection[72]. Four proteins including myelocytomatosis viral oncogene homolog avian (MYC) promote cell proliferation[73]. Chemokine ligand 2 (CCL2) prevents apoptosis[74]. The meaningful expression profiles of these genes show the sameness or similarity at some point while different at others, indicating that they may co-regulate responses to hypoxia. Among them, *trib3* was up- at 1st, 8th – 24th hour, 48th and 66th – 72nd hour after PH, and reached a peak at 48th hour that was 4.9 folds of control. *arnt2* was up- at 30th – 42nd, 60th, 72nd and 120th hour after PH, and reached a peak at 30th hour that was 6.8 folds of control. *drd2* was up- at 0.5th – 18th, 48th – 60th and 168th hour after PH, and reached a peak at 2nd hour that was 8.6 folds of control. *app* was up- at metaphase and anaphase after PH, and reached a peak at 168th hour that was 6.4 folds of control. *ccl2* was up- at 0.5th – 1st, 12th – 24th, 36th, 48th – 72nd and 120th hour after PH, and reached a peak at 48th hour that was 128 folds of control. *myc* was nearly up- all the LR, and reached a peak at 6th hour that was 19.7 folds of control. It is presumed that they play key roles in hypoxia response during LR.

Among the proteins associated with response to starvation, caspase 8 (CASP8) and myeloid cell leukemia sequence 1 (MCL1) promote apoptosis[75]. Cholecystokinin (CCK) and melanocortin 4 receptor (MC4R) stimulate digestion[76]. Five proteins including protein kinase AMP-activatedα1 catalytic subunit (PRKAA1) participate in the metabolism of carbohydrates and fats[77]. Cyclin E (CCNE1) stimulates transit from G1 into S phase. Aconitase 1 (ACO1) relates to cholesterolemia caused by excessive intake[78]. Solute carrier family 38 member 3 (SLC38A3) participates in sodium-dependent transportation of Glu, Asn and His[79]. Peroxisome proliferative activated receptor gamma coactivator 1α (PPARGC1A) can maintain temperature and stabilize metabolism[80]. The meaningful expression profiles of these genes are same or similar at some points, whereas different at others, suggesting that they may co-regulate responses to starvation. Among them, *prkaa1* was up- at 0.5th – 12th, 48th and 144th – 168th hour after PH, and reached a peak at 4th hour that was 7.5 folds of control, which was consistent with the results reported by Dransfeld *et al*[26]. *ccne1* was up at 1st – 2nd, 8th – 72nd and 120th hour after PH, and reached a peak at 24th hour that was 18.5 folds of control. *casp8* was up at 1st, 18th – 24th, 36th, 48th – 72nd and 120th – 168th hour after PH, having a peak at 48th hour that was 10.6 folds of control. It is assumed that the genes play vital roles in starvation response during LR.

In conclusion, the high-throughput gene expression analysis technique was used to investigate the expression changes of the genes associated with the responses to ischemia, hypoxia and starvation in long time range (0.5th hour – 7 days after PH) and multiple time points (total 23). It was primarily confirmed that PH can cause various physiological responses, such as hypoxia, hypoxia and starvation etc; that Rat Genome 230 2.0 Array was a useful tool analyzing the above responses-associated genes at transcriptional level. However, the processes DNA→ mRNA→ protein were influenced by many factors including protein interaction, we'll further analyze the above-mentioned results by the techniques, such as Northern blotting, protein chip, RNA interference, protein-interaction etc.

Acknowledgments

This study was supported by the National Natural Science Foundation of China, No. 30270673.

Correspondence to:

Cunshuan Xu
College of Life Science, Henan Normal University
Xinxiang, Henan 453007, China
Telephone: 86-373-3326001
Fax: 86-373-3326524
Email: xucs@x263.net

References

1. Evgen'ev MB, Garbuz DG, Zatsepina OG. Heat shock proteins: functions and role in adaptation to hyperthermia. Ontogenez 2005; 36 (4): 265 – 73.

2. Xu CS, Fracella F, Christiane RL, *et al*. Stress response of lysosomal, cysteine proteinases in rat C6 glioma cells. Comp Biochem Physiol B Biochem Mol Biol 1997; 117 (2): 169－78.
3. Dresios J, Aschrafi A, Owens GC, *et al*. Cold stress-induced protein Rbm3 binds 60S ribosomal subunits, alters microRNA levels, and enhances global protein synthesis. PNAS 2005; 102 (6): 1865－70.
4. Varela CA, Baez ME, Agosin E. Osmotic stress response: Quantification of cell maintenance and metabolic fluxes in a lysine-overproducing strain of corynebacterium glutamicum. Appl Environ Microbiol 2004; 70 (7): 4222－9.
5. Barbour E, Rawda N, Banat G, *et al*. Comparison of immunosuppression in dry and lactating Awassi ewes due to water deprivation stress. Vet Res Commun 2005; 29 (1): 47－60.
6. Vitetta L, Anton B, Cortizo F, *et al*. Mind-body medicine: Stress and its impact on overall health and longevity. Ann N Y Acad Sci 2005; 1057: 492－505.
7. Huelmos Rodrigo A, Garcia Velloso MJ, *et al*. Myocardial perfusion reserve studied by single-photon emission-computed tomography with thallium-201 and a drug stress test with adenosine triphosphate in patients with cardiovascular risk factors. Rev Esp Cardiol 1997; 50 (10): 696－708.
8. Muto Y, Sato K. Pivotal role of attractin in cell survival under oxidative stress in the zitter rat brain with genetic spongiform encephalopathy. Brain Res Mol Brain Res 2003; 111 (1－2): 111－22.
9. Hohenblum H, Gasser B, Maurer M, *et al*. Effects of gene dosage, promoters, and substrates on unfolded protein stress of recombinant Pichia pastoris. Biotechnol Bioeng 2004; 85 (4): 367－75.
10. Lucht JM, Mauch-Mani B, Steiner HY, *et al*. Pathogen stress increases somatic recombination frequency in Arabidopsis. Nat Genet 2002; 30 (3): 311－4.
11. Estes DM, Turaga PS, Sievers KM, *et al*. Characterization of an unusual cell type ($CD4^+$ $CD3^-$) expanded by helminth infection and related to the parasite stress response. J Immunol 1993; 150 (5): 1846－56.
12. Matsuzawa S, Suzuki T, Misawa M. Conditioned fear stress induces ethanol-associated place preference in rats. Eur J Pharmacol 1998; 341 (2－3): 127－30.
13. Ono H, Ichiki T, Ohtsubo H, *et al*. Critical role of Mst1 in vascular remodeling after injury. Arterioscler Thromb Vasc Biol 2005; 25 (9): 1871－6.
14. Oztas B, Akgul S, Arslan FB. Influence of surgical pain stress on the blood-brain barrier permeability in rats. Life Sci 2004; 74 (16): 1973－9.
15. Liu LM, Dubick MA. Hemorrhagic shock-induced vascular hyporeactivity in the rat: relationship to gene expression of nitric oxide synthase, endothelin-1, and select cytokines in corresponding organs. J Surg Res 2005; 125 (2): 128－36.
16. Hosford GE, Koyanagi KS, Leung WI, *et al*. Hyperoxia increases protein mass of 5-lipoxygenase and its activating protein, flap, and leukotriene B(4) output in newborn rat lungs. Exp Lung Res 2002; 28 (8): 671－84.
17. Hasan SS, Chaturvedi PK. Response of whole body X-irradiation to inanition stress. Strahlentherapie 1983; 159 (6): 351－7.
18. Spiler IJ, Molitch ME. Lack of modulation of pituitary hormone stress response by neural pathways involving opiate receptors. J Clin Endocrinol Metab 1980; 50 (3): 516－20.
19. Spector MP. The starvation-stress response (SSR) of Salmonella. Adv Microb Physiol 1998; 50 (3): 516－20.
20. Riezman H. Why do cells require heat shock proteins to survive heat stress? Cell Cycle 2004; 3 (1): 61－3.
21. Higgins GM, Anderson RM. Experimental pathology of the liver: restoration of the liver of the white rat following partial surgical removal. Arch Pathol 1931; 12: 186－202.
22. Fausto N, Campbell JS, Riehle KJ. Liver regeneration. Hepatology 2006; 43 (2): S45－S53.
23. Michalopoulos GK, DeFrances M. Liver Regeneration. Adv Biochem Eng Biotechnol 2005; 93: 101－34.
24. Taub R. Liver regeneration: from myth to mechanism. Nat Rev Mol Cell Biol 2004; 5 (10): 836－47.
25. Xu CS, Chang CF, Yuan JY, *et al*. Expressed genes in regenerating rat liver after partial hepatectomy. World J Gastroenterol 2005; 11 (19): 2932－40.
26. Dransfeld O, Gehrmann T, Köhhrer K, *et al*. Oligonucleotide microarray analysis of differential transporter regulation in the regenerating rat liver. Liver International 2005; 25 (6): 1243－58.
27. Li L, Roden J, Shapiro BE, *et al*. Reproducibility, fidelity, and discriminant validity of mRNA amplification for microarray analysis from primary hematopoietic cells. J Mol Diagn 2005; 7 (1): 48－56.
28. Hood L. Leroy Hood expounds the principles, practice and future of systems biology. Drug Discov Today 2003; 8 (10): 436－8.
29. Yue H, Eastman PS, Wang BB, *et al*. An evaluation of the performance of cDNA microarrays for detecting changes in global mRNA expression. Nucleic Acids Res 2001; 29 (8): E41－1.
30. Knepp JH, Geahr MA, Forman MS, *et al*. Comparison of automated and manual nucleic acid extraction methods for detection of enterovirus RNA. J Clin Microbiol 2003; 41 (8): 3532－6.
31. Nuyts S, Van Mellaert L, Lambin P, *et al*. Efficient isolation of total RNA from Clostridium without DNA contamination. J Microbiol Methods 2001; 44 (3): 235－8.
32. Arkin A, Ross J, McAdams HH. Stochastic kinetic analysis of developmental pathway bifurcation in phage lambda-infected *Escherichia coli* cells. Genetics 1998; 149 (4): 1633－48.
33. Eisen MB, Spellman PT, Brown PO, *et al*. Cluster analysis and display of genome-wide expression patterns. Proc Natl Acad Sci 1998; 95 (25): 14863－8.
34. Werner T. Cluster analysis and promoter modelling as bioinformatics tools for the identification of target genes from expression array data. Pharmacogenomics 2001; 2 (1): 25－36.
35. Qi YF, Shi YR, Bu DF, *et al*. Changes of adrenomedullin and receptor activity modifying protein 2 (RAMP2) in myocardium and aorta in rats with isoproterenol-induced myocardial ischemia. Peptides 2003; 24 (3): 463－8.
36. Suh JG, An SJ, Park JB, *et al*. Transcortical alterations

in Na^+-K^+ ATPase and microtubule-associated proteins immunoreactivity in the rat cortical atrophy model induced by hypoxic ischemia. Neural Plast 2002; 9 (3): 135－46.
37. Krick S, Hanze J, Eul B, *et al*. Hypoxia-driven proliferation of human pulmonary artery fibroblasts: cross-talk between HIF-1 alpha and an autocrine angiotensin system. FASEB J 2005; 19 (7): 857－9.
38. Maat MP, Pietersma A, Kofflard M, *et al*. Association of plasma fibrinogen levels with coronary artery disease, smoking and inflammatory markers. Atherosclerosis 1996; 121 (2): 185－91.
39. Cuzzocrea S, Di Paola R, Mazzon E, *et al*. PARG activity mediates intestinal injury induced by splanchnic artery occlusion and reperfusion. FASEB J 2005; 19 (6): 558－66.
40. McLeod CJ, Aziz A, Hoyt RF Jr, *et al*. Uncoupling proteins 2 and 3 function in concert to augment tolerance to cardiac ischemia. Biol Chem 2005; 280 (39): 33470－6.
41. Stitt AW, McGoldrick C, Rice-McCaldin A, *et al*. Impaired retinal angiogenesis in diabetes: role of advanced glycation end products and galectin-3. Diabetes 2005; 54 (3): 785－94.
42. Zugck C, Lossnitzer D, Backs J, *et al*. Increased cardiac norepinephrine release in spontaneously hypertensive rats: role of presynaptic alpha-2A adrenoceptors. J Hypertens 2003; 21 (7): 1363－9.
43. Koshida R, Rocic P, Saito S, *et al*. Role of focal adhesion kinase in flow-induced dilation of coronary arterioles. Arterioscler Thromb Vasc Biol 2005; 25 (12): 2548－53.
44. Mackness B, Durrington PN, Mackness MI. The paraoxonase gene family and coronary heart disease. Curr Opin Lipidol 2002; 13 (4): 357－62.
45. Bowron A, Scott J, Stansbie D. The influence of genetic and environmental factors on plasma homocysteine concentrations in a population at high risk for coronary artery disease. Ann Clin Biochem 2005; 42(Pt 6): 459－62.
46. Pallottini V, Montanari L, Cavallini G, *et al*. Mechanisms underlying the impaired regulation of 3-hydroxy-3-methylglutaryl coenzyme A reductase in aged rat liver. Mech Ageing Dev 2004; 125 (9): 633－9.
47. Kombian SB, Ananthalakshmi KV, Parvathy SS, *et al*. Substance P depresses excitatory synaptic transmission in the nucleus accumbens through dopaminergic and purinergic mechanisms. J Neurophysiol 2003; 89 (2): 728－37.
48. Schroder O, Schulte KM, Ostermann P, *et al*. Heat shock protein 70 genotypes HSPA1B and HSPA1L influence cytokine concentrations and interfere with outcome after major injury. Crit Care Med 2003; 31 (1): 73－9.
49. Matsumura I, Tanaka H, Kanakura Y. E2F1 and c-Myc in cell growth and death. Cell Cycle 2003; 2 (4): 333－8.
50. Sere KM, Janssen MP, Willems GM, *et al*. Purified protein S contains multimeric forms with increased APC-independent anticoagulant activity. Biochemistry 2001; 40 (30): 8852－60.
51. Miharada K, Hiroyama T, Sudo K, *et al*. Lipocalin 2 functions as a negative regulator of red blood cell production in an autocrine fashion. FASEB J 2005; 19 (13): 1881－3.
52. Kelly BD, Hackett SF, Hirota K, *et al*. Cell type-specific regulation of angiogenic growth factor gene expression and induction of angiogenesis in nonischemic tissue by a constitutively active form of hypoxia-inducible factor 1. Circulation Research 2003; 93 (11): 1074－81.
53. Imai H, Harland J, McCulloch J, *et al*. Specific expression of the cell cycle regulation proteins, GADD34 and PCNA, in the peri-infarct zone after focal cerebral ischaemia in the rat. Neurosci 2002; 15 (12): 1929－36.
54. Nagayama T, Nagayama M, Kohara S, *et al*. Post-ischemic delayed expression of hepatocyte growth factor and c-Met in mouse brain following focal cerebral ischemia. Brain Res 2004; 999 (2): 155－66.
55. Verhagen AM, Ekert PG, Pakusch M, *et al*. Identification of DIABLO, a mammalian protein that promotes apoptosis by binding to and antagonizing IAP proteins. Cell 2000; 102 (1): 43－53.
56. Orii KE, Lee Y, Kondo N, *et al*. Selective utilization of nonhomologous end-joining and homologous recombination DNA repair pathways during nervous system development. Proc Natl Acad Sci USA 2006; 103 (26): 10017－22.
57. Matsumori Y, Northington FJ, Hong SM, *et al*. Reduction of caspase-8 and -9 cleavage is associated with increased c-FLIP and increased binding of Apaf-1 and Hsp70 after neonatal hypoxic/ischemic injury in mice overexpressing Hsp70. Stroke 2006; 37 (2): 507－12.
58. Wang H, Vohra BP, Zhang Y, *et al*. Transcriptional profiling after bile duct ligation identifies PAI-1 as a contributor to cholestatic injury in mice. Hepatology 2005; 42 (5): 1099－108.
59. Tudor EL, Perkinton MS, Schmidt A, *et al*. ALS2/Alsin regulates Rac-PAK signaling and neurite outgrowth. J Biol Chem 2005; 280 (41): 34735－40.
60. Yang XP, Irani K, Mattagajasingh S, *et al*. Signal transducer and activator of transcription 3 alpha and specificity protein 1 interact to upregulate intercellular adhesion molecule-1 in ischemic-reperfused myocardium and vascular endothelium. Arterioscler Thromb Vasc Biol 2005; 25 (7): 1395－400.
61. Hurtado C, Ander BP, Maddaford TG, *et al*. Adenovirally delivered shRNA strongly inhibits Na^+-Ca^{2+} exchanger expression but does not prevent contraction of neonatal cardiomyocytes. J Mol Cell Cardiol 2005; 38 (4): 647－54.
62. Bhargava A, Fullerton MJ, Myles K, *et al*. The serum- and glucocorticoid-induced kinase is a physiological mediator of aldosterone action. Endocrinology 2001; 142 (4): 1587－94.
63. Ferrington DA, Yao Q, Squier TC, *et al*. Comparable levels of Ca-ATPase inhibition by phospholamban in slow-twitch skeletal and cardiac sarcoplasmic reticulum. Biochemistry 2002; 41 (44): 13289－96.
64. Kawaguchi K, Hickey RW, Rose ME, *et al*. Cyclooxygenase-2 expression is induced in rat brain after kainate-induced seizures and promotes neuronal death in CA3 hippocampus. Brain Res 2005; 1050 (1－2): 130－7.
65. Shoshani T, Faerman A, Mett I, *et al*. Identification of a novel hypoxia-inducible factor 1-responsive gene, RTP801, involved in apoptosis. Mol Cell Biol 2002; 22 (7): 2283－93.

66. D'Angelo G, Duplan E, Boyer N, *et al*. Hypoxia up-regulates prolyl hydroxylase activity: a feedback mechanism that limits HIF-1 responses during reoxygenation. J Biol Chem 2003; 278 (40): 38183－7.
67. Mayumi-Matsuda K, Kojima S, Suzuki H, *et al*. Identification of a novel kinase-like gene induced during neuronal cell death. Biochem Biophys Res Commun 1999; 258 (2): 260－4.
68. Mitsushima D, Funabashi T, Kimura F. Estrogen increases messenger RNA and immunoreactivity of aryl-hydrocarbon receptor nuclear translocator 2 in the rat mediobasal hypothalamus. Biochem Biophys Res Commun 2003; 307 (2): 248－53.
69. Lam SY, Fung ML, Leung PS. Regulation of the angiotensin-converting enzyme activity by a time-course hypoxia in the carotid body. J Appl Physiol 2004; 96 (2): 809－13.
70. Han MH, Bolanos CA, Green TA, *et al*. Role of cAMP response element-binding protein in the rat locus ceruleus: regulation of neuronal activity and opiate withdrawal behaviors. J Neurosci 2006; 26 (17): 4624－9.
71. Montagna P, Cevoli S, Marzocchi N, *et al*. The genetics of chronic headaches. Neurol Sci 2003; 24: S51－56.
72. Kogel D, Schomburg R, Schurmann T, *et al*. The amyloid precursor protein protects PC12 cells against endoplasmic reticulum stress-induced apoptosis. J Neurochem 2003; 87 (1): 248－56.
73. Liu J, Narasimhan P, Lee YS, *et al*. Mild hypoxia promotes survival and proliferation of SOD2-deficient astrocytes via c-Myc activation. J Neurosci 2006; 26 (16): 4329－37.
74. Tarzami ST, Calderon TM, Deguzman A, *et al*. MCP-1/CCL2 protects cardiac myocytes from hypoxia-induced apoptosis by a G (alphi)-independent pathway. Biochem Biophys Res Commun 2005; 335 (4): 1008－16.
75. Sieghart W, Losert D, Strommer S, *et al*. Mcl-1 overexpression in hepatocellular carcinoma: a potential target for antisense therapy. J Hepatol 2006; 44 (1): 151－7.
76. Kissileff HR, Carretta JC, Geliebter A, *et al*. Cholecystokinin and stomach distension combine to reduce food intake in humans. Am J Physiol Regul Integr Comp Physiol 2003; 285 (5): R992－8.
77. Horman S, Vertommen D, Heath R, *et al*. Insulin antagonizes ischemia-induced Thr172 phosphorylation of AMP-activated protein kinase alpha-subunits in heart via hierarchical phosphorylation of Ser485/491. J Biol Chem 2006; 281 (9): 5335－40.
78. Lemieux C, Gelinas Y, Lalonde J, *et al*. The selective estrogen receptor modulator acolbifene reduces cholesterolemia independently of its anorectic action in control and cholesterol-fed rats. J Nutr 2005; 135 (9): 2225－9.
79. Karinch AM, Lin CM, Wolfgang CL, *et al*. Regulation of expression of the SN1 transporter during renal adaptation to chronic metabolic acidosis in rats. Am J Physiol Renal Physiol 2002; 283 (5): F1011－9.
80. Leone TC, Lehman JJ, Finck BN, *et al*. PLoS PGC-1alpha deficiency causes multi-system energy metabolic derangements: muscle dysfunction, abnormal weight control and hepatic steatosis. Biol 2005; 3 (4): 1－16.

Received October 11, 2006

Effect of Thalidomide on Neuropathic Pain Induced by Lumbar 5 Ventral Rhizotomy in Rats

Jitian Xu[1], Wenjun Xin[2], Huiyin Tu[1], Xianguo Liu[2]

1. Department of Physiology, Basic Medical College, Zhengzhou University, Zhengzhou, Henan 450001, China

2. Department of Physiology, Zhongshan Medical School of Sun Yat-sen University, Guangzhou, Henan 510080, China

Abstract: Selective injury to motor fiber but keeping primary sensory neuron intact also induced behavioral signs of neuropathic pain. The underlying mechanism, however, is still unclear. Accumulating evidence showed that TNF-α plays an important role in the process of injured nerve degeneration and the production of abnormal pain behaviours after nerve injury. The present study was to examine the role of TNF-α in the development of neuropathic pain induced by lumbar 5 ventral rhizotomy (L5 VR), a model of selective injury to motor fibre in sciatic nerve, with intraperitoneal injection of thalidomide, an inhibitor of TNF-α synthesis, started before and after the surgery. The results showed that L5 VR induced robust and long-lasting abnormal pain behaviours in bilateral hind paws of rats. Compared with sham operated group and the pre-operated baseline, the significantly decrease of paw withdrawal threshold and paw withdrawal latency started 1 day after the surgery and persisted more than 4 weeks. Intraperitoneal injection of thalidomide, started 2 hours before surgery and once per day thereafter, significantly reduced the mechanical allodynia and thermal hyperalgesia in bilateral hind paws induced by L5 VR. Whereas, post-treatment with thalidomide as above started at the 7th day after operation, the established neuropathic pain induced by L5 VR was not affected. Taken together, the above data suggested that TNF-α might be playing an important role in the initiation, rather than maintenance, of the neuropathic pain induced by L5 VT. [Life Science Journal. 2006;3(4): 12-16] (ISSN: 1097-8135).

Keywords: ventral rhizotomy; neuropathic pain; TNF-α; thalidomide

Abbreviations: CCI: chronic constraint injury; DRG: dorsal root ganglia; L5 VR: lumbar 5 ventral rhizotomy; SIN: sciatic inflammatory neuropathy

1 Introduction

Peripheral nerve injury often results in neuropathic pain associated with hyperalgesia and allodynia. Although vast studies have been performed in the past decade, the underlying mechanisms are still remained largely unknown[1]. In clinic, the injured peripheral nerve, such as the lesion of sciatic nerve by accident, often includes afferent and efferent fibers. Therefore, it is important that verify the role of selective injury to efferent fiber in the development of neuropathic pain. Recently, several groups reported that selective injury to motor fiber with primary sensory neuron intact by Lumbar 5 ventral rhizotomy (L5 VR) also induce abnormal pain behaviors which last for several weeks after the surgery[2,3]. And the Wallerian degeneration of injured motor fiber contributes to the production of neuropathic pain after L5 VR[4-6]. Several lines of evidence demonstrated that cytokines and nerve growth factors play an important role in the process of injured fibre degeneration as well as the development of neuropathic pain subsequently[6-8]. Among them, TNF-α appears to play a key role for the initiation of injured nerve degeneration after sciatic nerve or spinal nerve injury[9-11]. Whereas, whether the TNF-α plays a role in the neuropathic pain induced by L5 VR is still unclear. So the present study was to examine the role of TNF-α in the induction and maintenance of the neuropathic pain induced by L5 VR with intraperitoneal injection of thalidomide, an inhibitor of TNF-α synthesis, started 2 hours before and the 7th day after L5 VR, respectively.

2 Materials and Methods

2.1 Animals

Male Sprague-Dawley rats weighing 180-250 g were used. The rats were housed in separated cages with free access to food and water. The room temperature was kept at 24 ± 1℃ under a 12 : 12 light-dark cycles. All animal experimental procedures were approved by the local animal care committee and were carried out in accordance with the

guideline of the National Institutes of Health on animal care and the ethical guidelines for investigation of experimental pain in conscious animal[12].

2.2 Surgical procedures of L5 VR

All experimental procedures were done on rats that were deeply anesthetized with sodium pentobarbital (50 mg/kg body weight, *i. p.*). Special care was paid to prevent infection and to minimize the influence of inflammation. The L5 VR was done following the procedures described by Li *et al*[2]. Briefly, after a midline skin incision in the L4 – S1 region, the left L5 vertebra was freed of its muscular attachment. An L5 hemilaminectomy was performed, and the dura matter and arachnoid membrane were incised. The L5 ventral root was identified as it lays at the most lateral side of spinal canal and just beneath the dorsal root. The ventral root was gently pulled out and carefully transected 2 – 3 mm proximal to the dorsal root ganglia (DRG). Great care was taken to avoid any damage to the nearby L5 dorsal root and its DRG. In the sham group, all procedures of operation were identical with the experimental group except that the exposed ventral root was not transected. After surgery, the wound was washed with saline and closed in layers with 3 – 0 silk thread. At the end of each study, animals in L5 VR groups were deeply anesthetized with intra-peritoneal 20% urethane and were dissected to verify that the lesions were done at the correct level. Animals that had a lesion at wrong level were excluded from the study.

2.3 Behavioural tests and drug delivery

The rats were accommodated to the testing environment by exposed to the testing chambers for a period of 15 – 20 minutes on three separate days just prior to the pre-operative testing. Mechanical sensitivity was assessed using von Frey hairs and the up-down method following the procedure described previously[13]. Briefly, three rats were placed under separate transparent Plexiglas chambers positioned on a wire mesh floor. Five minutes were allowed for habituation. Each stimulus consisted of 2 – 3 seconds application of the von Frey hair to the middle of the plantar surface of the foot with 5 minutes interval between stimuli. Quick withdrawal or licking of the paw in response to the stimulus was considered a positive response.

Heat hypersensitivity was tested using the plantar test (7370, UgoBasile, Comeria, Italy) according to the method described by Hargreaves *et al*[14]. Briefly, a radiant heat source beneath a glass floor was aimed at the plantar surface of the hind paw. Three measurement of latency were taken for each hind paw in each test session. The hind paw was tested alternately with greater than 5 minutes intervals between consecutive tests. The three measurements of latency per side were averaged as the result of per test. Two persons performed the behavioral tests and only one knew the design of the study.

To investigate the role of TNF-α in neuropathic pain induced by L5 VR, drug delivery was performed as follows. Thalidomide (Sigma, St. Louis, USA) was dissolved in dimethyl sulfoxide (DMSO) and then diluted in saline to a final concentration of 20 mg/ml (the concentration of DMSO was 10%, v/v). In one group of rats thalidomide was injected (50 mg/kg) intraperitoneally (*i. p.*) 2 hours before surgery and once per day thereafter until the 7th day after surgery. In another group of rats the same dose of thalidomide as above was injected at the 7th day after surgery, and once per day thereafter for 7 days. The control group received vehicle injection.

2.4 Statistical analysis

Differences in changes of values over time were tested using Friedman ANOVA followed by Wilcoxon matched pairs. The data between groups on a given testing day were analyzed with Mann-Whitney U test. Statistical test were performed with SPSS 10.0 (SPSS Inc, USA). All data are expressed as mean ± SE. $P < 0.05$ was considered significant.

3 Results

3.1 L5 VR induced mechanical and heat hypersensitivity in bilateral hind paws of rats

In consistence with a previous work[2], we found that selective transection of L5 ventral root produced robust and prolonged bilateral mechanical allodynia and thermal hyperalgesia. After L5 VR, the paw withdrawal thresholds on the ipsilateral side were significantly decreased compared with pre-operative baseline ($P < 0.001$) and with those in sham operated group ($P < 0.001$, Figure 1A). The paw withdrawal thresholds of contralateral hind paw were also significantly decreased after L5 VR. In the same group of rats paw withdrawal latencies to radiant heat on both ipsi- and contralateral sides were significantly lower compared with baseline ($P < 0.05$, Figure 1B) and with those in sham operated group ($P < 0.01$, Figure 1B). The behavioural signs of neuropathic pain persisted more than 4 weeks after L5 VR.

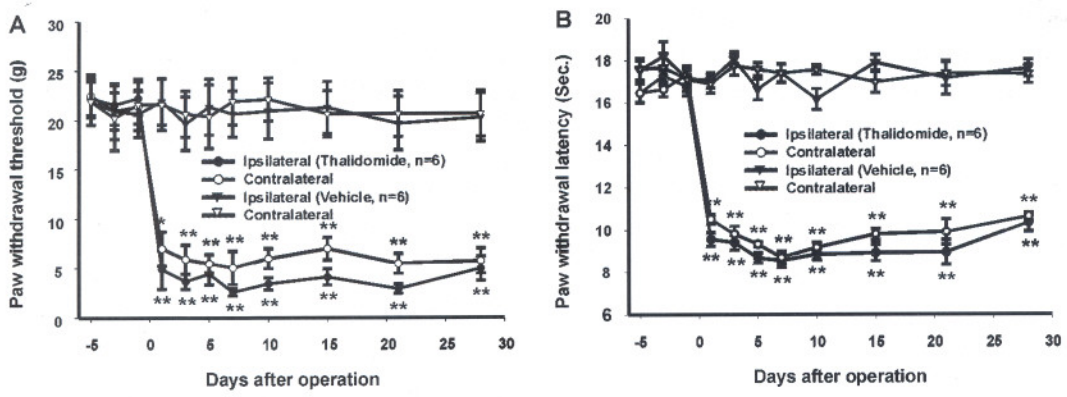

Figure 1. L5 VR induced pain-related behaviors in bilateral hind paws

A: Show the changes of paw withdrawal threshold in bilateral hind paws following L5 VR. B: Show the changes of paw withdrawal latency in bilateral hind paws following L5 VR. The results revealed that both paw withdrawal threshold and paw withdrawal latency exhibited a significantly decrease compared with pre-operative baseline as well as sham operated group starting on day 1 and persistent for more than 4 weeks after L5 VR. *: $P<0.05$, **: $P<0.01$ *vs*. the sham operated group, respectively.

3.2 The effects of pre-treatment with thalidomide intrapertoneal injection on L5 VR induced neuropathic pain in rats

To evaluate the role of TNF-α in the neuropathic pain induced by L5 VR, thalidomide, a specific inhibitor of TNF-α synthesis, was injected intraperitoneally (50 mg/kg) before L5 VR. In eight rats treated with the drug, started at 2 hours before L5 VR and once daily thereafter until 7 days after surgery, the paw withdrawal thresholds of bilateral hind paws displayed an initial decrease at the 1st day and 3rd day after operation, but returned to normal at the 7th day, and then maintained at the level up to 13 days after operation (Figure 2A). The paw withdrawal thresholds between thalidomide treated group and vehicle treated group were not significantly different until the 5th day after operation ($P>0.05$, Figure 2A). In the same group of rats the decrease of paw withdrawal latencies to radiant heat was completely abolished. In contrast, in vehicle treated group the paw withdrawal latency dropped significantly after L5 VR (Figure 2B). The difference of bilateral paw withdrawal latencies between thalidomide treated group and vehicle treated group was significant from the 1st day to the 13th day after surgery ($P<0.01$, Figure 2B).

3.3 The effects of post-treatment with thalidomide on the established neuropathic pain following L5 VR in rats

To evaluate the effect of thalidomide on the established neuropathic pain, administration of thalidomide was designed at the 7th day after surgery. Although the animals received injection of thalidomide once daily for 7 days, the paw withdrawal threshold as well as paw withdrawal latency between the thalidomide treated group and vehicle treated group was not different ($P>0.05$, Figure 3A－B). These results suggest that the abnormal pain behaviours can be abolished or alleviated by inhibition of the TNF-α synthesis at the early stage of the neuropathic pain rather than when it has been established.

4 Discussion

In the present study, we found that L5 VR induced long-lasting abnormal pain behaviours in bilateral hind paws in rats. Intraperitoneal injection of thalidomide started before surgery significantly reduced the mechanical allodynia and completely blocked the thermal hyperalgesia after L5 VR. Whereas, post-treatment with thalidomide started at the 7th day there is no effect on the established neuropathic pain. It suggests that the TNF-α might be playing an important role in the initiation, but not maintenance, of the neuropathic pain induced by L5 VR.

4.1 L5 VR induced neuropathic pain in rats

As reported by several groups previously[2,3], L5 VR in the present study also induced abnormal pain behaviours to a similar extent as in rats received lumbar 5 spinal nerve ligation. Ventral root consist of myelinated efferent fibers mainly, and the unmyelinated afferent fibers less than 4%. Furthermore, very recent study shows that selective transected L5 dorsal root failed induced pain-related behaviors[15]. Therefore, the motor fiber injury produced by L5 VR induced the pain related behaviors in the present study. It indicates that not only primary sensory afferents but also motor fibre injury responsible for the development of neuropathic pain after peripheral nerve injury.

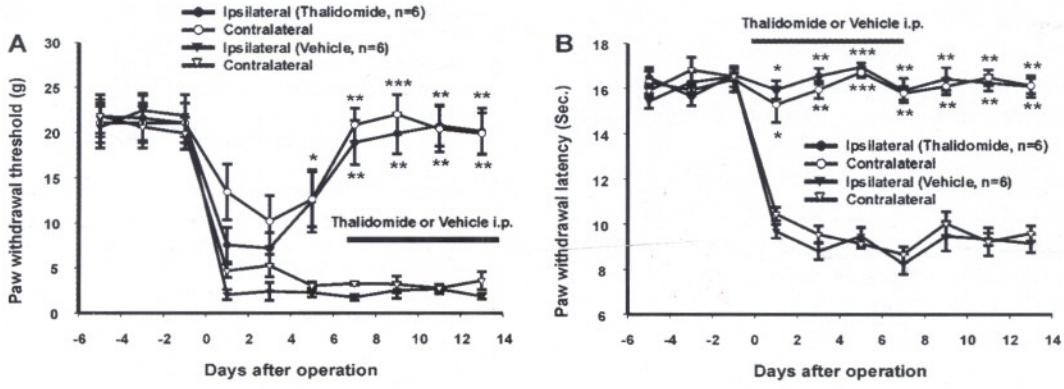

Figure 2. Pre-treatment with thalidomide reduced the pain-related behaviors produced by L5 VR

A－B: Intraperitoneal injection of thalidomide (50 mg/kg), applied 2 hours before L5 VRT and once daily thereafter until 7 days after surgery, attenuated mechanical allodynia (A) and thermal hyperalgesia (B). $^{*}P<0.05$; $^{**}P<0.01$; $^{***}P<0.001$ *vs*. vehicle group (thalidomide treated group, $n=8$; vehicle treated group, $n=6$).

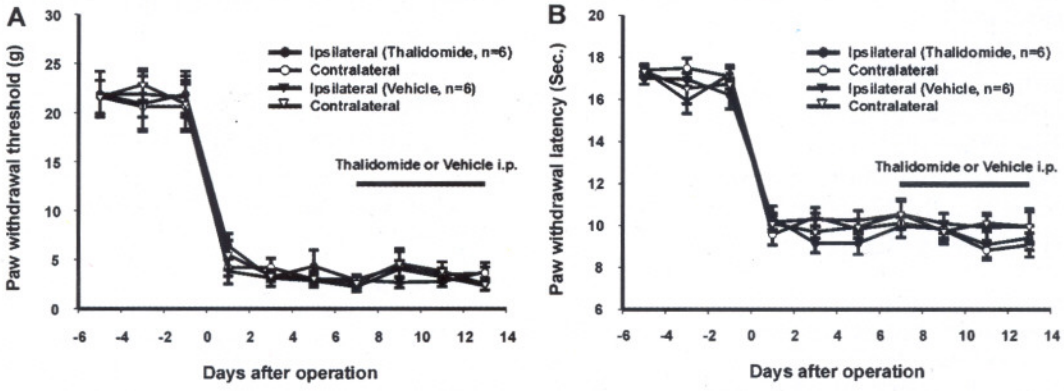

Figure 3. Effect of thalidomide on the established neuropathic pain induced by L5 VR

Compared with vehicle treated group, thalidomide applied at the 7th days after operation and once daily thereafter has no effect on the established mechanical allodynia (A) and thermal hyperalgesia (B).

4.2 The role of TNF-α in the development of neuropathic pain induced by L5 VR

Accumulating evidence shows that Wallerian degeneration contributes to the development of neuropathic pain after nerve injury. TNF-α is the pioneer cytokine, which released 4 to 6 hours after nerve injury, and play a key role in the initiation of the Wallerian degeneration of injured fibers and neuropathic pain subsequently[8;16－18]. L5 VR created a selective injury to motor fiber but keeping sensory neuron intact and induced neuropathic pain. One possible explanation for the result is that Wallerian degeneration of the injured fibers in the peripheral nerve leads to changes in adjacent, uninjured primary afferents. Therefore, inhibited the synthesis of TNF-α, may be delayed the process of Wallerian degeneration of the injured motor fibers and prevented the development of neuropathic pain. Thalidomide reduces TNF-α production in macrophages by reducing TNF-α mRNA half-life[19]. Previous studies showed that thalidomide also exhibits a potent inhibition to the production of TNF-α in injured nerve[20,21]. In the present study, pre-treatment with thalidomide intraperitoneal injection significantly reduced abnormal pain behaviours following L5 VR. However, thalidomide treatment started at 7 days after L5 VR there is no any effect on the established neuropathic pain. It indicates that TNF-α plays an important role in the initiation of the neuropathic pain induced by the selective motor fibre injury, and therefore our data provides a therapeutic window for treatment the patient of neuropathic pain with the blocker of TNF-α in clinic.

Previous studies have demonstrated that acute injection of zymosan around the sciatic nerve produces bilateral mechanical allodynia[22] and that spinal glia and proinflammatory cytokines, including TNF-α, play important roles in the so-called sciatic inflammatory neuropathy (SIN), since both ipsilateral and mirror image allodynia can be attenuated by a glial metabolic inhibitor or by blockage of

the action of TNF-α[23,24]. Apparently, it is in agreement with our discovery in the present study. It has been shown that intrathecal administration of low dose carbenoxolone, a gap junction decoupler, reverses mirror image pain, while leaving ipsilateral mechanical allodynia unaffected in SIN or chronic constraiut injury (CCI) model[25]. Accordingly, we speculate that the communications through gap junctions between ipsi- and contralateral spinal dorsal horn may contribute to L5 VR induced mirror image pain in contralateral hind paw.

Acknowledgments

This work was supported by grants from the National Natural Science Foundation of China (No. 30570599).

Correspondence to:
Jitian Xu, Ph.D.
Department of Physiology
Basic Medical College
Zhengzhou University
Zhengzhou, Henan 450001, China
Telephone: 86-371-6136-6390
Email: jtxu@zzu.edu.cn

References

1. Zimmermann M. Pathobiology of neuropathic pain. Eur J Pharmacol 2001;429: 23－37.
2. Li L, Xian CJ, Zhong JH, *et al*. Effect of lumbar 5 ventral root transection on pain behaviors: a novel rat model for neuropathic pain without axotomy of primary sensory neurons. Exp Neurol 2002; 175: 23－34.
3. Sheth RN, Dorsi MJ, Li Y, *et al*. Mechanical hyperalgesia after an L5 ventral rhizotomy or an L5 ganglionectomy in the rat. Pain 2002; 96: 63－72.
4. Wu G, Ringkamp M, Murinson BB, *et al*. Degeneration of myelinated efferent fibers induces spontaneous activity in uninjured C-fiber afferents. J Neurosci 2002; 22: 7746－53.
5. Li L, Xian CJ, Zhong JH, *et al*. Lumbar 5 ventral root transection-induced upregulation of nerve growth factor in sensory neurons and their target tissues: a mechanism in neuropathic pain. Mol Cell Neurosci 2003; 23: 232－50.
6. Obata K, Yamanaka H, Dai Y, *et al*. Contribution of degeneration of motor and sensory fibers to pain behavior and the changes in neurotrophic factors in rat dorsal root ganglion. Exp Neurol 2004; 188: 149－60.
7. George A, Buehl A, Sommer C. Wallerian degeneration after crush injury of rat sciatic nerve increases endo- and epineurial tumor necrosis factor-alpha protein. Neurosci Lett 2004; 372: 215－9.
8. Shamash S, Reichert F, Rotshenker S. The cytokine network of Wallerian degeneration: tumor necrosis factor-alpha, interleukin-1alpha, and interleukin-1beta. J Neurosci 2002; 22: 3052－60.
9. Schafers M, Geis C, Svensson CI, *et al*. Selective increase of tumour necrosis factor-alpha in injured and spared myelinated primary afferents after chronic constrictive injury of rat sciatic nerve. Eur J Neurosci 2003; 17: 791－804.
10. Schafers M, Sorkin LS, Geis C, *et al*. Spinal nerve ligation induces transient upregulation of tumor necrosis factor receptors 1 and 2 in injured and adjacent uninjured dorsal root ganglia in the rat. Neurosci Lett 2003; 347: 179－82.
11. Zelenka M, Schafers M, Sommer C. Intraneural injection of interleukin-1beta and tumor necrosis factor-alpha into rat sciatic nerve at physiological doses induces signs of neuropathic pain. Pain 2005; 116: 257－63.
12. Zimmermann M. Ethical guidelines for investigations of experimental pain in conscious animals. Pain 1983; 16: 109－10.
13. Chaplan SR, Bach FW, Pogrel JW, *et al*. Quantitative assessment of tactile allodynia in the rat paw. J Neurosci Methods 1994; 53: 55－63.
14. Hargreaves K, Dubner R, Brown F, *et al*. A new and sensitive method for measuring thermal nociception in cutaneous hyperalgesia. Pain 1988; 32: 77－88.
15. Obata K, Yamanaka H, Kobayashi K, *et al*. The effect of site and type of nerve injury on the expression of brain-derived neurotrophic factor in the dorsal root ganglion and on neuropathic pain behavior. Neuroscience 2006; 137: 961－70.
16. Liefner M, Siebert H, Sachse T, *et al*. The role of TNF-alpha during Wallerian degeneration. J Neuroimmunol 2000; 108: 147－52.
17. Cunha TM, Verri WA, Silva JS, *et al*. A cascade of cytokines mediates mechanical inflammatory hypernociception in mice. Proc Natl Acad Sci 2005; 102: 1755－60.
18. Zelenka M, Schafers M, Sommer C. Intraneural injection of interleukin-1beta and tumor necrosis factor-alpha into rat sciatic nerve at physiological doses induces signs of neuropathic pain. Pain 2005; 116: 257－63.
19. Moreira AL, Sampaio EP, Zmuidzinas A, *et al*. Thalidomide exerts its inhibitory action on tumor necrosis factor alpha by enhancing mRNA degeneration. J Exp Med, 1993; 177: 1675－80.
20. George A, Marziniak M, Schafers M, *et al*. Thalidomide treatment in chronic constrictive neuropathy decreases endoneurial tumor necrosis factor-alpha, increases interleukin-10 and has long-term effects on spinal cord dorsal horn met-enkephalin. Pain 2000; 88: 267－75.
21. Sommer C, Marziniak M, Myers RR. The effect of thalidomide treatment on vascular pathology and hyperalgesia caused by chronic constriction injury of rat nerve. Pain 1998; 74: 83－91.
22. Chacur M, Milligan ED, Gazda LS, *et al*. A new model of sciatic inflammatory neuritis (SIN): induction of unilateral and bilateral mechanical allodynia following acute unilateral peri-sciatic immune activation in rats. Pain 2001; 94: 231－44.
23. Milligan ED, Twining C, Chacur M, *et al*. Spinal glia and proinflammatory cytokines mediate mirror-image neuropathic pain in rats. J Neurosci 2003; 23: 1026－40.
24. Twining CM, Sloane EM, Milligan ED, *et al*. Peri-sciatic proinflammatory cytokines, reactive oxygen species, and complement induce mirror-image neuropathic pain in rats. Pain 2004; 110: 299－309.
25. Spataro LE, Sloane EM, Milligan ED, *et al*. Spinal gap junctions: potential involvement in pain facilitation. J Pain 2004; 5: 392－405.

Received October 5, 2006

Serum Proteomic Analysis on Invasive Cervical Cancer

Sheke Guo[1,2], Yuhuan Qiao[1], Huirong Shi[1], Xianlan Zhao[1], Liuxia Li[1]

1. Department of Gynaecology and Obstetrics, The First Affiliated Hospital, Zhengzhou University, Zhengzhou, Henan 450052, China

2. Department of Gynaecology and Obstetrics, Jiaozuo People's Hospital, Jiaozuo, Henan 454100, China

Abstract: Objective. To characterize the serum proteomic pattern and its relationship with surveillance and prognosis in judgment of patients with invasive cervical cancer. **Methods.** A total of 166 serum samples, including group A of 49 patients with invasive cervical cancer and 71 age-matched healthy women; and group B of 49 invasive cervical cancer patients, 24 invasive cervical patients with radical hysterectomy and pelvic lymphadenectomy and 22 review patients at the 3rd month after surgery, were tested by SELDI-TOF-MS with IMAC-Cu. Group A was to build a diagnosis model and detect the significant proteins that might be potentially as biomarkers. The significant proteins from group A were compared with group B. **Results.** 47 proteins were detected with a significant level of $P<0.01$ from group A. 6 proteins with m/z value of 8929.31, 7930.52, 9127.31, 8141.01, 7963.06 and 9280.63 had high score(>95%) in building a model of decision tree classification algorithm for invasive cervical cancer detection. The accuracy, sensitivity and specificity of m/z value of 8929.31 were 98.33%, 97.96% and 98.59% respectively. The 6 proteins, which appeared to be down-regulated in patients with invasive cervical cancer, had gradually retrieved in a level of $P<0.01$ after surgery, except m/z value of 9280.63, and continuously climbed in a level of $P<0.01$ at the time of 3 months postoperation including 9280.63. **Conclusions.** The six proteins as a novel group of biomarkers could potentially be used for the treatment surveillance and prognosis prediction of cervical cancer. [Life Science Journal. 2006;3(4):17-22] (ISSN: 1097-8135).

Keywords: SELDI-TOF-MS; cervical cancer; radical hysterectomy; pelvic lymphadenectomy; biomarker

Abbreviations: SELDI-TOF-MS: surface-enhanced laser desorption/ionization time-of-flight mass spectrometry

1 Introduction

Cervical cancer remains an important public health problem, ranking second only to breast cancer as the most common malignancy among women worldwide, especially in developing countries. According to Global Cancer Statistics published in 2005[1], the estimate annual number of new cases of cervical cancer worldwide is 492,000 and the estimated number of deaths is 274,000 in the year of 2002. However, there are only 83,000 new cases, 40,000 deaths in developed countries while 409,000 new cases and 234,000 deaths in developing countries. In general terms, it is much more common in developing countries. Routine screening has decreased the incidence of invasive cervical cancer, but invasive cervical cancer is still more common in women middle aged and older of poor socioeconomic status, who are less likely to receive regular screening and early treatment[1]. The cause of cervical cancer is not very clear. Infection with specific subtypes of human papillomavirus has been strongly implicated in cervical carcinogenesis but HPV infection alone is insufficient for malignant transformation[2,3]. The information regarding tumor type, grade, extent of invasion and metastasis and completeness of excision, etc were histopathologically provided. The treatment scheme and assessment of prognosis at present are based on clinical features[4-10], such as clinical stage, differentiation of the cancer cells, the metastasis of pelvic lymph nodes, surgical margin involved, deep stroma invasion and parametrial extension. And the prognosis of cervical cancer patients has improved in the past decade as a result of improvements in screening programs and early detection[1,11-15], advanced in surgery[4,16], radiotherapy and chemotherapy[17-20]. However, not all early stage patients with cervical cancer are cured. Some cases may be recurrent or even lead to death[21]. Cervical cancer related biomarkers have not been well characterized. Protein expression in serum of patients with invasive cervical cancer should contain information about cancer development and progression. Utilization of this information for discovering biomarkers that could be used to monitor the treatment response and to predict the prognosis of cervical cancer patients could be possible if a tool can be developed to rapidly analyze and display changes in protein expression. In fact, it appears that no single

biomarker, or few specific tumor markers will be effective in improving detection, treatment, and prognosis in cervical cancer. Proteomic technologies, especially the surface-enhanced laser desorption/ionization time-of-flight mass spectrometry (SELDI-TOF-MS) technology, are providing the tools needed to discover a group of disease-associating biomarkers[22-24]. The SELDI-TOF-MS technology coupled with different protein chips facilitates protein profiling of complex biological mixtures. Therefore, the present study was undertaken to characterize the serum proteomic patterns in cervical cancer and to correlate these molecules with cervical cancer prognosis.

2 Materials and Methods

2.1 Serum samples

A total of 166 serum specimens were obtained from the department of gynecology and medical examination center, the First Affiliated Hospital, Zhengzhou University (Zhengzhou, China) from June 1, 2005 to November 31, 2005. They were divided into two groups: group A of 49 patients with invasive cervical cancer and 71 age-matched healthy women; group B of 49 invasive cervical cancer patients, 24 patients with invasive cervical cancer whose serum samples were collected on the 10th day after radical hysterectomy and pelvic lymphadenectomy and 22 review patients at the time of 3 months after operation. All consenting patients with invasive cervical cancer were histopathologically diagnosed by biopsy and reconfirmed histopathologically after operation. Serum samples of patients with invasive cervical cancer were collected from the patients without any treatment such as chemotherapy, radiotherapy, etc. All blood samples were taken after overnight fasting. The medial age of patients with invasive cervical cancer was 47 years old (25 - 75 years old) and the medial age of the control group was 45 years old (22 - 73 years old). There was no statistically significant difference in the ages between the patients and controls ($P>0.05$). The clinical staging was according to the criteria of Federation of International Gynecologists and Obstetrician (FIGO). The clinical characteristics of 49 patients with invasive cervical cancer were listed in Table 1.

Table 1. Patients characteristics ($n=49$)

FIGO stage	
Ⅰb - Ⅱa	39(79.59%)
> Ⅱa	10(20.41%)
Histopathology	
Squamous cell	45(91.84%)
Others	4(8.16%)

2.2 Preparation of serum samples for SELDI analysis

3 ml blood sample was obtained and centrifuged with 2,000 rpm at 4 ℃ for 10 minutes within 30 minutes after collection. All serum samples were aliquoted into 100 μl and stored at −80 ℃ until use. Serum samples for SELDI-TOF analysis were prepared by vortexing 5 μl of serum with 10 μl (1:2) U9 (9 mol/L urea, 2% Chaps, 50 mmol/L Tris-HCl, pH 9.0) at 4 ℃ for 30 minutes, and then diluted to 1 : 12 in binding PBS buffer (pH 7.0), vortexed at 4 ℃ for 30 minutes. Eight-spot immobilized metal affinity capture array-Cu (IMAC-Cu) chips (Ciphergen Biosystems, Fremont, CA, USA) was put onto a bioprocessor, a device that holds chips. The spots were activated with 50 μl of 100 mmol/L $CuSO_4$ and vortexed for 5 minutes, followed by a deionized water rinse, then 50 μl of 100 mmol/L sodium acetate buffer (pH 4.0) was added to each array and shaken for 5 minutes, followed by a deionized water rinse again. The activated array surfaces were equilibrated with 150 μl of PBS (pH 7.0), agitated for 5 minutes, twice. 50 μl of diluted sample were applied onto the array surface and shaken at 4 ℃ for 60 minutes. Then the chips were washed twice, with 150 μl of PBS for 5 minutes each wash cycle. The chips were removed from the bioprocessor, air-dried. Before SELDI-TOF-MS analysis, 0.5 μl of a saturated EAM solution (sinapinic acid in 50% aqueous acetonitrile and 0.5% trifluoroacetic acid) was applied onto each spot twice and air-dried between each EAM application.

2.3 SELDI-TOF-MS analysis

The chips were placed in the PBS-Ⅱ mass spectrometer reader (Ciphergen Biosystems, Fremont, CA, USA). Time-of-flight mass spectra were generated by averaging 90 laser shots at a laser intensity of 180 and a detector sensitivity of 9. The spectra were calibrated by using the All-in-1 protein molecular mass standard (Ciphergen Biosystems, Fremont, CA, USA). The reproducibility of the SELDI-TOF system was determined using two representative serum samples: one from the healthy controls and the other from the cervical invasive cancer patients, according to the manufacturer's instructions.

2.4 Statistical analysis of SELDI-TOF-MS spectra

All spectra were compiled, and the peak intensities were normalized to the total ion current of mass to charge (m/z) values from 1,500 Da to 15,000 Da using ProteinChip Software 3.2.0 (Ciphergen Biosystems, Fremont, CA, USA). The cluster data was analyzed by using Biomarker Pat-

tern Software 4.0.1 and Biomarker Wizard Software (Ciphergen Biosystems, Fremont, CA, USA). The construction of the decision tree classification algorithm with ten fold cross validation were accomplished. It creates tree-like structured decision diagrams by splitting the original dataset (parent node) into two nodes (child nodes) of highest possible purity, in which splitting decision was defined as the intensity levels of one peak. Each child node then becomes a parent node at the time of creation and can be the origin of a new split. The splitting process continued till terminal nodes. The classification of terminal nodes was determined by the group of samples (i. e. invasive cervical cancer or control) representing the majority of samples in the corresponding node. Variable importance scores reflect the contribution of each variable to classification. The variable used to split the root node was ranked as the most important. The variable received a zero score, indicating that it did not play any role in the analysis as either primary splitters or surrogates. Sensitivity was calculated as the ratio of the number of correctly classified cancer samples to the total number of cancer samples while specificity was calculated as the ratio of the number of non-cancer samples correctly classified to the total number of non-cancer samples. *t* test and One-Way ANOVA (SPSS Software 11.0) were used for comparison the mass peaks of group B.

3 Results

47 qualified mass peaks were identified with a significant level of $P<0.01$ (Figure 1). 6 mass peaks of them with the m/z value of 8929.31, 7930.52, 9127.31, 8141.01, 7963.06 and 9280.63 were of importance as decision tree classification algorithm (classification score > 95%), which appeared to be down regulated in patients with invasive cervical cancer. The score in classification, intensity of split and the mean intensity were shown in Table 2. The decision tree model with m/z value of 8929.31 had automatically built with the least nodes and lowest ratio of mis-judged wrong classification (Figure 2). And the judgment of cancer or healthy control was made according to the rules of the model tree. This model has correct classification ratio of 98.33%, sensitivity of 97.96%, specificity of 98.59%. The mass spectrum and pseudogel view of m/z value of 8929.31 were shown in Figure 3. The intensity of this 6 mass peaks, had gradually retrieved in a level of $P<0.01$ after operation, except m/z value of 9280.63 (a little lower than preoperation 0.6307 ± 0.5789/0.4339 ± 0.2940), and continuously climbed in a level of $P<0.01$ at the time of 3 months postoperation including 9280.63. Comparison of intensities of this 6 mass peaks within group B was listed in Table 3. Results of *t* test for the 6 mass peaks of every variable in group B were shown in Tables 4 and 5.

4 Discussion

Proteins carry out most of the cellular functions. Therefore, the direct measurement of protein levels and activity within the cell is the best determinant of overall cellular function. However, as the range of protein expression and modification is dynamic, it is a clear need for high-throughput assays in proteomics. Here, the novel proteomic analytical technique referred to as SELDI technology becomes a valuable tool in determining the presence of protein within a sample. This high throughput, array-based technology can bring us closer to a better understanding of cellular functions at the protein level. It produces spectra based on the m/z of complex proteins and on their binding affinity to the chip surface[23-25].

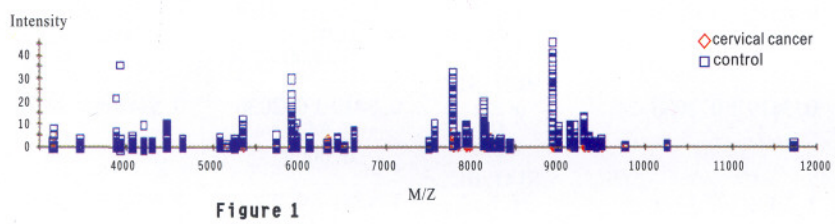

Figure 1

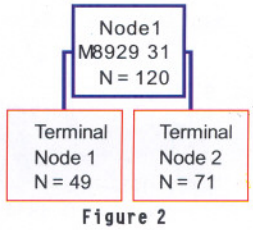

Figure 2

Figure 1. Serum proteomic mass peaks from 47 invasive cervical cancer patients and control group. Y axis represents the relative intensity of protein, X axis is the ratio of mass to charge of protein. Red circle represents cervical cancer patients, and blue square means the healthy women.

Figure 2. The decision tree model with m/z value of 8929.31. A case goes left if the intensity of 8929.31≤1.864 otherwise it goes right.

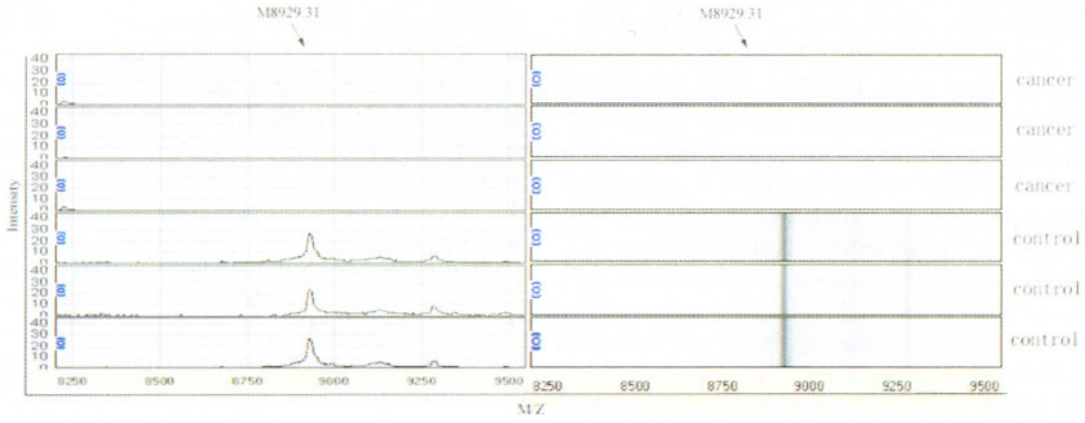

Figure 3. The mass spectra and gel view of M8929.31. Y axis is the relative intensity of proteins; X, the ratio of mass to charge.

Table 2. The score and split intensity in value of classification algorithm, mean intensity and standard deviation($\bar{x} \pm s$) of the six significant proteins in the sera of invasive cervical cancer patients and control group

m/z	Score	Split	Control($\bar{x} \pm s$)	Cervical cancer($\bar{x} \pm s$)	*P*
8929.310	100	1.864	19.88393 ± 13.34943	0.407668 ± 0.307375	0.0000
7930.527	98.25	1.427	4.541067 ± 2.145074	0.325958 ± 0.198719	0.0000
9127.317	98.25	0.746	4.884198 ± 2.960881	0.137516 ± 0.112587	0.0000
8141.019	98.12	1.506	5.043384 ± 1.486190	0.483423 ± 0.317135	0.0000
7963.060	97.35	1.406	3.343155 ± 1.106128	0.340217 ± 0.263501	0.0000
9280.430	97.00	2.650	7.370173 ± 2.190772	0.630661 ± 0.578872	0.0000

Table 3. Mean intensity and standard deviation($\bar{x} \pm s$) of the six mass peaks within group B (One-Way ANOVA)

m/z	Cervical cancer	Postoperation	3-month review	*F*	*P*
8929.31	0.4077 ± 0.2074	0.7062 ± 0.2409	1.6468 ± 0.6334	74.391	0.000
7930.53	0.3256 ± 0.1987	0.8375 ± 0.4328	2.5177 ± 1.0523	113.575	0.000
9127.32	0.1357 ± 0.1106	0.3419 ± 0.2036	0.5446 ± 0.2654	40.516	0.000
8141.02	0.4834 ± 0.3171	1.1481 ± 0.8371	2.0022 ± 0.6673	55.530	0.000
7963.06	0.3402 ± 0.2635	0.6518 ± 0.3728	1.6923 ± 0.4796	113.506	0.000
9280.43	0.6307 ± 0.5789	0.4339 ± 0.2940	1.3837 ± 0.6642	19.410	0.000

Table 4. Changes of the six mass peaks between invasive cervical cancer and postoperation (*t* test)

m/z	Cervical cancer	Postoperation
8929.31		
$\bar{x} \pm s$	0.4077 ± 0.2074	0.7062 ± 0.2409
t	4.0285	
P	0.0001	
7930.52		
$\bar{x} \pm s$	0.3256 ± 0.1987	0.8375 ± 0.4328
t	5.2984	
P	0.0000	
9127.31		
$\bar{x} \pm s$	0.1357 ± 0.1106	0.3419 ± 0.2036
t	4.4613	
P	0.0001	
8141.01		
$\bar{x} \pm s$	0.4834 ± 0.3171	1.1481 ± 0.8371
t	3.6098	
P	0.0014	
7963.06		
$\bar{x} \pm s$	0.3402 ± 0.2635	0.6518 ± 0.3728
t	4.0342	
P	0.0001	
9280.43		
$\bar{x} \pm s$	0.6307 ± 0.5789	0.4339 ± 0.2940
t	1.8964	
P	0.0621	

Table 5. Comparison intensities of the six mass peaks between postoperation and review (*t* test)

m/z	Postoperation	Review
8929.31		
$\bar{x} \pm s$	0.7062 ± 0.2409	1.6468 ± 0.6333563
t	6.5111	
P	0.0000	
7930.52		
$\bar{x} \pm s$	0.8375 ± 0.4328	2.5177 ± 1.0523
P	6.9259	
t	0.0000	
9127.31		
$\bar{x} \pm s$	0.3419 ± 0.2036	0.5446 ± 0.2654
P	2.8431	
t	0.0069	
8141.01		
$\bar{x} \pm s$	1.1481 ± 0.8371	2.0022 ± 0.6673
P	3.7421	
t	0.0005	
7963.06		
$\bar{x} \pm s$	0.6518 ± 0.3728	1.6923 ± 0.4796
P	8.0343	
t	0.0000	
9280.43		
$\bar{x} \pm s$	0.4339 ± 0.2940	1.3837 ± 0.6642
t	6.1332	
P	0.0000	

Comparisons of the protein peak patterns obtained from samples representing different status are expected to provide detailed diagnostic patterns classifying cellular or pathological status. It needs low amounts of complex biological specimens, no protein tagging and can be run automatically. Only the mass values detected both reproducibly and reliably are required to make a correct classification or diagnosis without necessary to know the identities of the masses only for the purpose of differential diagnosis. SELDI-TOF-MS technology provides a better and easier tool to identify the complex serum protein profiling. This technology has been successfully applied for analyzing protein expression in several kinds of cancer, such as breast cancer[26], prostate cancer[27], cancer of digestive system[28-30], gynecologic cancer[31-33], etc. Most of those studies demonstrated the diagnostic ability of SELDI for protein profiles and its potential utility for cancer detection and diagnosis.

To our best knowledge, cervical cancer has not been found potential biomarkers, which can be used for detection, diagnosis, treatment surveillance and prognosis prediction. Treatment surveillance and prognosis prediction has played a pivotal role in a complete treatment scheme of patients with cervical cancer. It could not only rely on the experiences of gynecologists and oncologists but also on some objective signs such as biomarkers. In this study, 6 peaks were identified as the potential biomarkers with a significant level of $P<0.01$ and a significant score in a decision tree classification algorithm with high sensitivity and specificity. The 6 mass peaks, down regulated in patients with invasive cervical cancer, were slowly retrieved after operation except m/z value of 9280.43, a little lower than preoperation ($P>0.05$). Afterwards they were continuously climbed in a level of $P<0.01$ including m/z of 9280.43 until 3-month review after operation. However, they were still more less than in healthy women even at the time of 3-month review. So they would be thought as a group of protective factors or tumor-suppressor, proteins or peptides. They are of importance in the initiation, progression of cervical cancer. Therefore it would be possible that the 6 mass peaks could be used as novel potential biomarkers for monitoring and assessing the treatment effect, predicting the prognosis of invasive cervical cancer. If one or more of them is declined or keeps same level after treatment, the treatment scheme for patients with cervical cancer would not be ideal or the remaining cancer cells would be proliferating. Based on this, we may proceed with further studies using this SELDI-TOF-MS technology in a large population, particularly in review patients with formal treatment for invasive cervical cancer, at least up to the 5-year survival year. And the further efforts would be invested in purifying, identifying and characterizing these proteins or peptides for better understanding what biological role these proteins or peptides may play in the carcinogenesis of cervical cancer. So their exact identities will be possible to find a more simple way to test them for clinical uses.

Acknowledgments

We are grateful to Professor Lidong Wang, Henan Key Laboratory for Esophageal Cancer and Laboratory for Cancer Research of Experimental Center for Medicine, Zhengzhou University, China, for his important help in study design, methodological and manuscript preparation. We also thank Ms. Xiuli Zhang, Laboratorial Center of Anal-colorectal Surgery, 150th Center Hospital of P. L. A., China, for technical assistance.

This work was funded by National Outstanding Young Scientist Award of China 30025016 and Foundation of Henan Education Committee.

Correspondence to:
Yuhuan Qiao, M.D.
Department of Gynaecology
The First Affiliated Hospital
Zhengzhou University
Zhengzhou, Henan 450052, China
Telephone and Fax: 86-371-6699-9848

References

1. Parkin DM, Bray F, Ferlay J, *et al*. Global cancer statistics, 2002. CA Cancer J Clin 2005; 55:74-108.
2. Haverkos HW. Viruses, chemicals and co-carcinogenesis. Oncogene 2004; 23:6492-9.
3. Haverkos HW. Multifactorial etiology of cervical cancer: a hypothesis. Med Gen Med 2005; 7:57-64.
4. Ng HT, Yen MS, Chao KC, *et al*. Radical hysterectomy: past, present, and future. Eur J Gynaecol Oncol 2005; 26: 585-8.
5. Sananes C, Giaroli A, Soderini A, *et al*. Neoadjuvant chemotherapy followed by radical hysterectomy and postoperative adjuvant chemotherapy in the treatment of carcinoma of the cervix uteri: long-term follow-up of a pilot study. Eur J Gynaecol Oncol 1998; 19:368-73.
6. Umanzor J, Aguiluz M, Pineda C, *et al*. Concurrent cisplatin/gemcitabine chemotherapy along with radiotherapy in locally advanced cervical carcinoma: a phase II trial. Gynecol Oncol 2006; 100:70-5.
7. Shimada M, Kigawa J, Takahashi M, *et al*. Stromal invasion of the cervix can be excluded from the criteria for using adjuvant radiotherapy following radical surgery for patients with cervical cancer. Gynecol Oncol 2004; 93: 628-31.
8. Ho CM, Chien TY, Huang SH, *et al*. Multivariate

analysis of the prognostic factors and outcomes in early cervical cancer patients undergoing radical hysterectomy. Gynecol Oncol 2004; 93:458－64.
9. Memarzadeh S, Natarajan S, Dandade DP, *et al*. Lymphovascular and perineural invasion in the parametria: a prognostic factor for early-stage cervical cancer. Obstet Gynecol 2003; 102:612－9.
10. Memarzadeh S, Natarajan S, Dandade DP, *et al*. Lymphovascular and perineural invasion in the parametria: a prognostic factor for early-stage cervical cancer. Obstet Gynecol 2003; 102:612－9.
11. Goldie SJ, Gaffikin L, Goldhaber JD, *et al*. Cost-effectiveness of cervical-cancer screening in five developing countries. N Engl J Med 2005; 353:2158－68.
12. Soler ME, Gaffikin L, Blumenthal PD. Cervical cancer screening in developing countries. Prim Care Update Ob Gyns 2000; 7:118－23.
13. Abdel-Hady ES, Emam M, Al-Gohary A, *et al*. Screening for cervical carcinoma using visual inspection with acetic acid. Int J Gynaecol Obstet 2006; 93:118－22.
14. Niikura H, Okamura C, Akahira J, *et al*. Sentinel lymph node detection in early cervical cancer with combination 99mTc phytate and patent blue. Gynecol Oncol 2004; 94:528－32.
15. Herzog TJ. New approaches for the management of cervical cancer. Gynecol Oncol 2003; 90:S22－7.
16. Hoffman MS. Extent of radical hysterectomy: evolving emphasis. Gynecol Oncol 2004; 94:1－9.
17. Umanzor J, Aguiluz M, Pineda C, *et al*. Concurrent cisplatin/gemcitabine chemotherapy along with radiotherapy in locally advanced cervical carcinoma: a phase Ⅱ trial. Gynecol Oncol 2006; 100:70－5.
18. Tanaka T, Kokawa K, Umesaki N. Preoperative chemotherapy with irinotecan and mitomycin for FIGO stage Ⅲb cervical squamous cell carcinoma: a pilot study. Eur J Gynaecol Oncol 2005; 26:605－7.
19. Linghu H, Xu XR, Mei YY, *et al*. Response of early stage bulky cervical squamous carcinoma to preoperative adjuvant chemotherapy. Chin Med Sci J 2004; 19:116－9.
20. Candelaria M, Garcia-Arias A, Cetina L, *et al*. Radiosensitizers in cervical cancer. Cisplatin and beyond. Radiat Oncol 2006; 5:1－15.
21. Goto T, Kino N, Shirai T, *et al*. Late recurrence of invasive cervical cancer: twenty years' experience in a single cancer institute. J Obstet Gynaecol Res 2005; 31:514－9.
22. Wiesner A. Detection of tumor markers with ProteinChip technology. Curr Pharm Biotechnol 2004; 5: 45－67.
23. Li L, Tang H, Wu Z, *et al*. Data mining techniques for cancer detection using serum proteomic profiling. Artif Intell Med 2004; 32:71－83.
24. Issaq HJ, Conrads TP, Prieto DA, *et al*. SELDI-TOF MS for diagnostic proteomics. Anal Chem 2003; 75:148－55.
25. Caputo E, Moharram R, Martin BM. Methods for on-chip protein analysis. Anal Biochem 2003; 321:116－24.
26. Abramovitz M, Leyland-Jones BR. A systems approach to clinical oncology: focus on breast cancer. Proteome Sci 2006; 4:5－10.
27. Pan YZ, Xiao XY, Zhao D, *et al*. Application of surface-enhanced laser desorption/ionization time-of-flight-based serum proteomic array technique for the early diagnosis of prostate cancer. Asian J Androl 2006; 8:45－51.
28. Engwegen JY, Helgason HH, Cats A, *et al*. Identification of serum proteins discriminating colorectal cancer patients and health controls using surface-enhanced laser desorption ionization-time of flight mass spectrometry. World J Gastroenterol 2006; 12:1536－44.
29. Qian HG, Shen J, Ma H, *et al*. Preliminary study on proteomics of gastric carcinoma and its clinical significance. World J Gastroenterol 2005; 11:6249－53.
30. Rosty C, Christa L, Kuzdzal S, *et al*. Identification of hepatocarcinoma-intestine-pancreas/pancreatitis-associated protein I as a biomarker for pancreatic ductal adenocarcinoma by protein biochip technology. Cancer Res 2002; 62:1868－75.
31. Kong F, Nicole WC, Xiao X, *et al*. Using proteomic approaches to identify new biomarkers for detection and monitoring of ovarian cancer. Gynecol Oncol 2006; 100:247－53.
32. Yoshizaki T, Enomoto T, Nakashima R, *et al*. Altered protein expression in endometrial carcinogenesis. Cancer Lett 2005; 226:101－6.
33. Wong YF, Cheung TH, Lo KW, *et al*. Protein profiling of cervical cancer by protein-biochips: proteomic scoring to discriminate cervical cancer from normal cervix. Cancer Lett 2004; 211:227－34.

Received October 5, 2006

Expressions of P33ING1 and P53 Protein in Human Lung Cancer Tissues

Haiyan Dong, Yongjun Wu, Yiming Wu

College of Public Health, Zhengzhou University, Zhengzhou, Henan 450052, China

Abstract: Aim. The inhibitor of growth 1 (*ING1*) gene is a novel candidate tumor suppressor gene and involve in the regulation of the cell cycle, senescence, and apoptosis. This study aims to evaluate the expression of P33ING1 protein, the product of *ING1*, with P53 protein in the same human lung cancer tissues. **Methods.** Human lung tissues were collected and classified into three groups, 31 cases of tumor tissues (A), 21 and 12 cases of tumor-adjacent lung tissues which were 3 cubic cm (B) and 5 cubic cm (C) by volume, respectively. 21 cases from group A were paired with those from group B (A-B); 12 cases from A-B were paired with those from group C (A-B-C). Immunoblotting was employed to detect P33ING1 expression in both tumor and tumor-adjacent lung tissues to ascertain the co-occurrence of P33ING1 with P53 protein. **Results.** The expression level of P53 was elevated of tissues in group A (12 of 21, 57.1%). In contrast, the expression level of P33ING1 decreased (14 of 21, 66.7%) of the tissues from the same group. There was not significant linear relationship between P53 and P33ING1 protein expression ($P>0.05$) by correlation analysis and McNemar's Test. **Conclusions.** This study first demonstrated that P33ING1 protein was down-regulated in lung cancer tissues, implying that it might play a role in carcinogenesis of lung cancer. In contrast to previous reports, this study didn't find the correlation between P33ING1 and P53 protein expression. Further studies will be conducted on gene polymorphism by larger volume of tissue samples. [Life Science Journal. 2006;3(4):23-26] (ISSN: 1097-8135).

Keywords: Lung cancer; P33ING1; P53

Abbreviations: ING1: inhibitor of growth 1

1 Introduction

Recently, studies on genes and their functional products have become hot in life science research. Exploration of interactions among diverse gene products is a critical issue in the field of proteomics. *ING1* (inhibitor of growth 1), a new candidate tumor suppressor gene, was identified in the subtelomeric region of human chromosome $13q^{33-34}$. Suppression of *ING1* expression is associated with increased proliferation and immortalization. This growth inhibitor participates in cell cycle regulation. Overexpression of *ING1* from transfected DNA constructs efficiently decreases S-phase fraction through blocking the entry of cell into S-phase, further leading to inhibition of normal cell growth. The repression of *ING1* expression frequently occurs with tumor development of breast cancer, stomach cancer, lymphoma, and so on. It has been reported that the growth inhibitory effect of P33ING1 directly cooperates with P53 protein *in vivo*. However, the expression of *ING1* gene has not been determined yet in lung carcinoma tissue. P53 protein plays a critical role in the regulation of cell proliferation, apoptosis and cellular aging, and is associated with tumor development. The mutation of *p53* gene is an early event in the pathogenesis of lung cancer[1], so *p53* could be applied for early lung cancer forecast. However, there are about 50% cases of lung cancer without *p53* gene mutation. It is shown that *p53* suppressing effect on tumor growth is regulated and modulated by other genes or proteins. So far, it is very obscure about the network for P53 protein regulation. Any efforts on uncovering one of those links will shed light on understanding of the development of lung cancer. So Western blot was used to detect protein expression of P33ING1 in tumor and tumor-adjacent tissues to unveil the correlation between P33ING1 and P53 protein.

2 Materials and Methods

2.1 Subjects

The fresh tissues including tumour tissues (A), 3 cubic cm (B) and 5 cubic cm (C) by volume, were harvested from the same patient and frozen in liquid nitrogen immediately after surgery and then stored at −80 ℃ until the extraction of protein. Three groups, 31 cases in group A, 21 cases in group B and 12 cases in group C, were harvested from 22 cases with lung squamous cell carcinoma, 7 cases with lung adenocarcinoma, 1 case with small cell lung cancer, and 1 case of large cell lung cancer. 21 cases from group A were pair-

matched with those from group B (A-B); 12 cases from A-B were pair-matched with those from group C (A-B-C).

2.2 Western blot

Protein isolation was conducted according to the published procedure in *Molecular Cloning: A Laboratory Manual*. Specifically, 0.1 g – 0.5 g lung tissue was washed with ice-cold PBS buffer, then homogenized immediately in lysis buffer at 0 ℃ (100 μg/mL PMSF, 1 μg/mL aprotinin, 0.001 mol/L EDTA(pH 8.0), 0.01 mol/L Tris·HCl(pH 7.6), 0.1 mol/L NaCl). The lysates were further sonicated to shear DNA prior to centrifugation with 10,000 rpm for 10 minutes at room temperature. The supernatants were collected and stored at −20 ℃. Protein contents were measured before use.

The supernatant was mixed with an equal volume of 2× SDS sample buffer (100 mmol/L Tris·HCl, (pH 6.8), 200 mmol/L dithiothreitol, 4% SDS, 20% glycerin) and boiled for 10 minutes. After normalization for protein content, cell extracts were subjected to 12% SDS-PAGE. Proteins were then electroblotted onto nitrocellulose.

The membrane was blocked with 20% fetal bovine serum in PBS, then washed and incubated with goat anti-ING1 antibody (sc-7566) at room temperature for 1 hour. After wash, the blots were incubated with a horseradish peroxidase-conjugated secondary antibody and counterstained with 3′3 diaminobenzidine (DAB). The images were taken with Bio-Imaging System. The horseradish peroxidase-conjugated secondary antibody and Kalerdoscope Prestained standards were purchased from Santa Cruz Biotechnology. DAB was obtained from Sigma.

2.3 Statistic analysis

Experiment data was processed using SAS software(6.12). Normal distribution was first tested. The data of Normal distribution was denominated by $\bar{x} \pm s$, and the data of abnormal distribution was denominated by 50% Med. Difference among three independent groups were determined by analysis of variance(ANOVA) and least significant difference t test. Differences between independent ratios were determined by Chi-square test. Significance was set at $P<0.05$.

3 Results

3.1 Expression of P53 protein

The expression level of P53 was increased in 57.1%(12 of 21) of tissues from group A, which was consistent with the previous reports (50% – 60%); in A-B-C, there was no significant difference in P53 expression between group A and the combined group B ($P>0.05$) (Tables 1 – 3). However, the differences of P53 expression of group A *vs*. group C, group B *vs*. C were significant ($P<0.05$), respectively(Table 3).

Table 1. The different expression of P53 in different groups

Group	n	P53($\bar{x} \pm s$)
A	31	33380.1±11841.3*
B	21	33704.6±12984.9
C	12	25000.1±11961.7

* *vs*. group C, $P<0.05$; group A *vs*. group B, group A *vs*. group C, $P>0.05$

Table 2. The different expression of P53 in A-B

Group	n	P53($\bar{x} \pm s$)
A	21	31139.8±13233.0
B	21	33704.6±12984.9

$t=-0.8325$ $P=0.4149$

Table 3. The different expression of P53 in A-B-C

Group	n	P53($\bar{x} \pm s$)
A	12	33130.5±11572.8
B	12	32254.8±9703.9
C	12	25000.1±11961.7*

* *vs*. group A, group B, $P<0.05$; group B *vs*. group A, $P>0.05$.

From Table 3, it was shown that compared with adjacent tissues which were 5 cubic cm from the cancer tissue, the expression level of P53 in tumor tissues and tissues which were 3 cubic cm from the cancer tissue were increased significantly.

3.2 Expression of P33ING1 protein

The expression level of P33ING1 was decreased in 66.7% (14 of 21) of the tissues from group A. In A, B, C and A-B-C, compared with group C, the expression level of P33ING1 in group A was decreased significantly ($P<0.05$) (Tables 4 – 6). However, the differences in P33ING1 expression between the group A and group B, group B and group C were not significant ($P>0.05$), respectively (Table 4).

Table 4. The different expression level of P33ING1 in different groups

Group	n	P33ING1($\bar{x} \pm s$)
A	31	22156.8±4654.2*
B	21	23983.5±5586.2
C	12	26021.9±5079.8

* *vs*. group C, $P<0.05$; group A *vs*. group B, group B *vs*. group C, $P>0.05$.

Table 5. The different expression of P33ING1 in A-B

Group	*n*	P33ING1 (50% Med)	Significance M(sign)	*P*
A	21	20654	—	—
B	21	23412	10.5	0.001

Table 6. The different expression of P33ING1 in A-B-C

Group	*n*	P33ING1($\bar{x} \pm s$)
A	12	22528.4±3716.4
B	12	25812.8±5278.3
C	12	26021.9±5079.8

Group A *vs*. group B, group A *vs*. group C, $P<0.05$; group B *vs*. group C, $P>0.05$

From Table 6, these results showed that compared with tissues which were 3 cubic cm and 5 cubic cm from the cancer tissues, the expression level of P33ING1 in tumor tissues were decreased significantly.

3.3 Correlation between P53 and P33ING1 expression

66.7% cancer tissues that expressed less P33ING1, P53 protein was expressed at a higher level. Meanwhile, 55.6% tissues with decreased P33ING1 levels did not exhibit an elevated expression of P53. However, there was no significant linear relationship between P53 and P33ING1 protein by correlation analysis and McNemar's Test ($P>0.05$) (Tables 7 and 8).

Table 7. The different expression level of P53 and P33ING1 in A-B

P53	P33ING1		Total
	Decreased	Increased	
Decreased	6	3	9
Increased	8	4	12
Total	14	7	21

$\chi^2=2.273, P=0.132$

Table 8. Linear correlation analysis

Group	*n*	*r*	*P*
A	31	0.0358	0.8482
B	21	0.2646	0.2464
C	12	0.2723	0.3920

4 Discussion

The normal expression of P53 protein can induce growth suppression and apoptosis. Vicious cycle of abnormal cell proliferation, immortalization, and malignant tumor may take place if P53 loses its function or is mutated. Up to now, it has been accepted that there exists a close relationship between p53 mutation and human tumor development. Previous studies have shown that 50% – 60% of 5,000 cases of tumor derived from 43 kinds of tissues produced with mutated *p53* gene[2]. This study demonstrated an abnormal expression of P53 (57.1%), which was consistent with previous reports. There was no significant difference in P53 expression between lung cancer tissues and the cancer-adjacent tissues. The explanation for these phenomena may lie on two aspects. First, due to the irregular infiltration of malignant tumor, abnormal differentiation cell or cancer cell may exist in cancer-adjacent tissues, which may express mutated P53; second, wild type P53 protein might be combined with other molecular chaperones (such as MDM-2)[3], thus caused elongation of its half life, which may interfere the detection of mutated P53 protein. Further studies on gene expression need to be conducted to confirm these explanations.

The data demonstrated that the expression of P53 in lung cancer tissues (A) was significantly higher than that in the tissues which were 5 cm (C) from cancer tissues and the same was true of A-B-C of 12 patients. These are consistent with previous reports. In addition, an expression of P53 increased in lung cancer. And also the expression of P53 in the 3 cubic cm tissues from the cancer tissue was statistically higher than that in 5 cubic cm tissues away in A-B-C. However, analysis on groups A, B and C that were not paired, there were no significant differences in P53 expression between tissues that were 3 cubic cm and 5 cubic cm from the cancer tissue. These might be caused by unpaired groups A, B and C, since the result of analysis of variance in A-B-C showed that match factors could interfere the expression level of P53 protein ($P<0.05$), and would confound the results while taking the comparison in unpaired groups A, B and C.

*ING*1 gene is located in the subtelomeric region of human chromosome $13q^{33-34}$. Previous studies showed[4-8] that P33ING1 protein was the product of *ING*1 gene, located in nuclear, and participated in cell cycle regulation and its suppression was associated with increased cell proliferation and formation of neoplasm. Recently, it has been discovered that *ING*1 gene products had interaction with P53, and P53 protein took part in the regulation of cell proliferation, apoptosis and cellular aging[4].

Some investigations reported that the expression of *ING*1 gene was decreased in stomach cancer[9], breast cancer[10], and others, which implied that *ING*1 gene was relevant to the occurrence and

development of carcinoma. P33ING1 expression was determined in this study, which showed an increase in its expression in tumor tissues(A), tissues which were 3 cubic cm(B) and 5 cubic cm(C) from cancer tissue, respectively. It was assumed that the decreased expression of P33ING1 could be one of the mechanisms of abnormal cell growth, and played an important role in the procession of the occurrence and development of pulmonary carcinoma.

It has been reported that the expression of P33ING1 was correlated with P53 protein in stomach cancer, breast cancer, and so on; however, analysis on the correlation between P33ING1 and P53 in the study revealed that in 66.7% of the tissues that down-regulated P33ING1 the level of P53 protein was up-regulated. In addition, 55.6% of the tissues with decreased P33ING1 expression did not show altered P53 protein expression. There was no significant linear relationship between P53 and P33ING1 protein by correlation analysis and McNemar's Test ($P>0.05$). Further study needs to be carried out to confirm this observation based on the following reasons: *ING*1 gene encodes alternative transcripts of P47ING1, P33ING1 and P24ING1 in human cell, three of them exert different function through different channel.

In summary, the decreased expression of P33ING1 was determined in lung cancer tissues in the study; this suggested that it might play a role in the occurrence and development of lung cancer. This study provided a new clue for further study of pathogenesis and diagnosis of lung cancer, also gave a new idea and direction to gene therapy. But we did not find the correlation between P33ING1 and P53. Future studies on the gene polymorphism will be conducted. However, the exertion of tumor suppressor P53 function is regulated by multiple factors; most of them occur in different temporal and spatial segments of cell proliferation and interact with each other through expression modulation. Therefore, it is difficult to figure out their interactions by analyzing a single or few factors. Nevertheless, elucidation of certain events may be helpful in understanding carcinogenesis.

Acknowledgements

The authors thank the anonymous referees for their comments, suggestions and the very helpful review of manuscript, especially thank Weidong Wu, Research Assistant Professor (faculty), University of North Carolina at Chapel Hill, USA, for his constructive advice. Thanks are also given to the technical staff of Henan Key Laboratory of Molecular Medicine (HKLMM) for competent and kind assistance.

This study is supported by sustentation fund of National Natural Science Foundation of China (30571552) and "211 Project" of Ministry of Education of China.

Correspondence to:
Yiming Wu
College of Public Health
Zhengzhou University,
Zhengzhou, Henan 450001, China
Telephone: 86-371-6665-8011, 6665-8960
Email: wuym@zzu.edu.cn

References

1. Wu YM, Li ZW, Chen C, *et al*. The predication value of the detection of serum level of P53 protein in occupational lung cancer. J Henan Medical Univ 2000; 35(3): 206-8.
2. Greenblatt M, Bennett W, Hollsteain M, *et al*. Mutations in the *p*53 tumor suppressor gene: clues to cancer etiology and molecular pathogenesis. Cancer Res 1994; 54: 4855.
3. Hartwell L, Kastan MB. Cell cycle control and cancer. Science 1994; 266:1820-8.
4. Garkavtsev I, Grigorian IA, Ossovskaya VS, *et al*. The candidate tumour suppressor P33ING1 cooperates with *p*53 in cell growth control. Nature 1998; 391(6664): 295-8.
5. Garkavtsev I, Kazarov A, Gudkov A, *et al*. Suppression of the novel growth inhibitor P33ING1 promotes neoplastic transformation. Nat Genet 1996; 14(4): 415-20.
6. Garkavtsev I, Boland D, Mai J, *et al*. Specific monoclonal antibody raised against the P33ING1 tumor suppressor. Hybridoma 1997;16(6): 537-40.
7. Garkavtsev I, Demetrick D, Riabowol K. Cellular localization and chromosome mapping of a novel candidate tumor suppressor gene (*ING*1). Cytogenet Cell Genet 1997; 76(3-4): 176-8.
8. Garkavtsev I, Riabowol K. Extension of the replicative life span of human diploid fibroblasts by inhibition of the P33ING1 candidate tumor suppressor. Mol Cell Biol 1997; 17(4): 2014-9.
9. Oki E, Maehara Y, Tokunaga E, *et al*. Reduced expression of *p*33(*ING*1) and the relationship with *p*53 expression in human gastric cancer. Cancer Lett 1999; 147(1-2): 157-62.
10. Tokunaga E, Maehara Y, Oki E, *et al*. Diminished expression of *ING*1 mRNA and the correlation with p53 expression in breast cancers. Cancer Lett 2000; 152(1): 15-22.

Received April 28, 2006

High-level Expression of Human α-1,2-fucosyltransferase Gene in Transgenic Mice Enhances Heart Function in *ex vivo* Model of Xenograft Rejection

Peihuan Li[1], Bingqian Liu[2], Yudong Wu[2], Lixia Zhang[3], Guangsan Li[3]

1. *Department of Pathology, Institute of Hematology, Chinese Academy of Medical Sciences and Peking Union Medical College, Tianjin 300052, China*
2. *Department of Urology, The First Affiliated Hospital of Zhengzhou University, Zhengzhou, Henan 450052, China*
3. *Institute of Genetics and Development Biology, Chinese Academy of Sciences, Beijing 100080, China*

Abstract: Background. Hyperacute rejection (HAR) of discordant xenotransplantation is the consequence of binding of natural antibodies to galactose-α-1,3-galactose (Gal) of vascular endothelium of the xenograft that activates complement system. Expression of human α-1,2-fucosyltransferase (HT) eliminating α-Gal antigen in donor organs has proven to be a promising approach to dealing with HAR. The aim of the paper was to investigate the effect of expressing human *HT* gene *in vivo* on α-Gal antigen and the role of human HT in overcoming HAR. **Methods.** Transgenic mice were produced by microinjection of gene construct for the enzyme human HT. PCR and Southern blot were used to screen the positive transgenic mice. Real-time PCR analysis was used to detect the level of human *HT* mRNA expression in transgenic mice. Expressions of H antigen and α-Gal antigen on peripheral blood mononuclear cells (PBMCs) of transgenic mice were detected by Flow Cytometry (FCM). In addition, the hearts of transgenic mice were perfused *ex vivo* with 12% human plasma by using a modified Langendoff apparatus, and the effect on cardiac function was determined. **Results.** 1176 injected and surviving zygotes were implanted into the oviducts of pseudopregnant foster mothers. Integration rate of human *HT* gene was 10.2% (14/137). Expression of human *HT* mRNA was detected in the heart, liver, kidney and muscle of transgenic mice, and expression rate was 78.6% (11/14). FCM analysis showed high-level expression of H antigen and with reduction of α-Gal antigen on PBMCs in transgenic mice. When perfused *ex vivo* with 12% human plasma, hearts from transgenic mice showed prolongation in survival time, compared to normal controls. **Conclusion.** A transgenic mice model with overexpression of human *HT* was successfully established. The transgene was integrated and transmitted into chromosome of transgenic mice. The present study suggests that the expression of human *HT* gene can reduce expression of the α-Gal antigen, and be effective in prolonging survival of xenograft and overcoming HAR. [Life Science Journal. 2006;3(4):27-32] (ISSN: 1097-8135).

Keywords: xenotransplantation; α-1,2-fucosyltransferase; hyperacute rejection; transgene

Abbreviations: α-Gal: galactose-α-1,3-galatose; HAR: hyperacute rejection; HT: α-1,2-fucosyltransferase; FCM: flow cytometry; PBMCs: peripheral blood mononuclear cells; XNAs: xenoreactive natural antibodies

1 Introduction

Notable improvements in the success of organ transplantation have created a severe imbalance between organ supply and demand. Xenotransplantation using porcine organs is currently viewed as a possible solution to overcome the worldwide shortage of donor organs for transplantation[1,2]. However, hyperacute rejection (HAR) must be overcome before organs can be transplanted between disxordant species[3]. HAR is primarily mediated by the binding of xenoreactive natural antibodies (XNAs) to the galactose-α-1,3-galatose (α-Gal) on vascular endothlium of the xenograft followed by complement activation, and is initiated within minutes of reperfusion[3]. Therefore, elimination of this interaction will be highly beneficial to overcoming HAR. The α-Gal antigen is synthesized by the enzyme α-1, 3-galactosyltransferase (α-1, 3-GT). Human α-1,2- fucosyltransferase (HT) was shown to efficiently compete with α-1,3-GT for the same substrate, N-acetyl lactosamine, impeding the transfer of the temrminal galactose residue that gives rise to the α-Gal antigen[4]. Furthermore, HT generates fucosylated residues that are universally tolerated[5]. So we can utilize the expression

of HT to down-regulate α-Gal antigen expression.

This study was designed, with a transgenic mice model, to investigate the effects of expressing the human HT on α-Gal antigen. In addition, function of human HT expression was studied by using an *ex vivo* heart perfusion model.

2 Materials and Methods

2.1 Animals

Kunming mice were purchased from Institute of Genetics and Development Biology, Chinese Academy of Sciences.

2.2 Chemicals and reagents

Restriction endonucleases *Not* I and *Pvu* I, Trizol, and RT-PCR kit were purchased from Invitrogen Inc. (USA). DIG-High Prime DNA labeling and detection starter kit I and nylon membranes were purchased from Roche (Switzerland). PCR kit was purchased from TaKaRa (Japan). Fluorescein isothiocyanate (FITC) -conjugated UEA I and GS-IB4 were purchased from Sigma (USA). Red blood cell lysate was purchased from BD Company (USA). Proteinase K was purchased from Merck (Germany).

2.3 Plasmid

The pRc-CMV plasmid containing full-length sequences of human *HT* cDNA was offered by Dr. Hiroshi Kimura (Department of Forensic Medicine and Human Genetics, Kurume, Japan). The pCMV-MCS plasmid was purchased from Merck (Germany).

2.4 Production of transgenic mice

Gene construct used to generate transgenic mice has been described previously[6]. The pCMV-MCS-HT recombinent plasmid was indetified by enzyme digests. It consists of CMV promoter, β-globin intron, *hHT* cDNA and hGH polyadenylation signal (Figure 1). Transgenic mice were generated as described by Gordon[7]. Transgene construct was microinjected into pronuclei of one-cell embryos with dosage of 5 μg/ml. The injected and surviving zygotes were reimplanted into the oviducts of pseudopregnant female mice and allowed to develop to term.

Figure 1. Schematic diagram of the target transgene construct

2.5 PCR

Genomic DNA of mice was extracted from the tail[8,9], and were screened for integration of human *HT* gene by PCR with the following primers: up-stream: 5′-AAC GTG CTG GTC TGT GTG CG-3′; down-stream: 5′-CTC CGA TGT GGC ACC TTT CA-3′. PCR cycling parameters were: initial denaturation at 95 ℃ for 10 minutes, 30 cycles (denaturation at 95 ℃ for 40 seconds, anneal at 60 ℃ for 40 seconds, extension at 72 ℃ for 50 seconds), and a final extension at 72 ℃ for 10 minutes. Positive PCR reaction using the primer generate a 915 bp fragment. For Southern blot analysis, mouse genomic DNA was digested with restriction enzyme *Eco*RI/*Bam*HI, product was subjected to electrophoresis in a 1.0% agarose gel and transferred to nylon membrane according to the manufacturer's instruction. Hybridization was performed with a DIG labeled human *HT* cDNA probe under stringent condition according to the protocol of DIG DNA labeling and detection kit.

2.6 RT-PCR

Total RNA was isolated by using Trizol Reagent as described by the manufacturer. Expression of human *HT* mRNA was evaluated by RT-PCR from total mRNA samples of heart, liver, kidney and spleen. First strand cDNA was prepared by reverse transcription using AMV reverse transcriptase and used for PCR. The primers designed according to the sequence of cDNA of human *HT* gene: up-stream: 5′-GAC TTT CTT CCA CCA TCT CC-3′; down-stream: 5′-TAA TGC CCA CCC ACT CG-3′. The expected PCR products is 544 bp. The β-actin primers: up-stream: 5′-CCA ACT GGG ACG ACA TGG AG-3′; down-stream: 5′-AGG TCC AGA CGC AGG ATG GC-3′. The products is 300 bp. Reaction condition: denaturation at 96 ℃ for 2 minutes; then for 30 cycles (denaturation at 94 ℃ for 30 seconds, annealing at 65 ℃ for 60 seconds), extension at 72 ℃ for 60 seconds; and a final extension at 72 ℃ for 7 minutes.

2.7 Flow cytometry analysis of α-Gal and H antigen

Mice blood was collected by orbital eye-bleed and erythrocytes lysed by incubation in red blood cell lysate. Peripheral blood leukocytes were collected by centrifugation and washed 3 times in phosphate-buffered saline, containing 2% heat-inactivated febovine serum and NaN_3, and then incubated with FITC-conjugated lectins GS-IB4 and UEAI for expression of α-Gal and H antigen respectively on ice for 30 minutes, washed twice in Hanks' balanced salt solution. The expression on peripheral blood mononuclear cells (PBMCs) was analyzed by Flow cytometry (FCM) as described[10].

2.8 *Ex vivo* isolated perfused heart model

Mouse hearts were perfused on a Landendorff

apparatus essentially as reported[11]. Mice were anethetized with pentobarbitone sodium, and the hearts were removed and immersed 20 ml of ice-cold modified heparin-containing Krebs-Henseleit buffer to arrest cardiac activity. Hearts were then attached to a 21-gauge cannula via the aortic root, connected to the perfusion apparatus and perfused in a retrograde manner. Heart rate and force of contraction were monitored using PowerLab 4.0 software at 5 minutes intervals, and heart work was calculated as the product of heart rate multiply force of contraction. After a 20-minute period of stabilization perfused with K-H buffer, pooled human plasma was added at 5 minutes intervals to final concentration of 12%.

2.9 Statistical analysis

All data were expressed as mean ± standard deviation and analyzed by SPSS 11.0 software, statistical significance was determined by Student's test, significance was defined as a P value <0.05.

3 Results

3.1 Identification of human *HT* transgene construct

The length of the resulting construct pCMV-MCS-HT plasmid was about 5.6 kb containing 1.85 kb human *HT* cDNA. The electrophoresis assay showed: 1.1 kb and 4.5 kb in the *Eco*RI/*Bam*HI digest, and 2 fragments containing 2.85 kb and 2.75 kb in the *Not*I digest, and 3 fragments containing 2.85 kb, 1.4 kb and 1.35 kb in the *Pvu*I/ *Not*I digest (Figure 2), indicating that human *HT* cDNA was correctly inserted and linked.

3.2 Sequence data

Sequence data showed that the sequenced fragment was the same as human *HT* in the Genebank, and no ATG was present in the 60 bp vector fragment between CMV promoter and human *HT* cDNA on the recombinment plasmid.

3.3 Screening of transgenic mice

Tail genomic DNA from G_0 mice was screened by PCR, which amplify a 915 bp fragment from transgenic mice but not from non-transgenic mice littermates (Figure 3). Southern blot revealed the same results of PCR (Figure 4).

3.4 Transgenic efficiency of transgenic mice

To create transgenic mice, a total 1,300 fertilized embryos was microinjected with purified human *HT* transgene construct. 1,176 surviving injected embryos were reimplanted into 55 pseudopregnant foster mice, and 43 of whom gave birth to 137 mice. Pregnancy rate was 78.2% (43/55), and birthrate was 11.6% (137/1176). Among 137 G_0 mice, transgene integration was confirmed by PCR and Southern blot in 11 mice. Integration efficiency was 8.0% (11/137).

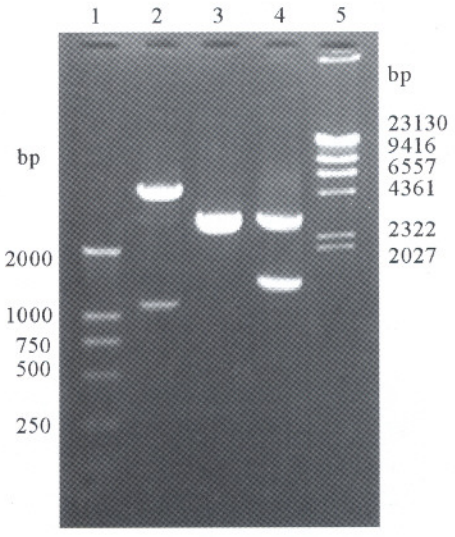

Figure 2. Identification of recombinant pCMV-MCS-HT plasmid by enzyme digestion
Lane 1: DL2000 Marker; Lane 2: Plasmid digested with *Eco*RI/*Bam*HI(1.1 kb and 4.5 kb); Lane 3: Plasmid digested with *Not*I (2.85 kb and 2.75 kb); Lane 4: Plasmid digested with *Pvu* I / *Not* I (2.85 kb, 1.4 kb and 1.35 kb); Lane 5: λ-*Hind* III Marker

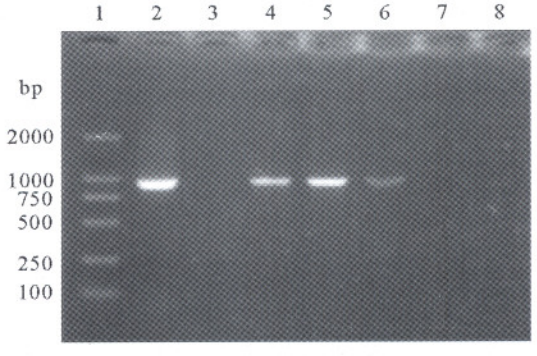

Figure 3. Identification of transgenic mice by PCR
Lane 1: DL2000 Marker; Lane 2: pCMV-MCS-HT plasmid as positive control; Lane 4,5,6: positive mice; Lane 3,7: negative mice; Lane 8: normal mice as negative control

3.5 Expression of human *HT* mRNA in transgenic mice

RT-PCR anslysis was used to determine *hHT* RNA expression in various tissues derived from control and transgenic mice. Total RNA was isolated from heart, liver, kidney and spleen. Human *HT* mRNA expression was detected in 8 mice among 11 G_0 transgenic mice, and expression was positive in organs of transgenic mice including

heart, liver, kidney and spleen, no specific PCR products were observed in any of the non-transgenic littermate. Endogenously-expressed β-actin was used as a control to confirm the integrity of all samples tested by PCR (Figure 5).

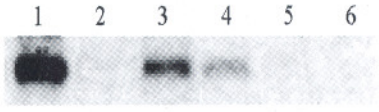

Figure 4. Identification of transgenic mice by Southern blot
Lane 1: pCMV-MCS-HT plasmid; Lane 3 and Lane 4: positive mice; Lane 2 and Lane 5: negative mice; Lane 6: normal mice as negative control

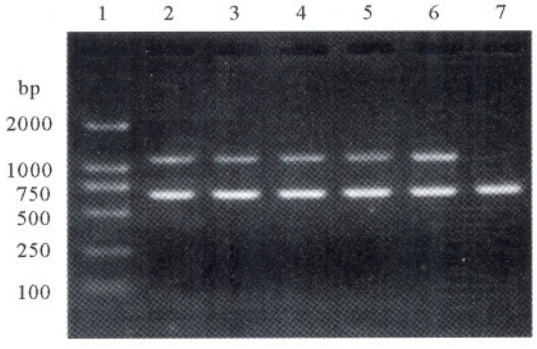

Figure 5. The expression of human *HT* gene in transgenic mice detected by RT-PCR
Lane 1: DL2000 Marker; Lane 2: positive control; Lane 3: heart; Lane 4: liver; Lane 5: kidney; Lane 6: muscle; Lane 7: negative control

3.6 FCM analysis

H antigen and α-Gal antigen expression was evaluated by FCM on PBMCs. Control mice cells showed only background staining for H antigen, but cells from transgenic mice expressed high levels of this antigen. Staining with GS-IB4 for α-Gal revealed a fourfold reduction in mean fluorescence intensity of transgenic mice cells relative to controls (Figure 6).

3.7 *Ex vivo* heart perfusion

Six hearts from control and transgenic mice were removed quickly respectively. The hearts were attached to a modified Langendorff perfusion apparatus, then perfused with 12% human plasma[11]. Heart work from control mice dropped sharply to below 20% of maximum within 20 minutes of plasma addition. In contrast, hearts from transgenic mice were still functioning at 30% of maximum after 60 minutes perfusion. 100% work is defined as heart work measured immediately before time 0 (Figure 7).

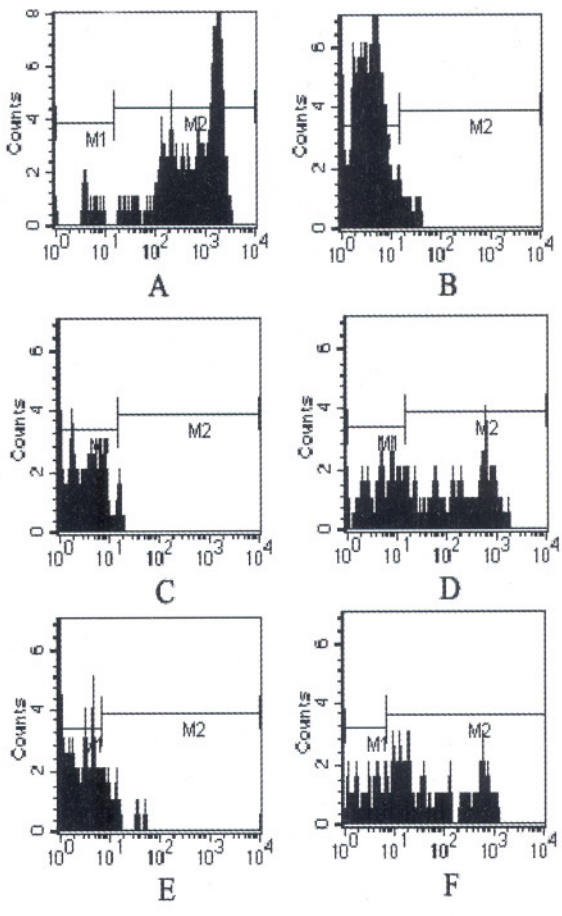

Figure 6. Expression of various levels of H and Gal antigen.
A: Gal of normal mice; B: H of normal mice; C: Gal of human; D: H of human; E: Gal of transgenic mice; F: H of transgenic mice

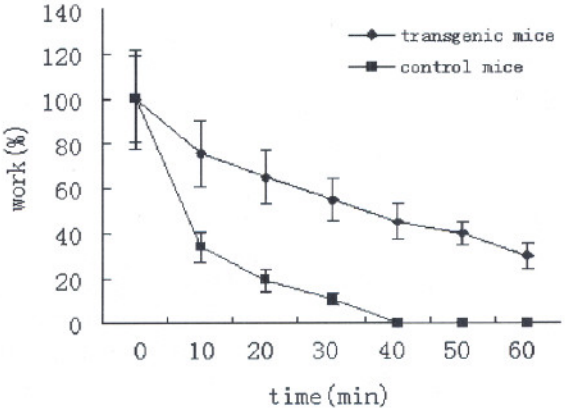

Figure 7. Function of mice hearts perfused *ex vivo* with human plasma

4 Discussion

Rapid improvement in the success of organ

transplantation have created an obvious imbalance between organ supply and demand. The serious shortage of human organs available for allotransplantation has stimulated people to look at the possibility of using animals as donors. Xenotransplantation using pig organs is currently regarded as a feasible approach to solving the problem, but the immediate barrier to the transplantation of vascularized pig organ to primates is HAR[12,13].

It is now clear that the binding of XNAs to α-Gal on vascular endothelium of xenograft is key mediator of HAR[14], therefore elimination of this interaction will be highly beneficial to overcoming HAR. The strategies could be classified as recipients or donors directed. The disadvantages of the former are that their effect is transient, and impose an additional burden on the recipient. Therefore genetic engineering of the donor organ has greater potential for effectively inhibiting xenograft rejecting with reduced risk to recipient. Transgenic expression of human complement regulation proteins (CRPs) in donor organs has significantly prolonged the survival of xenografts[15]. However, expression of CRPs without eliminating xenogeneic natural antibody reactivity may not provide sufficient protection for clinical application.

α-Gal is a major antigen involved in HAR of xenotransplantation that is synthesized by the enzyme α-1,3-galactosyltransferase. Removal of α-Gal antigen from pigs would prevent HAR, and prolong survival of xenograft[4,16]. The production of GT-KO mice and pigs has been reported recently, these GT-KO animals would, by definition, be deficient in α-Gal antigen, theoretically leaving no target for human natural antibodies. Some investigators suggest, however, that eliminating the α-Gal antigen would expose underlying "cryptic" oligosaccharide determinanta against which human may also have preformed antibody[17]. So, an alternative transgenic approach was developed that based on the competition between α-1,3-GT and human HT for a common substrate – N-acetyllactosamine, transgenic expression of human HT is currently viewed as the feasible strategy to reduce α-Gal expression in pigs[18]. The strategy has been to significantly reduce Gal expression on a variety of cells in transgenic mice and pigs. However its ability at prologing xenograft survival is yet to be demonstrated.

Thus, we obtained transgenic mice by microinjection of human *HT* transgene construct, and to investigate the effect of expressing human HT *in vivo* on α-Gal antigen and the role in overcoming HAR. α-Gal was expressed in all tissues and organs of normal mice, so we chosed CMV promoter to achieve ubiquitous expression of human HT. The result suggested that human *HT* mRNA was expressed in most organs of transgenic mice including heart, liver, kidney and spleen. According to expression of H antigen and α-Gal on PBMCs was the same as on vacular endothelium[19], we evaluted expression of them on PBMCs. FCM analysis showed that overexpression of human HT could greatly reduce the amount of α-Gal antigen on PBMCs.

In the study, we tested the ability of human HT expressed in transgenic mice to protect organs against HAR when perfused *ex vivo* with human plasma. As expected, the cardiac function of hearts from control mice perfused with 12% human plasma dropped sharply to 20% of maximum work within 20 mintutes from plasma addition and stopped beating at the 35th minute. In constrast, the function of human HT transgenic hearts was only reduced by 50% – 65% after 20 minutes, and was maintained approximately 35% after 60 minutes. Therefore, as far as HAR concerned, the results would suggest that the human *HT* expression is effective in protecting against XNAs and complement mediated HAR.

However, FCM analysis showed that there was still α-Gal expression on PBMCs of transgenic mice. It is suggested that overexpression of human *HT* gene would be unlikely to totally eradicate α-Gal. Whether transgenic expression of human *HT* is sufficient to avoid HAR and whether residual α-Gal is related to subsequent acute vascular rejection (AVR) of xenotransplantation is not clear and is under examination. And xenotransplantation is related to many factors[20], so a combination of human HT transgene approach, together with the transgenic expression of human complement inhibitory proteins, may lead to murine heart entirely resistant to HAR. The present study provide a helpful technique for the further research of transgenic pigs.

Acknowledgments

This subject is supported by Doctor Invention Foundation of Tianjin Medical University.

Correspondence to:
Bingqian Liu
Department of Urology
The First Affiliated Hospital
Zhengzhou University
Zhengzhou, Henan 450052, China
Telephone: 86-371-6686-1002
Email: liubq76@yahoo.com.cn

References

1. Deschamps JY, Roux FA, Sai P, *et al*. History of xenotransplantation. Xenotransplantation 2005;12(2): 91 – 109.
2. Dwyer KM, MB BS, Cowan PJ, *et al*. Xenotransplantation: Past achievements and future promise. Heart, Lung and Circulation 2002;11(1): 32 – 41.
3. Madsen JC. Feasibility of xenotransplantation. Surg Clin N Am 2004;84(1): 289 – 307.
4. Cohney S, Mckenzie IF, Patton K, *et al*. Down-regulation of Gal alpha (1,3) Gal expression by alpha1,2-fucosyltransferase: Further characterization of alpha1,2-fucosyltransferase transgenic mice. Transplantation 1997;64 (3): 495 – 500.
5. Costa C, Zhao L, Burton WV, *et al*. Transgnic pigs designed to express human CD59 and H-transferase to avoid humoral xenograft rejection. Xenotransplantation 2002;9 (1):45 – 57.
6. Ma ZF, Liu BQ, Zhang Y, *et al*. The production of microinjected DNA fregment for transgenic mouse in studying xenotransplantation. Chinese Remedies Clinics 2004, 4(12): 912 – 5.
7. Gordon JW. Production of transgenic mice. San Diego: Academic Press Inc 1993; 768 – 71.
8. Wan LX, Chung SK, Yang YZ, *et al*. Transgenic mice with overexpression of human scavenger receptor A on endothelial cells. Chin Med J 2001; 114(10): 1078 – 83.
9. Sambrook J, Russell DW. Molecular Cloning: A Laboratory Manual. 3rd ed. Cold Spring Harbor Laboratory Press 2002. 1: 479 – 82.
10. Van D, Bryce JW, Pearse MJ, *et al*. Expression of functional decay-accelerating factor (CD55) in transgenic mice protects against human complement-mediated attack. Transplantation 1996;61(4): 582 – 8.
11. Wu SH, Ma H, Huang SJ, *et al*. CD59 prevents human complement-mediated injuries in isolated guinea pig hearts. Chin Med J 2002;115(2): 175 – 8.
12. Khalpey Z, Koch CA, Platt JL. Xenograft transplantation. Anesthesiology Clin N Am 2004; 22(4): 871 – 5.
13. Evans RW. Coming to terms with reality: why xenotransplantation is a necessary. In: Platt JL, ed. Xenotransplantation. Washinton, DC: ASM Press, 2001;29.
14. Sharma A, Okabe J, Birch P, *et al*. Reduction in the level of Gal(α1,3)Gal in transgenic mice and pigs by the expression of an α(1,2)fucosyltransferase. Proc Natl Acad Sci 1996; 93(14): 7190 – 5.
15. Masayoshi N, Masayuki S, Takashi O, *et al*. Adenovirus-mediated gene transfer of triple human complement regulating proteins (DAF, MCP, CD59) in the xenogeneic porcine-to-human transplantation medel. Transpl Int 2002; 15(5): 205 – 19.
16. Uri G. The alpha-gal epitope (Gal alpha 1-3Gal beta 1-4GlcNAc-R) in xenotransplantation. Biochimie 2001; 83 (7): 557 – 63.
17. David KC. Clinical xenotransplantation – how close are we? Lancet 2003; 362(9383): 557 – 9.
18. Cowan PJ, Chen CG, Shinkel TA, *et al*. Knock out of alpha1,3-galactosyltransferase or expression of alpha 1,2-fucosyltransferase further protects CD55- and CD59-expressing mouse hearts in an *ex vivo* model of xenograft rejection. Transplantaion 1998; 65(12): 1599 – 604.
19. Cowan PJ, Aminian A, Barlow H, *et al*. Renal xenografts from triple-transgenic pigs are not hyperacutely rejected but cause coagulopathy in non-immunosuppressed baboons. Transplantation 2000; 69(12): 2504 – 15.
20. David TC, Anthony DC, Robert CR. The road to clinical xenotransplantation: A worthwhile journey. Transplantation 2004; 78(8): 1108 – 9.

Received June 5, 2006

Effects of Sparfloxacin on Delayed Rectifier Potassium Current of Ventricular Myocyte in Guinea Pig

Ying Jing[1,2], Shengna Han[1], Yingna Wei[1], Peng Qiao[1], Zhao Zhang[1,3]

1. Department of Physiology, Basic Medical College, Zhengzhou University, Zhengzhou, Henan 450052, China

2. Stem Cell Center, Zhengzhou University, Zhengzhou, Henan 450052, China

3. Jiangsu Province Key Laboratory for Molecular Medical Biological Technique, College of Life Science, Nanjing Normal University, Nanjing, Jiangsu 210097, China

Abstract: Administration of fluoroquinolone antibiotics in human has proven to induce prolongation of QT interval, which is mainly assumed the blockade of some kind of potassium channel(s). This study is to examine the effect of sparfloxacin on delayed rectifier potassium current of ventricular myocyte in guinea pig. Single ventricular cells were dissociated from guinea pig heart and continuously superfused with sparfloxacin solution of different concentrations. Delayed rectifier potassium current (I_K) was recorded with whole-cell patch clamp technique. Results showed that sparfloxacin decreased the current amplitude of I_K in a concentration dependent manner. When the concentration was from 0.1 μM to 1,000 μM, the inhibitory capacity of drug on I_K peak current gradually enhanced; and depressed rates of the tail currents increased too. Sparfloxacin displayed an IC_{50} value of 14.89 μM. These results indicate that sparfloxacine inhibits I_K concentration-dependently to the ventricular myocyte. [Life Science Journal. 2006;3(4):33-36] (ISSN: 1097-8135).

Keywords: sparfloxacin; ventricular myocyte; delayed rectifier potassium current; whole-cell patch-clamp

Abbreviations. IC_{50}: 50% inhibitory concentration; I_K: delayed rectifier potassium current

1 Introduction

There is considerable interest in ventricular repolarization, since prolonged repolarization is associated largely with ventricular tachyarrhythmia, syncope and sudden death, known as long-QT syndrome. It is the delayed rectifier potassium current (I_K) that plays a critical role in cardiac repolarization. Therefore any congenial or environmental variation that interferes with I_K might underlie long QT syndrome. Recently, it has been suggested that some antibiotics, such as fluoroquinolone antibacterial drugs, are a hint to the occurrence of long QT syndrome[1,2]. Sparfloxacin belongs to fluoroquinolone class and has been widely prescribed in clinic since 1993 for the treatment of infection. The present study was designed to examine *in vitro* the effects of sparfloxacine on I_K of isolated ventricular myocyte, in order to explore the pharmacological mechanism of cardiac inhibition, and to provide support for clinical drug application.

2 Materials and Methods

2.1 Cardiomyocyte isolation

Adult guinea-pigs (300±50 g) were adopted. The operation followed previous reports with slight modification[3]. In brief, animals were sacrificed by blunt trauma to the head. Hearts were rapidly excised, rinsed and mounted on a Langendorff system. Hearts were perfused for 10 minutes with Ca^{2+}-free Tyrode solution containing: NaCl 140 mM, KCl 5.4 mM, $MgCl_2$ 1 mM, HEPES 10 mM, and glucose 10 mM(pH 7.4). Then the perfusion was switched to normal Tyrode solution (25 μM $CaCl_2$) complemented with 0.36 g/L collagenase (type B, Roche) and 0.26 g/L protease (type XIV, Sigma). When the flow-out appeared viscous and the heart was obviously dilated, digestion process was ceased by perfusing solution consisting of: Glutaminc acid 120 mM, KOH 80 mM, KCl 20 mM, $MgCl_2$ 1 mM, EGTA 0.3 mM, HEPES 10 mM, and glucose 10 mM(pH 7.4±0.5). Ventricular free walls were removed, cut into pieces, gently agitated in Ca^{2+}-free Tyrode solution and filtrated through 200 μm nylon sieve. Harvested myocytes were placed at room temperature (18-22℃) in Ca^{2+}-free Tyrode solution.

2.2 Whole-cell patch clamp recording

Microelectrodes (hard, thin-wall glass capillaries with inner diameter of 1.5 mm) were pulled with the micropipette puller (Narishige PP-83,

Japan). Resistance when filled with inner solution was 2 – 3 MΩ. Inner solution of the pipette contained: KCl 140 mM, Mg-ATP 4 mM, $MgCl_2$ 1 mM, HEPES 10 mM, and EGTA 5 (pH 7.3). Isolated cells were bathed and continuously perfused with oxygen-saturated Tyrode solution containing: NaCl 140 mM, KCl 5.4 mM, $MgCl_2$ 1 mM, $CaCl_2$ 0.025 mM, HEPES 10 mM, and glucose 10 mM (pH 7.4). Rod-shaped ventricular cells with smooth edge and clear striates were selected for recording.

I_K was recorded using conventional whole cell clamp protocol at room temperature. Whole-cell current records were performed with an amplifier (2300E, Axon Instruments, America), filtered at 1 kHz and sampled at 0.25 kHz. After reaching "sealing", series resistance and capacitive resistance were compensated to minimize the resistance impact and to ensure the recording stability. Both voltage pulses delivering and current signals collecting were processed automatically by pClamp 5.51 software (Axon Instruments, America). Step-voltage depolariztions were fired from – 10 mV to + 80 mV with + 10 mV step, maintaining 5 seconds each. Before recording, 0.3 mM $CdCl_2$ was added to external solution to block L-type Ca^{2+} channels. A pre-stimulating pulse of – 40 mV was applied to ensure inactivation of Na^+ channel and T-type Ca^{2+} channels.

2.3 Group and data analysis

I_K recorded in normal Tyrode solution were the control group. Five test groups included I_K recorded when the cells were for 20 minutes each immersed in drug of different concentrations from 0.1 μM to 1,000 μM. Data were noted as current density (pA/pF) (that is, current on each unit of membrane surface, I_K/C_m). I_K value came from real measurement using pClamp 6.0 Software (Axon Instrument); and C_m, the capacitance of cellular membrane which represents the superficial area, was calculated from formula $C_m = \tau \times I/V$, among which I(pA) stands for the amplitude of the capacity current, τ(ms) is for the attenuation constant of uncompensated capacitance current, and V(mV) is for a constant of 10 mV depolarization. In this experiment the mean membrane capacitance obtained was 61.12 pF ± 2.64 pF ($n = 30$), which is consistent with the published data[4].

All data were presented as mean ± SD. Difference significance was statistically determined by Student's t test ($\alpha = 0.05$). Statistical analysis was performed using Origin 6.0 Software.

3 Results

Sparfloxacine reduced the current amplitude of I_K. As shown in Figure 1, the comparison of current amplitudes before and after drug administration indicated that sparfloxacine had inhibitory effect on I_K (both peak current and tail current). The inhibition occurred steadily after the cells were exposed to drug superfusion more than 20 minutes. In the span of testing voltages the inhibitory capacity increased with the voltage steps, which can be observed from the I-V (current-voltage) curves (Figure 2). The compounds couldn't be easily washed-out.

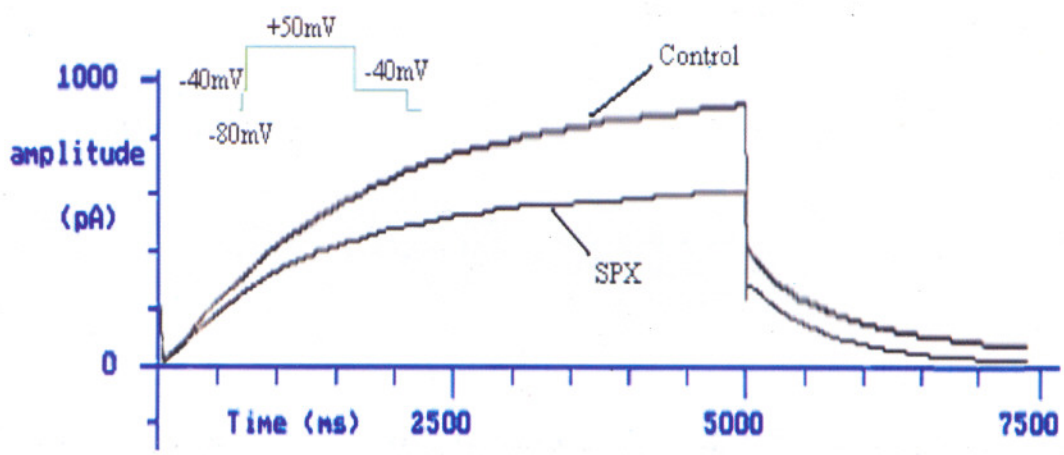

Figure 1. Inhibitory effect of sparfloxacine on I_K. Whole-cell I_K were elicited by a 5-second depolarizing pulse to + 50 mV from a holding potential of – 80 mV. Then potential was returned to – 40 mV to generate a large outward tail current. The effect of 100 μM sparfloxacine was displayed to reduce the I_K significantly ($P < 0.05$).

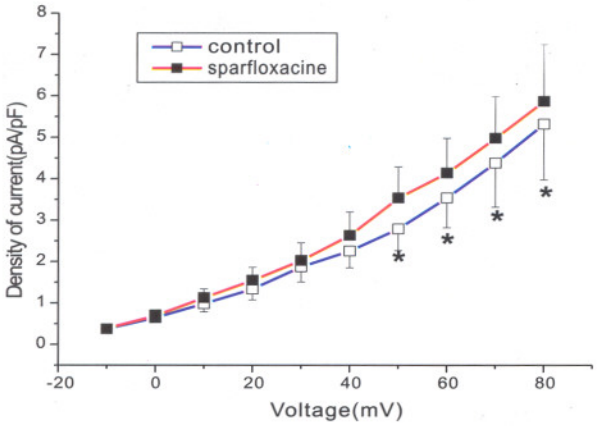

Figure 2. I-V curves of I_K

Cells were held at −80 mV and depolarized for 5 seconds to potentials ranging from −10 mV to +80 mV with +10 mV increments, and then returned to −40 mV to generate outward tail currents. Currents influenced with and without 100 μM sparfloxacine were measured and pictured. It showed that the inhibitory capacity increased with the voltage steps ($P<0.05$).

At +50 mV, I_K reduction (depressed rate) was calculated by dividing the depressed current value with the current amplitude of the control group. As listed in Table 1, in the concentration of 0.1 μM, the depressed rate of sparfloxacine on I_K peak current was (12.94 ± 3.09)%, and that of tail current was (7.66 ± 2.72)%. While the concentration increased to 10^4 times, depressed rates of I_K peak and tail currents reached to (38.40 ± 5.13)% and (60.64 ± 6.53)% separately, which were obviously different with those in low dose.

So concentration/response relationship was calculated by a non-linear squares fit of equation: $f = 1/(1 + (x/IC_{50})^{nH})$ to the data (Figure 3). Sparfloxacine inhibited I_K with an IC_{50} of 14.89 μM.

Table 1. Depressed rates of I_K impacted by different doses of sparfloxacine solutions(%)($n=25$)

0Concentration (μM)	$I_{K,step}$(%)	$I_{K,tail}$(%)
0.1	12.94 ± 3.09	7.66 ± 2.72
1	16.26 ± 2.21	10.03 ± 1.48
10	24.70 ± 2.78	17.78 ± 3.21
100	32.23 ± 3.19	32.90 ± 3.91
1000	38.40 ± 5.13	60.64 ± 6.53

4 Discussion

The results indicated that sparfloxacine did inhibit ionic current of I_K in even a relatively low concentration. I_K is a current conducted by two types of potassium channels-one is rapid activating channel; the other slow activating channel. In this study, two kinds of potassium channels had not been further identified, but surely one or both of them might be blocked by sparfloxacine, which led directly to abatement of I_K. Furthermore, sparfloxacine blocked I_K in a dose (concentration) dependent manner. The inhibitory impact occurred slightly in lower dose; with the raise of concentration, depressed effect could be greatly enhanced.

The QT interval is an electrocardiographic measurement of the period between ventricular depolarization and the completion of repolarization. The acquired form of the long QT interval syndromes is caused by various agents that reduce the magnitude of outward repolarizing K^+ currents, enhance inward depolarizing Na^+ or Ca^{2+} currents, thereby triggering the arrhythmia. The electrophysiological action of I_K blockade observed in this study, may translate into prolongation of the QT interval and then may predispose to development of torsades de pointes in clinic. According to the available reports, the fluoroquinolones in the market present a low risk of drug-induced QT prolongation, with a frequency approximately 0.2−2.7 per million prescriptions[5]. The safest member of the class appears to be ciprofloxacin[6]. Sparfloxacine represents comparably less secure one.

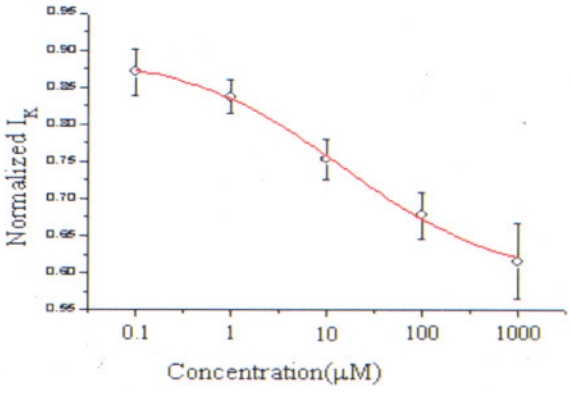

Figure 3. Concentration-response relationship of sparfloxacine response of peak currents at +50 mV was used to generate the concentration-response curve. The points represented the rates of remained currents to non-pressed ones. The slopes of the curves ranged from 87.06% for 0.1 μM to 61.60% for 1,000 μM.

Fortunately, judged from the relationship between drug concentration and inhibition response, the IC_{50} value of sparfloxacine was 14.89 μM, which fell far above the therapeutic peak concentration in patient blood (1.8 μM)[7]. So sparfloxacine is still reliable in clinical treatment of infection, ex-

cept that extra attention should be paid to the monitoring of electrocardiograph, especially when heavy dose is applied or excessive accumulation happens because of liver or kidney damage.

Correspondence to:
Zhao Zhang
Jiangsu Province Key Laboratory for Molecular Medical Biological Technique
College of Life Science
Nanjing Normal University
Nanjing, Jiangsu 210097, China
Email: nnuzhangzhao@163.com

References

1. Alexandrou AJ, Duncan RS, Sullivan A, *et al*. Mechanism of hERG K^+ channel blockade by the fluoroquinolone antibiotic moxifloxacin. Br J Pharmacol 2006; 147(8): 905 – 16
2. Kim EJ, Kim KS, Shin WH. Electrophysiological safety of DW-286a, a novel fluoroquinolone antibiotic agent. Hum Exp Toxicol 2005; 24(1):19 – 25
3. Xu YF, Dong PH, Zhang Z, *et al*. Presence of a calcium-activated chloride current in mouse ventricular myocytes. Am J Physiol Heart Circ Physiol 2002; 283 (1): H302 – 14.
4. Molecot CO, BitoV, Argibay JA. Rutheniurn red as an effective blocker of calcium and sodium currents in guinea pig isolated ventricular heart cells. British J Pharmacol 1998;124: 465 – 72.
5. Morganroth J, Talbot GH, Dorr MB, *et al*. Effects of single ascending, supratherapeutic doses of sparfloxacin on cardiac repolarization (QTc interval). Clin Ther 1999;21(5):818 – 28
6. Morganroth J, Hunt T, Dorr MB, *et al*. The cardiac pharmacodynamics of therapeutic doses of sparfloxacin. Clin Ther 1999; 21:1171 – 81.
7. Kang J, Wang L, Chen XL, *et al*. Interactions of a series of fluoroquinolone antibacterial drugs with the human cardiac K^+ channel HERG. Mol Pharmacol 2001; 59: 122 – 6.

Received June 18, 2006

A Survey of Human Myocarditis Cases Diagnosed Using Alexa Immunofluorescence Dyes and Confocal Microscopy

George E Sandusky, Jennifer C Offen, Michael A Clark

Department of Pathology and Laboratory Medicine, Indiana University School of Medicine, Indianapolis, Indiana, USA

Abstract: Sudden death as a result of viral myocarditis is a rare but distressing event because it usually occurs in young healthy individuals. Myocarditis is a relatively common complication of viral infections. Specifically, enteroviruses, influenza viruses and adenoviruses have been associated with this disease. In many cases the etiology remains unknown when routine methods are used for diagnosis. With the advent of new molecular techniques such as RT-PCR, stronger amplification techniques such as Alexa dyes for immunofluorescence, and confocal microscopy for reduction of background staining, some of these viruses can be identified. The incidence, clinical history, grosses and microscopic pathology were examined in 22 myocarditis cases that died suddenly. Viral identification was performed on sections from all 22 hearts by Alexa immunofluorescence with confocal microscopy. Influenza A, Coxsackie 3, and Coxsackie 5 were evaluated on all 22 hearts. Cell culture controls transfected with the virus were used as positive controls. One of 22 patients was positive for Influenza A. Six cases were positive for Coxsackie B5, two of which were also positive for Coxsackie B3. Fifteen cases were negative for all antibodies examined. [Life Science Journal. 2006;3(4):37-41] (ISSN: 1097-8135).

Keywords: myocarditis; viral; sudden death

1 Introduction

For the past two centuries, myocarditis has been classified as an inflammatory disease of the myocardium (Carthy, 1997; Feldman, 2000; Bergler-Klein, 2001; Calabrese, 2003). The natural history and pathogenesis is largely still unknown (Hyypia, 1993; Feldman, 2000; Noutsias, 2003). The disease is often fatal and diagnosed on post mortem autopsy (Waller, 1992; Lopes, 2001; Mounts, 2001; Weissel, 2001). The common etiologies are idiopathic, autoimmune and infectious (Furukawa, 2001; Hill, 2001; Leonard, 2004; Pauschinger, 2004; Whitton, 2004). Viral agents, especially the Coxsackie B viruses, are commonly associated with fatal myocarditis (Hyypia, 1993; Carthy, 1997; Feldman, 2000). Other viruses less commonly associated with fatal myocarditis have been Parvovirus (Murry, 2001), Influenza A (Nolte, 2000) and B (Engblom, 1983), Hepatitis C (Matsumori, 2001), HIV, Mumps virus, Cytomegalovirus, Adenovirus (Lozinski, 1994), Echovirus, Poliovirus, and Infectious mononucleosis (Fournier, 2001; Weissel, 2001; Leonard, 2004). In most of the reported studies, only about 20% to 37% of the cases have a definitive viral diagnosis.

Myocarditis has been viewed as the acute stage in the progression of disease leading to heart failure and cardiomyopathy (D'Ambrosio, 2001; Furukawa, 2001; Calabrese, 2003; Mason, 2003; Noutsias, 2003; Whitton, 2004). Generally, myocarditis is viewed histologically as sparse, focal, or diffuse inflammation of the heart associated with focal to multifocal cardiac myocyte necrosis. In end-stage idiopathic cardiomyopathy, the histologic pattern is focal to diffuse myocyte hypertrophy and multifocal to diffuse interstitial fibrosis (Vasiljevic, 2001). In one study using PCR techniques, Hepatitis C was found in a few cases of idiopathic cardiomyopathy (Pauschinger, 2004).

In this study, we report the immunofluorescence analysis using Alexa immunofluorescence amplification of 22 individual cases of fatal myocarditis over a period of 1985 to 2001. As with previous studies, we found a definitive viral etiology in 31% of the cases examined.

2 Materials and Methods

2.1 Tissue specimens

All tissue specimens were retrieved from the Tissue Bank of Indiana University Medical Center Department of Forensic Pathology. All heart specimens were collected from autopsy cases obtained during the period extending from 1985 to 2001. Nine of these cases were collected in the winter of 1997-1998. Three normal cases were used as negative control samples. The samples were selected based on the presence of inflammation after a review by two pathologists using Hematoxylin and

Eosin stained slides. For each of the hearts, two to three histological sections of the left ventricle were examined and at least one section involved a left ventricular papillary muscle.

2.2 Antibodies

The following antibodies were used for immunohistochemistry:

Coxsackie B5 (Chemicon Temecula, Ca)

Coxsackie B3 (Chemicon Temecula, Ca)

Influenza A monoclonal (Chemicon, Temecula, Ca)

2.3 Tissue preparation

Tissues were fixed overnight in 10% neutral buffered formalin and then transferred to 70% ethanol prior to processing through paraffin. Five-micron sections were microtomed, and the sections were placed on positive charged slides. The slides were then baked overnight at 60 ℃ in an oven.

2.4 Immunostaining

The slides were then deparaffinized in xylene and rehydrated through graded alcohols to water. Antigen retrieval was performed by immersing the slides in target retrieval solution (Dako) for 20 minutes at 90 ℃ in a water bath, cooling at room temperature for 10 minutes, washing in water and then proceeding with immunostaining. All subsequent staining steps were performed on the Dako immunostainer. Incubations were done at room temperature. Tris buffered saline plus 0.05% Tween 20, pH 7.4 (TBS - Dako Corp.) was used for all washes and diluents. Thorough washing was performed after each incubation. Slides were blocked with protein blocking solution (Dako) for 45 minutes. After washing, 5 μg/ml of the primary antibodies were added to the slides, and then incubated overnight at room temperature. The secondary antibody, Alexa anti-mouse or anti-rabbit fluorescent dye (Molecular Probes, Eugene OR) was added for 1 hour (Panchuk-Voloshina, 1999). The slides were washed, coverslipped and examined.

2.5 Confocal microscopy

A Bio-Rad MRC-1024ES confocal microscope equipped with a krypton/argon laser and a 60×1.4 numerical aperture objective was used to examine the hearts and obtain images. For each heart, the negative control was used to establish a pixel intensity that eliminated 99% of the background signal. Background fluorescence was then subtracted by applying this threshold to all images, and the percent pixels with the remaining signal and average signal intensity were recorded for each image.

2.6 Slide evaluation

Two investigators using a fluorescence microscope to evaluate the intensity and localization of the staining reviewed the slides. Staining was defined as negative (total absence of staining), 1+ (weak staining), 2+ (moderate), or 3+ (strong, intense staining).

3 Results

Histologic examination showed the inflammatory infiltrate to consist of macrophages and plasma cells without neutrophils. No acute inflammation was observed in any case. The inflammatory lesions were focal in the majority of cases and multifocal to diffuse in a few cases. Some cases were severe and diffuse, going transmural from the endocardium to the epicardial surface such as case number 18 (Figure 1). In this case all multiple histologic sections of the left ventricular myocardium were involved (six sections from different LV areas), and there was severe myodegeneration and myocytolysis. Most cases showed evidence of myofiber degeneration. See Table 1 for histologic scoring of the lesions.

Immunofluorescence revealed strong staining with Coxsackie B5 antibody in 6 of the 22 cases, two of which also stained with the Coxsackie B3 antibody. One case out of the 22 stained with the Influenza A antibody. Table 2 summarizes the immunofluorescence in the myocarditis cases with the three antibodies examined. The cell culture specimens used as positive controls were positive with the specific antibodies and did not cross-react to different antibodies against other viruses. The normal human myocardial cases did not stain with any of the viral antibodies.

The immunolocalization of the Coxsackie antibodies were generally confined to degenerating myocardial cells from sections in the left ventricle (Figure 2). There was no antibody staining with any of the antibodies in normal human heart tissues. Degenerating myocardial cell cytoplasm was distinctly stained with the three antibodies in the myocarditis cases. Occasionally the nucleus was stained with some of the antibodies.

In the one influenza myocarditis case, there was staining of lymphocytes and monocytes in the blood vessels within the myocardium in addition to the degenerating myocytes (Figure 3).

Table 1. Histological assessment of myocardium

Case #	Tissue	Inflammatory infiltrate	Myocyte necrosis	Fibrosis	Diagnosis
1	Heart	2	...	0	Myocarditis
2	Heart	3		1	Acute viral myocarditis
3	Heart	3		0	Viral myocarditis
4	Heart	1		0	Myocarditis
5	Heart	0		2	Myocarditis
6	Heart	1	1	2	Myocarditis
7	Heart	3	2	0	Acute myocarditis
8	Heart	2	1	0	Acute myocarditis
9	Heart	3		1	Viral myocarditis (childe sexual abuse)
10	Heart	2		0	Viral myocarditis
11	Heart	0		1	Viral myocarditis
12	Heart	0		0	Myocarditis
13	Heart	3		2	Myocarditis (lymphocytic, plasmacytic)
14	Heart	1		1	Myocarditis
15	Heart	1		0	Viral myocarditis and viral encephalitis
16	Heart	1		0	Resolving viral myocarditis
17	Heart	1		1.5	Eonsinophilic myocarditis
18	Heart	4	4	0	Myocarditis
19	Heart	1		0	Myocarditis
20	Heart	2	0	0	Acute myocarditis
21	Heart	3 F	0	3 F	Giant cell myocarditis
22	Heart	2		0	Myocarditis

Table 2. Immunofluorescence of viral antigens in heart

Case #	Tissue	Coxsackie B3	Coxsackie B5	Influenza A mono
1	Heart	Negative	2+ myocytes	Negative
2	Heart	Negative	Negative	Negative
3	Heart	Negative	2+ myocytes	Negative
4	Heart	Negative	Negative	Negative
5	Heart	Negative	Negative	Negative
6	Heart	Negative	Negative	endothelial
7	Heart	1+ myocytes	1+ myocytes	endothelial
8	Heart	Negative	Negative	Negative
9	Heart	Negative	3+ myocytes	Negative
10	Heart	1+ myocytes	2+ myocytes	1.5+ lymphocytes
11	Heart	Negative	2+ myocytes	Negative
12	Heart	Negative	Negative	Negative
13	Heart	Negative	Negative	2+ endothelial/macrophage
14	Heart	Negative	Negative	Negative
15	Heart	Negative	Negative	Negative
16	Heart	Negative	Negative	Negative
17	Heart	Negative	Negative	Negative
18	Heart	Negative	Negative	2+ myocytes
19	Heart	Negative	Negative	Negative
20	Heart	Negative	Negative	Negative
21	Heart	Negative	Negative	Negative
22	Heart	Negative	1+ endothelial	1.5+ macrophage

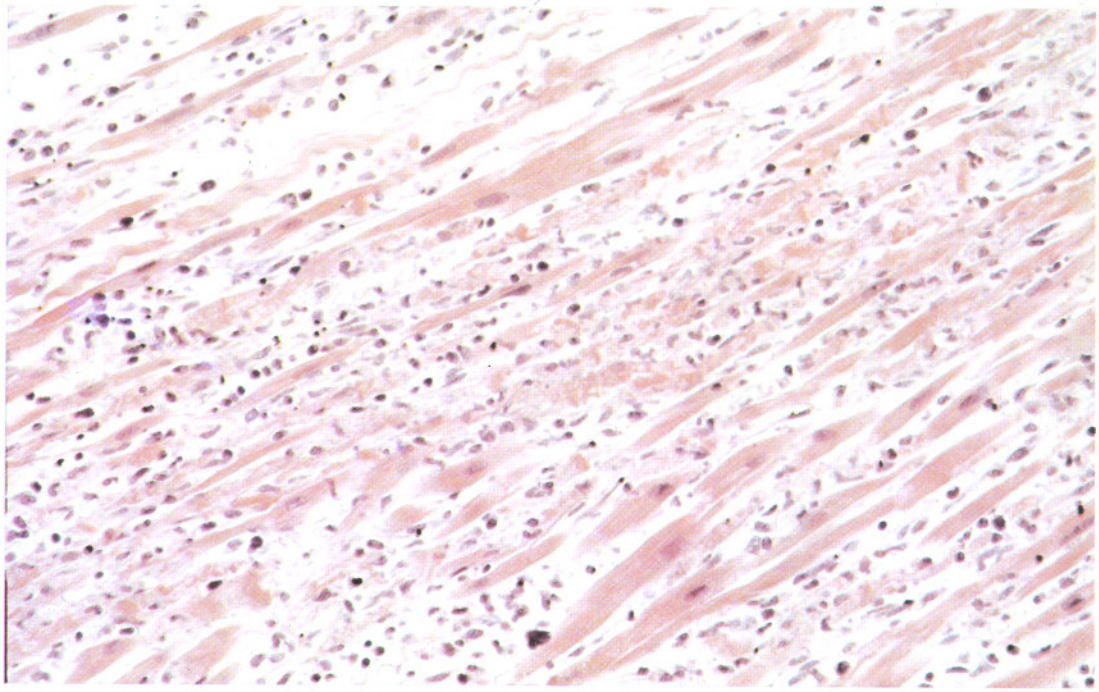

Figure 1. Hematoxylin and Eosin stain on case 18

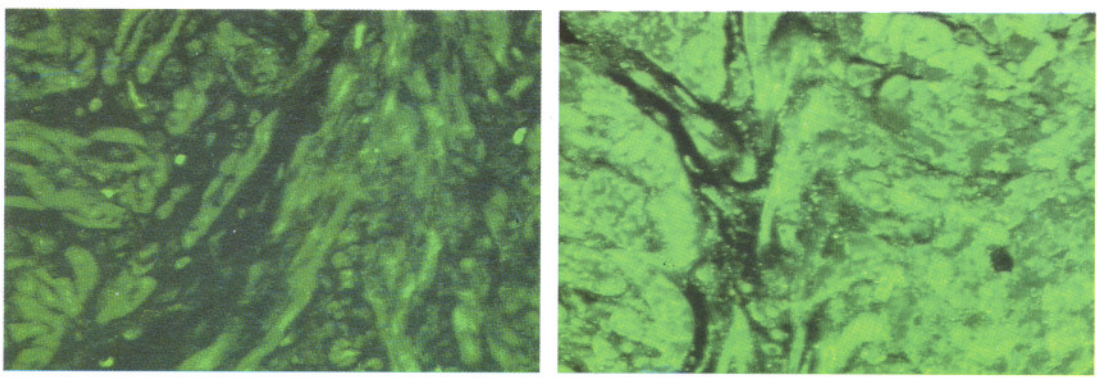

Figure 2. Coxsackie B5 antibody on case 9 (right). Negative control without antibody on case 9 (left).

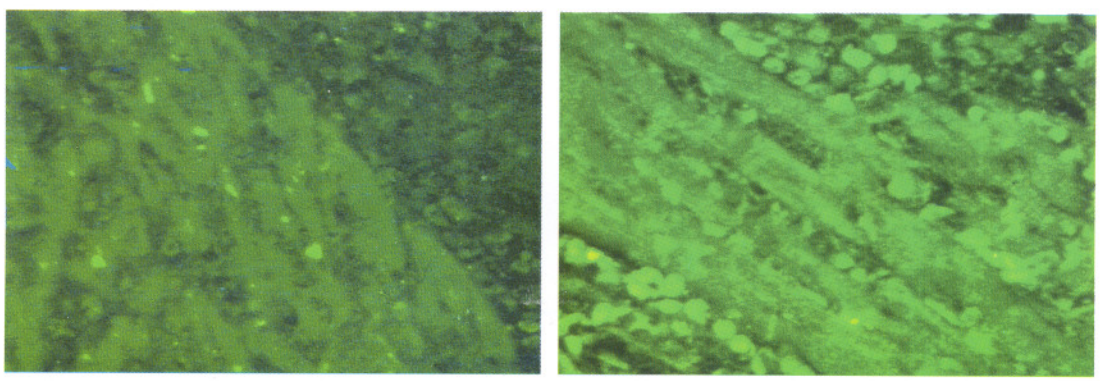

Figure 3. Influenza A antibody on case 18 (right). Negative control without antibody on case 18 (left).

Generally, the surrounding connective tissue stroma, blood vessel smooth muscle, endothelial cells, and associated inflammatory cells in and around the areas of active myocarditis lesions were

not stained with any of the antibodies examined. However, staining was seen in elastic tissue in small arteriole muscular arteries within the myocardium in most cases.

4 Discussion

In this survey we found that about 31% of the cases were positive for viral etiology. This is similar to previous review studies and studies involving collections of human viral myocarditis cases (Hyypia, 1993; Feldman, 2000). Just a few case reports on Influenza A have been reported (Engblom, 1983; Nolte, 2000). This acute case in our survey was very severe, with a severe transmural myocyte degeneration, necrosis, and inflammation.

In this study we used confocal microscopy to evaluate the myocarditis with the new Alexa dyes. These antibodies required long antigen retrieval pretreatment with the Dako antigen retrieval solution in a 90-degree water bath for 25 minutes to obtain reasonable immunofluorescence staining.

The procedure involved long overnight incubation with the Alexa amplification technique to be able to visualize any staining. The confocal microscope allowed us to remove any background scatter fluorescence to see a strong positive signal.

In summary, this survey was similar to previous studies reported in the literatures. This is the first report using confocal microscopy to evaluate human cases of myocarditis.

Correspondence to:
George Sandusky
Lilly Research Labs
Bldg 98, DC0424
Indianapolis, Indiana 46285
Telephone: 317-277-4631
Fax: 317-276-6510
Email: gsandusk@iupui.edu

References

1. Bergler-Klein J, Stanek G. Myocarditis. N Engl J Med 2001;344(11):857; author reply 858.
2. Calabrese F, Thiene G. Myocarditis and inflammatory cardiomyopathy: microbiological and molecular biological aspects. Cardiovasc Res 2003;60(1):11-25.
3. Carthy CM, Yang D, Anderson DR, *et al*. Myocarditis as systemic disease: new perspectives on pathogenesis. Clin Exp Pharmacol Physiol 1997;24(12):997-1003.
4. D'Ambrosio A, Patti G, Manzoli A, *et al*. The fate of acute myocarditis between spontaneous improvement and evolution to dilated cardiomyopathy: a review. Heart 2001;85(5):499-504.
5. Engblom E, Ekfors TO, Meurman OH, *et al*. Fatal influenza A myocarditis with isolation of virus from the myocardium. Acta Med Scand 1983;213(1):75-8.
6. Feldman AM, McNamara D. Myocarditis. N Engl J Med 2000;343(19):1388-98.
7. Fournier PE, Etienne J, Harle J, *et al*. Myocarditis, a rare but severe manifestation of Q fever: report of 8 cases and review of the literature. Clin Infect Dis 2001; 32(10):1440-7.
8. Furukawa Y, Kobuke K, Matsumori A. Role of cytokines in autoimmune myocarditis and cardiomyopathy. Autoimmunity 2001;34(3):165-8.
9. Hill SL, Rose NR. The transition from viral to autoimmune myocarditis. Autoimmunity 2001; 34(3): 169-76.
10. Hyypia T. Etiological diagnosis of viral heart disease. Scand J Infect Dis Suppl 1993;88:25-31.
11. Leonard EG. Viral myocarditis. Pediatr Infect Dis J 2004;23(7):665-6.
12. Lopes Rocha JL. Myocarditis. N Engl J Med 2001;344(11):857-8.
13. Lozinski GM, Davis GG, Krous HF, *et al*. Adenovirus myocarditis: retrospective diagnosis by gene amplification from formalin-fixed, paraffin-embedded tissues. Hum Pathol 1994;25(8):831-4.
14. Mason JW. Myocarditis and dilated cardiomyopathy: an inflammatory link. Cardiovasc Res 2003;60(1):5-10.
15. Matsumori A. Hepatitis C virus and cardiomyopathy. Intern Med 2001;40(2):78-9.
16. Mounts AW, Amr S, Jamshidi R, *et al*. A cluster of fulminant myocarditis cases in children, Baltimore, Maryland, 1997. Pediatr Cardiol 2001;22(1):34-9.
17. Murry CE, Jerome KR, Reichenbach DD. Fatal parvovirus myocarditis in a 5-year-old girl. Hum Pathol 2001;32(3):342-5.
18. Nolte KB, Alakija P, Oty G, *et al*. Influenza A virus infection complicated by fatal myocarditis. Am J Forensic Med Pathol 2000;21(4):375-9.
19. Noutsias M, Pauschinger M, Poller WC, *et al*. Current insights into the pathogenesis, diagnosis and therapy of inflammatory cardiomyopathy. Heart Fail Monit 2003;3(4):127-35.
20. Panchuk-Voloshina N, Haugland RP, Bishop-Stewart J, *et al*. Alexa dyes, a series of new fluorescent dyes that yield exceptionally bright, photostable conjugates. J Histochem Cytochem 1999;47(9):1179-88.
21. Pauschinger M, Chandrasekharan K, Noutsias M, *et al*. Viral heart disease: molecular diagnosis, clinical prognosis, and treatment strategies. Med Microbiol Immunol (Berl) 2004;193(2-3):65-9.
22. Vasiljevic JD, Popovic ZB, Otasevic P, *et al*. Myocardial fibrosis assessment by semiquantitative, point-counting and computer-based methods in patients with heart muscle disease: a comparative study. Histopathology 2001;38(4):338-43.
23. Waller BF, Catellier MJ, Clark MA, *et al*. Cardiac pathology in 2007 consecutive forensic autopsies. Clin Cardiol 1992;15(10):760-5.
24. Weissel M. Myocarditis. N Engl J Med 2001;344(11):857; author reply 858.
25. Whitton JL, Feuer R. Myocarditis, microbes and autoimmunity. Autoimmunity 2004;37(5):375-86.

Received July 6, 2006

Cloning and Sequence Analysis of Adhesion Gene *hpaA* of *Helicobacter pylori*

Xueyong Huang[1,2], Yi Ren[3], Guangcai Duan[1,2], Qingtang Fan[2], Yuanlin Xi[1], Zhigang Huang[1,2], Chunhua Song[1]

1. *Department of Epidemiology, College of Public Health, Zhengzhou University, Zhengzhou, Henan 450052, China*
2. *Henan Key Laboratory of Molecular Medicine, Zhengzhou, Henan 450052, China*
3. *Department of Labor and Environmental Health, College of Public Health, Zhengzhou University, Zhengzhou, Henan 450052, China*

Abstract: Objective. To clone the adhesion gene *hpaA* of *Helicobacter pylori* strain MEL-Hp27 isolated from a patient in Zhengzhou City, and analyze the *hpaA* gene nucleotide and putative amino acid sequences. **Methods.** *hpaA* gene of the *Helicobacter pylori* MEL-Hp27 was amplified by PCR. After purified, the target fragment was cloned into plasmid pBluescriptb Ⅱ and subject to nucleotide sequenced. The homologies of the nucleotide and putative amino acid sequences of *hpaA* were respectively analyzed. **Results.** *hpaA* gene of 783 bp, encoding the polypeptides of 260 amino acids, was obtained from the *Helicobacter pylori* strain MEL-HP27 genomic DNA. The homologies of the nucleotide and putative amino acid sequences compared with the published *hpaA* gene sequences were 94.76% – 97.19% and 95.38% – 98.46%, respectively. **Conclusions.** The recombined plasmid carring *hpaA* gene has been successfully constructed, and sequence analysis indicates that *hpaA* is a highly conserved prokaryotic gene and might be a potential candidate for *Helicobacter pylori* vaccine development. [Life Science Journal. 2006;3(4):42 – 48] (ISSN: 1097 – 8135).

Keywords: *Helicobacter pylori*; *hpaA* gene; cloning; sequence analysis

Abbreviations: HpaA: *Helicobacter pylori* adhesion; MALT: mucosa associated lymphoid tissue

1 Introduction

Helicobacter pylori is one of the common gram-negative bacteria causing chronic infection, which infects more than 50% of the human population. Infection of the gastric mucosa with *Helicobacter pylori* results in a number of disease outcomes including gastritis, which precedes the development of peptic ulcer disease, gastric cancer and lymphomas of the mucosa associated lymphoid tissue(MALT)[1,2]. Although significant progress has been made in treating *Helicobacter pylori* infection with current triple or quadruple therapy based on antibiotics, given in conjunction with bismuth compounds and proton pump inhibitor, the limitations of pharmacological therapy such as side effects, poor compliance, high cost, and most importantly, rapid emergence of antibiotic resistance have set the stage for the development of less costly and more efficient means to prevent and control *Helicobacter pylori* infections[3,4]. Immunization against the bacterium represents a cost-effective strategy to prevent *Helicobacter pylori* infection, the selection of antigenic targets is critical in the design of *Helicobacter pylori* vaccine[5]. *Helicobacter pylori* adhesion(HpaA) is a flagellar sheath protein with approximately 29 kDa located in the bacterial outer membrane[6]. So in this study, the recombinant plasmid inserted with *hpaA* of *Helicobacter pylori* was constructed and the homologies of the nucleotide and putative amino acid sequences were respectively analyzed, which will be helpful for determining whether the HpaA becomes one of the good candidates as an antigen in *Helicobacter pylori* vaccine.

2 Materials and Methods

2.1 Materials

The strain MEL-HP27 of *Helicobacter pylori* and cloning pBluescriptb Ⅱ were preserved by our laboratory, *E. coli* strains JM109 were purchased from New England Biolabs (Beijing) LTD (Beijing China). Pyrobest DNA polymerase, restriction endonuclease enzymes (*Bam*HI, *Hind* Ⅲ), T4 DNA

ligase, DNA gel extraction kit and 100 bp DNA marker were provided by TaKaRa Company (Dalian, China).

2.2 Bacterial culture and preparation of DNA template

Helicobacter pylori MEL-HP27 strains were grown on solid Columbia agar with 100 ml/L frozen-melting sheep blood, 50 ml/L fetal bovine serum, and antibiotic supplement (vancomycin 10 mg/L, polymyxin B 0.33 mg/L, amphotericin A 5 mg/L, trimethoprim 5 mg/L) in a microaerophilic atmosphere for 3 days to 4 days at 37 °C.

The *Helicobacter pylori* strains were harvested and suspended in 1 ml sterile normal saline and pelleted by centrifugation at 10,000 g for 5 minutes. The precipitate was resuspended in lysis buffer (10 mM Tris-HCl, pH 8.0, 0.1 M EDTA, pH 8.0, 0.5 % (w/v) SDS, 20 μg/ml RNase), and then, protease K was added in to a final concentration of 100 μg/ml, the lysate was incubated in a water bath at 42 °C for 2 hours. The solution was cooled to room temperature, and mixed with an equal volume of phenol equilibrated. The two phases were separated by centrifugation at 10,000 g for 10 minutes at room temperature, and the aqueous phase was extracted with phenol twice again. Afterwards, 0.1 volume of 2.5 M ammonium acetate and 2 volume of ethanol were added to the aqueous phase. The precipitate was collected by centrifugation at 10,000 g for 2 minutes, washed twice with 70% ethanol, and dissolved in an appropriate volume of TE buffer (pH 8.0)[7,8]. The DNA concentration was measured by ultraviolet spectrophotometry.

2.3 Synthetic primers and PCR

Oligonucleotide primers were designed to amplify *hpaA* gene from *Helicobacter pylori* strain MEL-HP27 based on the published corresponding genome sequence of 26695 and J99. The sequence of sense primer with a restriction endonuclease site of *Bam* HI was: 5′-CGGGATCCATGAAAGCAA ATAATC-3′. The sequence of antisense primer with a restriction endonuclease site of *Hind* Ⅲ was: 5′-CGCAAGCTTTTATCGGTTTCT-3′. PCR was performed in a 50 μl reaction mixture in 0.6 ml tube in an automatic thermal cycler. The PCR mixture contained 5 μl of 10×PCR buffer, 2.5 μl of sample DNA, 4 μl of 2.5 mmol/L deoxynucleoside triphoshpate, 2 μl of 0.25 μmol/L oligonucleotide primers, 0.5 μl Pyrbest DNA polymerase (1.25 U), 34 μl of MilliQ H_2O. The parameters for PCR were as follows: 95 °C for 5 minutes, 1 cycle; 94 °C for 60 seconds, 45 °C for 50 seconds, 72 °C for 50 seconds, 30 cycles; 72 °C for 10 minutes, 1 cycle. The amplified products (3 μl) were observed by electrophoresis on 10 g/L agarose gel containing 0.1 μg of ethidium bromide per ml in TBE buffer. The PCR product was visualized under UV light and photographed.

2.4 Construction of recombinant plasmids

PCR products were digested by restriction endonucleases *Bam*HI and *Hind* Ⅲ, meanwhile pBluescriptb Ⅱ plasmid was digested by *Bam*HI and *Hind* Ⅲ, too. The target fragments of *hpaA* and pBluescriptb Ⅱ were recovered by DNA gel extraction kit, and then these two fragments were ligated by using T4 DNA ligase at a molar ratio of 6:1 at 16 °C for 12 hours. The recombinant plasmid was transformed into *E. coli* JM109. The *E. coli* JM109 containing the recombinant plasmid was amplified in LB solid medium containing ampicillin (100 mg/L). Clones were picked out randomly through blue/white screening and cultivated in 4 ml LB medium containing 100 mg/L of ampicillin, at 200 r/min at 37 °C overnight. Finally the recombinant plasmids were extracted by Sambrook's method and identified by PCR and restriction endomuclease enzyme digestion.

2.5 Sequence determination and homology analysis

The sequence determination of *hpaA* gene of recombinant plasmid was carried out by Shanghai DNA Biotechnologies Company (China), in the meantime, the sequence of *hpaA* gene and amino acid were analyzed by software Omiga. 2.0 and DNAmen, and compared the homology based on the GenBank (No. NC000915, strain 26695; No. NC000921, strain J99; No. X92502, strain 11637; No. AF479028, strain CH-TX1; No. U35455, strain CCUG 17874; No. X61574, strain 8826; No. DQ115385, strain K51; No. AY714223, strain Y06).

3 Results

3.1 PCR amplification of *hpaA* encoding sequence

The *hpaA* of MEL-HP27 strain was amplified by PCR from the above primers. The PCR product was electrophoresed and visualized by 10 g/L agarose gel (Figure 1). It revealed that the size of *hpaA* DNA fragment amplified by PCR was 783 bp, and was compatible with the expectant size.

3.2 Construction and identification of recombinant plasmids

Recombinant plasmid pBluescriptb Ⅱ-hpaA was digested with *Bam*HI and *Hind* Ⅲ and confirmed by PCR, then digestive product and PCR product were visualized on 10 g/L agarose gel (Figure 2). It demonstrated that recombinant plasmid was digested to 3,000 bp and 783 bp DNA fragment, which contained the objective gene, and

hpaA gene was amplified from the recombinant plasmid by PCR.

3.3 Sequence analysis

Sequencing results showed that the *hpaA* gene consists of 783 base pairs and encodes the polypeptides of 260 amino acids. The sequencing results of *hpaA* from strain MEB-HP27 are published in the

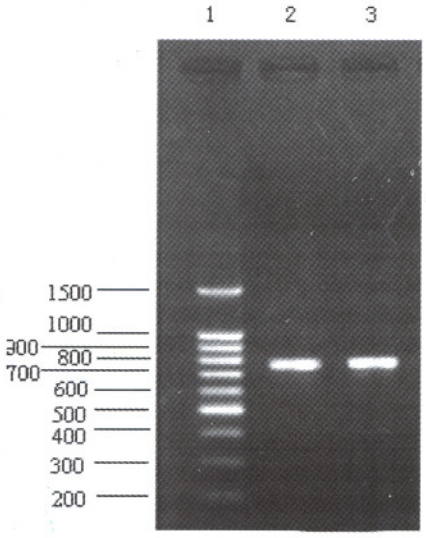

Figure 1. The result of *hpaA* gene amplification using PCR Lane 1:100 bp DNA ladder; Lane 2 and Lane 3: PCR product of *hpaA* gene.

GenBank, the accession number is DQ353891. The homologies of the nucleotide and putative amino acid sequences compared with eight published *hpaA* gene sequences were 94.76% – 97.19% and 95.38% – 98.46%, respectively (Figures 3, 4). The strain MEL-HP27 was quite identical to NCTC11637 than the others with nucleotide homologies of 97.19%, and the amino acid identity was 97.31% against NCTC11637. There are only 22 base pairs different between MEL-HP27 and NCTC11637, at 62nd site codon AAG/N→AGG/R, at 100th site codon AAT/N→AGC/S, at 112th site codon GCG/A→TCG/S, at 124th site codon AGT/S→AAT/N at 137th site codon ACA/T→ATA/I, at 164th site codon ATC/I→GCT/V, at 256th site codon AAC/N→GGC/G (codon/amnio acid). These analysis indicated that the *hpaA* gene sequence and the putative amino acid sequence were quite conservative and might be a potential antigen candidate for *Helicobacter pylori* vaccine development.

4 Discussion

Helicobacter pylori adhesion is a flagellar sheath potein located in the bacterial outer membrane. The outer membrane is a continuous structure on the surface of gram-negative bacteria, which have bilateral particular significance as a potential target for protective immunity and bacterial pathogens[9,10]. In other studies, outer membrane vaccines have been used with considerable success to induce protection against a number of organisms[4,11]. The *hpaA* gene is located in genome DNA of *Helicobacter pylori* and considerably conservative for its nucleotide and amino acid sequences. HpaA is one of the major structural outer membrane proteins of *Helicobacter pylori* and plays an important role in adhesion of the microbe[12,13]. Furthermore, antibody against HpaA almost could be found in all *Helicobacter pylori* infected patients sera, which will be an ideal antigen candidate for *Helicobacter pylori* vaccine. In this study, the *hpaA* gene was cloned from strain MEL-HP27, which consists of 783 base pairs and encodes the polypeptides of 260 amino acids. The homologies of the nucleotide and putative amino acid sequences of *hpaA* gene from *Helicobacter pylori* strain MEL-HP27 compared with the 8 published *hpaA* gene sequences were as high as 94.25% – 97.32% and 95.38% – 98.46%, respectively. These data indicate that the mutation level of the *hpaA* gene of *Helicobacter pylori* strain MEL-HP27 is within the range reported by GenBank, and suggest that HpaA is an excellent and ideal antigen for developing *Helicobacter pylori* vaccine.

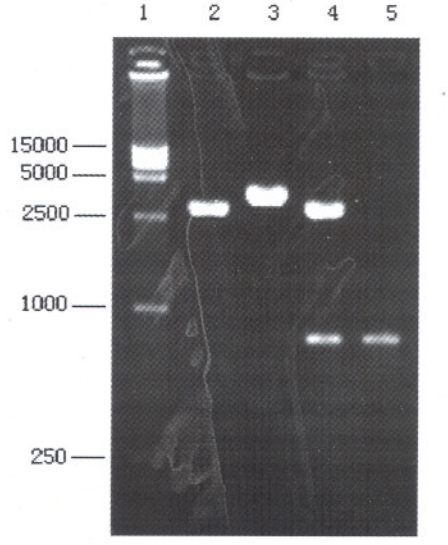

Figure 2. Identification of recombinant plasmid pBluescript-hpaA by restriction enzyme digestion
Lane 1: 15000bp DNA ladder; Lane 2: pBluescriptb Ⅱ digested by *Bam*HI and *Hind* Ⅲ; Lane 3: pBluescript-hpaA digested by *Hind* Ⅲ; Lane 4: pBluescript-hpaA digested by *Bam*HI and *Hind* Ⅲ; Lane 5: *hpaA* gene amplified by PCR from recombinant plasmid pBluescript-hpaA.

```
MEL-HP27    ATGAAAGCAAATAATCATTTTAAAGATTTTGCATGGAAAAAATGCCTTTT   50
26695       --------------------------------------------------   50
J99         ------a-----gg---------g--------------------t----   50
11637       ----g---------------------------------------------   50
CH-CTX1     ------a-----gg---------g--------------------------   50
CCUG17874   ------a-----gg---------g--------------------------   50
8826        ------a-----gg---------g--------------------------   50
K51         --------------------------------------------------   50
Y06         ----g---------------------------------------------   50

MEL-HP27    AGGCGCGAGCGTGGTGGCTTTGTTAGTGGGATGCAGTCCGCATATTATTG   100
26695       ---t----------------------------------c----------   100
J99         --------------------a--------g--t--c--------------   100
11637       --------------------a-------------c--------------   100
CH-CTX1     ---------t----------a-------------c--------------   100
CCUG17874   ------------gc-----a-------------c--------------   100
8826        ----a---------------a--------g-----c--------------   100
K51         ---t----------------------------c--------------   100
Y06         ----------------------g----------c--------------   100

MEL-HP27    AAACCAATGAAGTCGCTTTGAAATTGAATTACCATCCAGCTAGCGAGAAA   150
26695       --------------------------------------------------   150
J99         ------------t-------------------------------------   150
11637       --------------------------------------------------   150
CH-CTX1     --------------------------------------------------   150
CCUG17874   ---------------------g----------------------------   150
8826        ---------g-----------------------------------------g   150
K51         --------------------------------------------------   150
Y06         --------------------------------------------------   150

MEL-HP27    GTTCAAGCGTTAGATGAAAAGATTTTACTTTTAAAGCCAGCTTTTCAATA   200
26695       ----------------------------g-------g---------------   200
J99         ----------------------------------g---------c-----   200
11637       ----------------------------g-------g---------c-----   200
CH-CTX1     ----------------------------g-------g---------c-----   200
CCUG17874   ----------------------------g-------g---------------   200
8826        ----------------------------g-----------------c-----   200
K51         ----------------------------g-------g---------------   200
Y06         ------------------------c--g-------g---------------   200

MEL-HP27    CAGCGATAATATTGCTAAAGAGTATGAAAACAAATTCAAGAATCAAACCG   250
26695       --------------------------------------------------   250
J99         ----------------------------------------------------a   250
11637       t----------c-------------------------------------   250
CH-CTX1     --------------------------------------------------   250
CCUG17874   --------------------------------------------------   250
8826        ---------c--------------------t------------------a   250
K51         --------------------------------------------------   250
Y06         ----------------------------------------------------a   250

MEL-HP27    CGCTCAAGGTTGAACAGATTTTGCAAAATCAGGGCTATAAGGTTATTAAT   300
26695       ----------------------------------------------gc   300
J99         ----t--a------g----c--------------------------------   300
11637       ------------------------------a-----------------gc   300
CH-CTX1     ------------------------------------c--------c---   300
CCUG17874   t-------------------------------------------------   300
8826        ----t--a------g----c-----------------c--------c---   300
K51         ----------------------------------------------gc   300
Y06         ----t---------g----c-----------a----------------gc   300

MEL-HP27    GTAGATAGCAGCGATAAAGACGATCTTTCTTTTGCGCAAAAAAAAGAAGG   350
26695       ------------------------------t-----------------   350
J99         --g---------------------t--------------------------   350
11637       ------------------------t----------a---------------   350
CH-CTX1     --g-----t---------------t--------------------------   350
CCUG17874   --g---------------------t--------------------------   350
8826        --g---------------------t--------------------------   350
K51         ------------------------------t-----------------   350
Y06         ------------------------------t-----------------   350

MEL-HP27    GTATTTGGCCGTTGCTATGAGTGGCGAAATTGTTTTACGCCCCGATCCTA   400
26695       ---------t----------a--------------------------   400
J99         -------*--t--c-------a--------------------------   400
11637       ---------g----------a--------------------------   400
CH-CTX1     ---------g----------a--------------------------   400
CCUG17874   ---------t--c-------a---t----------------------   400
8826        ---------g----------t--------------------------   400
K51         ---------t----------a--------------------------   400
Y06         ------------c-------a--------------------------   400
```

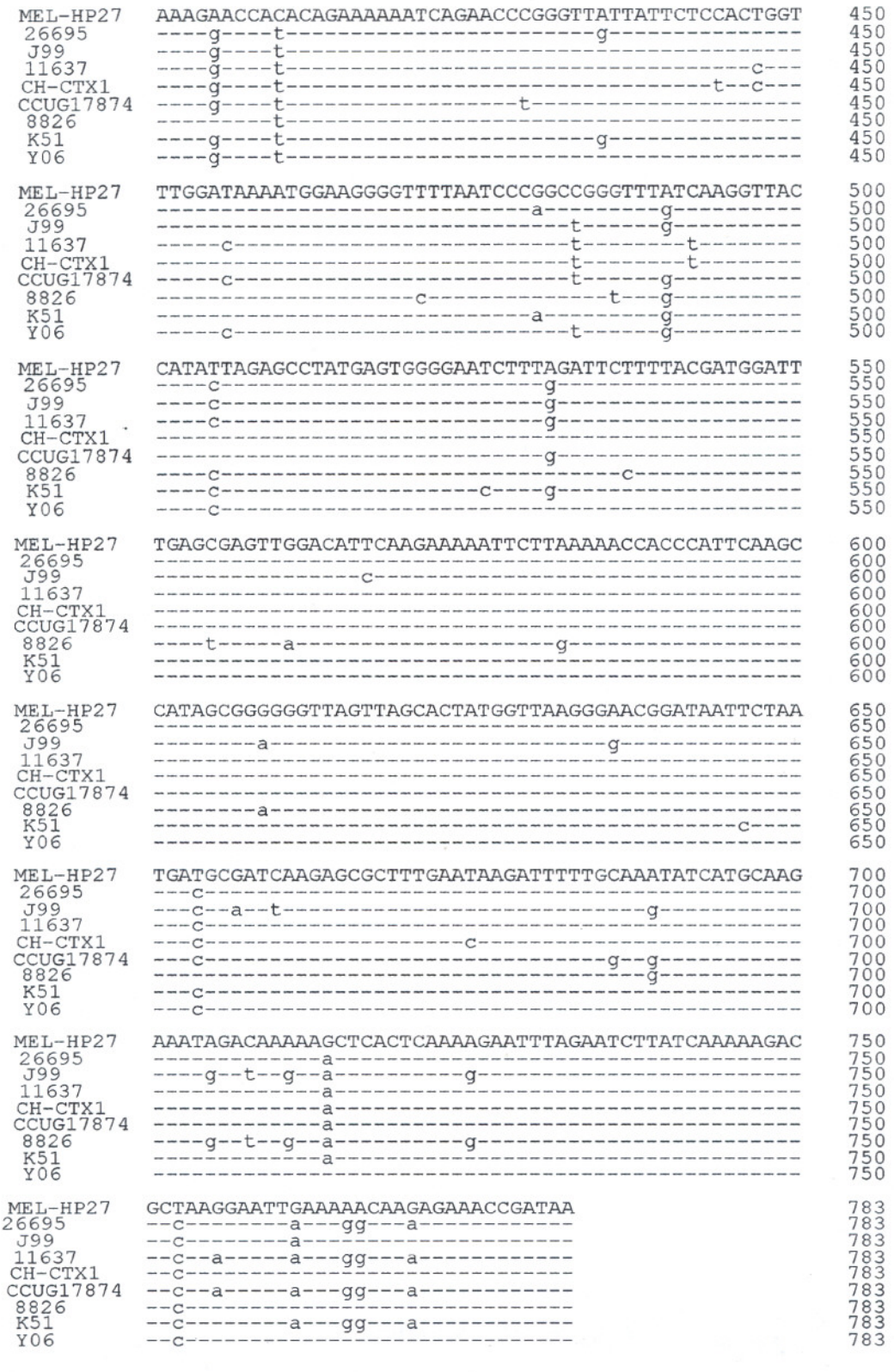

Figure 3. Homology comparison of *hpaA* gene nucleotide sequences

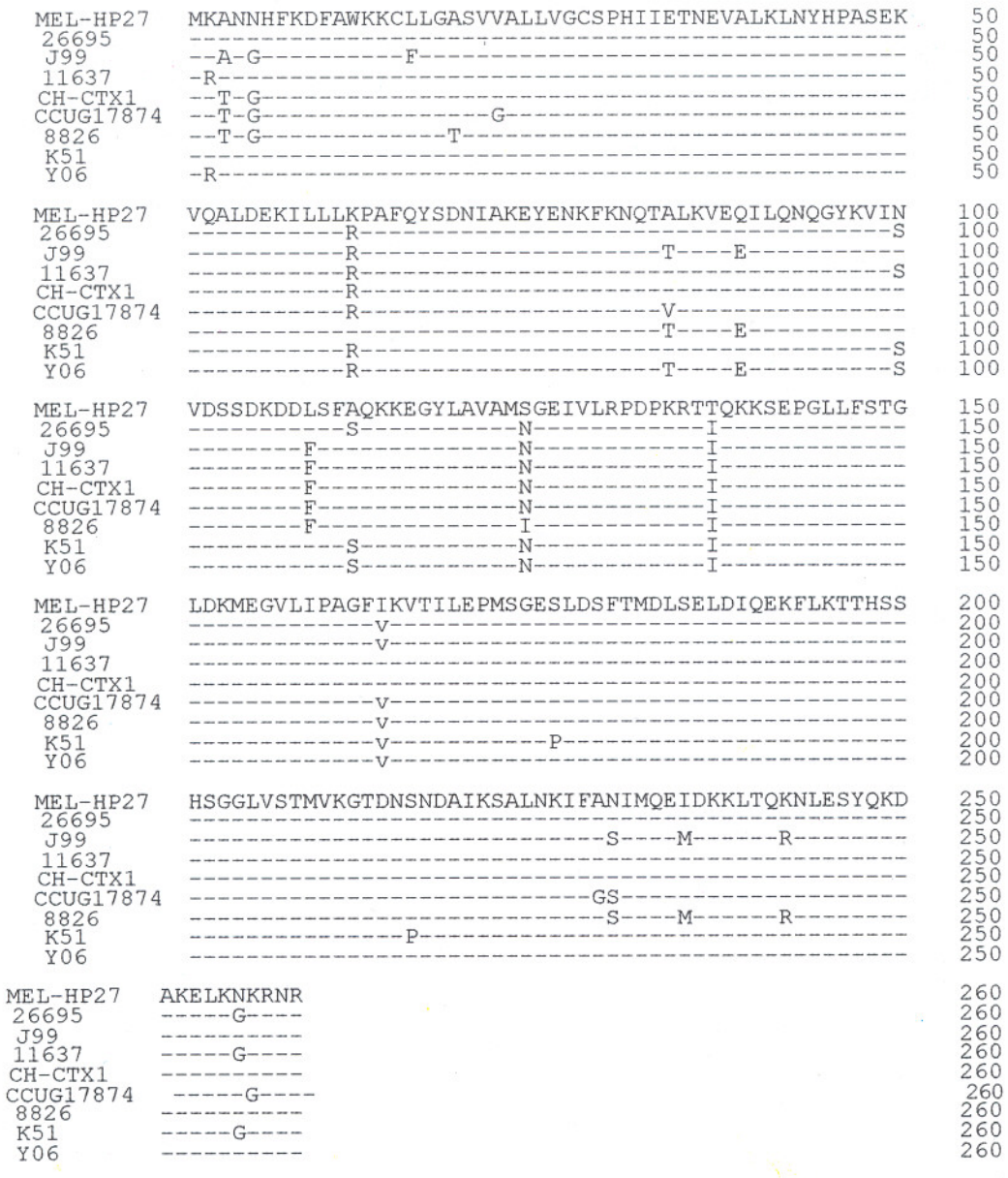

Figure 4. Homology comparison of the putative amino acid sequences of *hpaA* gene

Correspondence to:
Guangcai Duan
Department of Epidemiology
College of Public Health
Zhengzhou University
Zhengzhou, Henan 450052, China
Telephone: 86-0371-6696-9270
Email: gcduan@public.zz.ha.cn

References

1. Ohata H, Kitauchi S, Yoshimura N, *et al*. Progression of chronic atrophic gastritis associated with *Helicobacter pylori* infection increases risk of gastric cancer. Int J Cancer 2004; 109(1):138－43.
2. Kauser F, Hussain MA, Ahmed I, *et al*. Comparing genomes of *Helicobacter pylori* strains from the high-altitude desert of Ladakh, India. J Clin Microbiol 2005; 43(4):1538－45.
3. Graham DY. Therapy of *Helicobacter pylori*: current status and issues. Gasteroenterology 2000; 118: S2－S8.
4. Liu XF, Hu JL, Zhang X, *et al*. Oral immunization of mice with attenuated *Salmonella typhimurium* expressing *Helicobacter pylori* urease B subunit. Chinese Medical Journal 2002;115(10):1513－6.
5. Hatzifoti C, Wren BW, Morrow JW. *Helicobacter pylori* vaccine strategies-triggering a gut reaction. Immuno Today 2000; 21: 615－9.

6. Valkonen KH, Wadstrom T, Moran AP. Identification of the N-acetylneuraminyllactose-specific laminin-binding protein of *Helicobacter pylori*. Infect Immun 1997; 65 (3):916 – 23.
7. Yuan JP, Li T, Shi XD, *et al*. Deletion of *Helicobacter pylori* vacuolating cytotoxin gene by introduction of directed mutagenesis. World J Gastroenterol 2003;9(10): 2251 – 7.
8. Chen XJ, Yan J, Shen YF. Dominant cagA/vacA genotypes and coinfection frequency of *H. pylori* in peptic ulcer or chronic gastritis patients in Zhejiang Province and correlations among different genotypes, coinfection and severity of the diseases. Chinese Medical Journal 2005; 118(6):460 – 7.
9. Richard AA, James B, Beth M, *et al*. Comparative genomics of *Helicobacter pylori*: analysis of the outer membrane protein families. Infection and Immunity 2000; 68 (7):4155 – 68.
10. Keenan IJ, Allardyce AR, Bagshaw FP. Lack of protection following immunization with *Helicobacter pylori* membrane vesicles highlight santigenic differences between *H. felis* and *Helicobacter pylori*. FEMS Microbiology Letters 1998;161:21 – 7.
11. Jiang Z, Tao XH, Huang AL, *et al*. A study of recombinant protective *H. pylori* antigens. World J Gastroenterol 2002; 8: 308 – 11.
12. Jones AC, Logan RP, Foynes S, *et al*. A flagellar sheath protein of *Helicobacter pylori* is identical to HpaA, a putative N-acetylneuraminyllactose-binding hemagglutinin, but is not an adhesin for AGS cells. J Bacteriol 1997;179: 5643 – 7.
13. Alm RA, Ling SL, Moir DT, *et al*. Genomic-sequence comparison of two unrelated isolates of the human gastric pathogen *Helicobacter pylori*. Nature 1999;397: 176 – 80.

Received June 18, 2006

Expression of Recombinant Human MT1G Gene with C Terminal of His-tag in EC9706 Cells

Xinfang Hou[1], Qingxia Fan[1], Liuxing Wang[1], Ruilin Wang[1], Shixin Lu[1,2]

1. *Department of Oncology, The First Affiliated Hospital of Zhengzhou University, Oncology Center of Zhengzhou University, Zhengzhou, Henan 450052, China*

2. *Cancer Institute, Chinese Academy of Medical Sciences, Beijing 100021, China*

Abstract: Objective. To construct a recombinant eukaryotic expression plasmid of MT1G and express it in human esophageal cancer cell line EC9706. **Methods.** The target sequence was amplified by PCR from pACT2-MT1G plasmid containing human *MT1G* cDNA and cloned into eukaryotic expression vector pcDNA3.1/Myc-His(-) with C terminal of myc epitope and 6×His-tag. After restriction endonuclease digestion and DNA sequencing confirmation, the recombinant plasmid was tranfected into EC9706 cell by lipofectamine 2000. The positive monoclone was screened by G418. RT-PCR and Western blotting were used to detect the expression of mRNA and fusion protein of *MT1G* gene respectively. **Results.** The eukaryotic expression vector pcDNA3.1/Myc-His(-)-MT1G was successfully constructed and MT1G fused protein with His-tag was expressed in tranfected EC9706 cell. **Conclusion.** The human MT1G recombinant plasmid and the EC9706 cell strain stably expressing MT1G fused protein with His-tag were obtained, which provide the basis for further study on biology functions of MT1G. [Life Science Journal. 2006;3(4):49-53] (ISSN: 1097-8135).

Keywords: metallothionein 1G; esophageal cancer; eukaryotic expression

Abbreviations: MTs: Metallothioneins

1 Introduction

Metallothioneins (MTs) are a cystein-rich, low molecular weight proteins, which can bind to heavy metals such as zinc and copper and is involved in their intracellular homeostasis[1]. In humans, MTs are encoded by a family of genes consisting of 10 functional MTs isoforms and the encoded proteins are conventionally subdivided into four groups viz, MT-1, MT-2, MT-3 and MT-4 proteins[2-5]. While a single MT-2A gene encodes MT-2 protein, MT-1 protein comprises many subtypes encoded by a set of MT-1 genes (MT-1A, MT-1B, MT-1E, MT-1F, MT-1G, MT-1H and MT-1X) accounting for the microheterogeneity of the MT-1 protein[6]. Although MTs have been linked with tumorigenesis and progression, there is not much information available in the literature on the functional roles of the different MT isoforms. To investigate the biological roles of MT1G in human esophageal cancer cell line, we constructed the recombinant eukaryotic expression vector pcDNA3.1/Myc-His (-)-MT1G and expressed it in EC9706 cells.

2 Materials and Methods

2.1 Materials

Esophageal cancer cell EC9706, eukaryotic expression vector pcDNA3.1/Myc-His(-), *E. coli.* strain DH5a and strain DH5a containing pACT2-MT1G were from department of Etiology and Carcinogenesis, Cancer Institute, Chinese Academy of Medical Sciences. Taq DNA polymerase, T4 DNA ligase, *Xba*I and *Bam*HI restriction enzyme, 100 bp Ladder marker, RT-PCR kit were Takara. Lipofectamine™ 2000, TRIZOL reagents were Invitrogen. Rabbit polyclonal His antibody, peroxidase-conjugated secondary antibody were purchased from Beijing Zhongshan Biotechnology Company.

2.2 Methods

2.2.1 Design of primers and amplication of target gene

According to MT1G gene sequences published in GenBank, the primers were designed to amplify the full length of the human MT1G cDNA with an enzyme digest site of *Xba*I added to the 5′ end of the forward primer and an enzyme digest site of the *Bam*HI added to the 5′ end of the reverse primer. The forward primer was 5′-TAG TCT AGA ATG GAC CCC AAC TGC TCC -3′ and the reverse primer was 5′-TAT GGA TCC GGC GCA GCA GCT GCA CT -3′. MT1G cDNA was amplified using plasmid pACT2-MT1G as template. PCR conditions were as follows: 1 cycle at 94 ℃ for 2 minutes, 35 cycles with 30 seconds at 94 ℃ for denat-

uration, 45 seconds at 56 ℃ for annealing, 1 minute at 72 ℃ for extension and a final extension at 72 ℃ for 10 minutes. PCR products were identified with 1.5% agarose gel electrophoresis.

2.2.2 Construction and identification of recombinant eukaryotic expression vector pcDNA3.1(−)-MT1G

PCR products were purified by PCR purification kit and digested by *Xba* I and *Bam* HI. At the same time the plasmid pcDNA3.1(−) was also digested by *Xba* I and *Bam* HI. Later, the digested products of the 2 above mentioned were ligated by T4 DNA ligase for overnight at 16 ℃. The ligation products were transferred into competent cells of *E. coli* DH5a. Amp-resistant clones were selected and positive clones were verified by PCR. The positive clone containing MT1G cDNA fragment was named pcDNA3.1(−)-MT1G. The construction procedure of recombinant vector is shown in Figure 1.

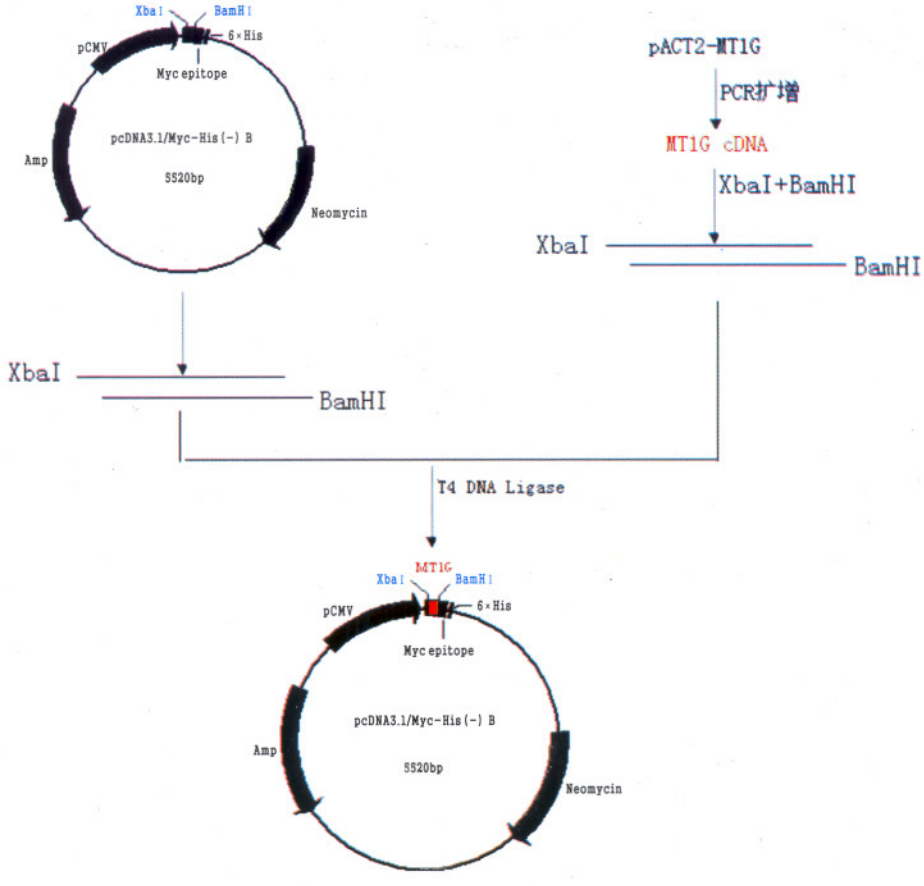

Figure 1. The construction procedure of recombinant vector pcDNA3.1(−)/Myc-His-MT1G

2.2.3 Cell tranfection and positive clone screening

According to the protocol of Lipofectamine™ 2000, plasmids pcDNA3.1(−)-MT1G were transfected into esophageal cancer cell EC9706. And pcDNA3.1(−) also was transfected transfected into EC9706 cells as negative control. Two groups cells were screened in the medium containing geneticin (G418) of 400 mg/mL for 48 hours. After two weeks' selection, positive clones were isolated and further expanded which were named EC9706-MT1G and EC9706-null cells respectively.

2.2.4 Identification of transfection

RT-PCR: Total RNA were extracted with TRIZOL reagent according to the manufacturer's instructions. Concentration and purity of RNA were measured by ultraviolet spectrophotometer. 0.5 μg RNA was used to synthesize cDNA, and PCR was performed as follows: 94 ℃ for 2 minutes;35 cycles of 94 ℃ for 30 seconds, 54 ℃ for 30 seconds, 72 ℃ for 1 minute; 72 ℃ for 5 minutes. The primers for MT1G were : 5′-TCG CTT

GGG AAC TCT AGT CTC-3′ (forward), and 5′-GCA AAG GGG TCA AGA TTG TAG -3′ (reverse), amplification fragment lengths were 309 bp. β-actin primers were 5′-CAT CCT GCG TCT GGA CCT-3′ (forward), and 5′-TCA GGA GGA GCA ATG ATC TTG-3′ (reverse), amplification fragment lengths were 480 bp. RT-PCR products were visualized by ethidium bromide-stained 1.5% agarose gel.

Westem blot: Cells were washed for 3 times with PBS and lysed in RIPA lysis buffer. Protein concentration in each lysate was detected by Bradford method. The protein were mixed with 5 × loading buffer and boiled for 5 minutes. Protein samples were resolved by SDS-PAGE by the same volume and transferred to 0.2 μm PVDF membrane. After blocking with 5% skim milk, proteins were incubated with rabbit anti-human His antibody for overnight at 4 ℃ and then with peroxidase-conjugaated secondary antibody for 1 hour. After washed for 5 times with PBST, the membrane was then stained using DAB kit.

3 Results

3.1 Identification of recombinant plasmid pcDNA3.1(−)-MT1G

Target gene fragment was obtained by PCR amplification from plasmid pACT2-MT1G containing human MT1G cDNA and inserted into pcDNA3.1(−) eukaryotic expression vector to construct pcDNA3.1(−)-MT1G recombinant plasmid. After digesting with double restriction endonuclease *Xba* I and *Bam* HI, around 5.4 kb and 192 bp fragments were obtained. The former is plasmid fragment digested and the latter was target gene fragment digested (Figure 2). Recombinant plasmid was sequenced, and the result was the same as MT1G cDNA sequence published in Genebank (Figure 3). This confirmed that eukaryotic expression vector pcDNA3.1(−)-MT1G was constructed successfully.

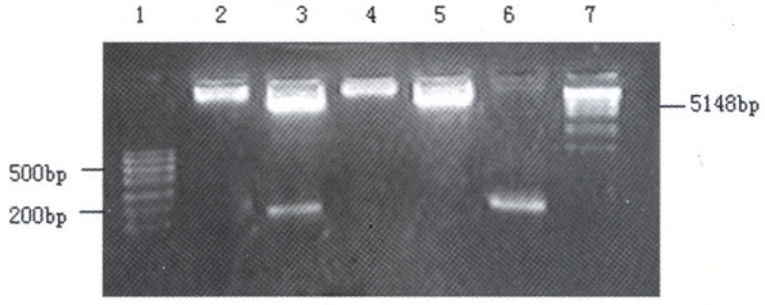

Figure 2. RCR analysis of recombinant plasmid pcDNA3.1(−)-MT1G
Lane 1: 100 bp ladder marker; Lane 2: pcDNA3.1(−)-MT1G; Lane 3: pcDNA3.1(−) -MT1G digested by *Xba* I and *Bam* HI; Lane 4: pcDNA3.1(−); Lane 5: pcDNA3.1(−) digested by *Xba* I and *Bam* HI; Lane 6: PCR product of MT1G Lane 7: λDNA/*Hind* Ⅲ + *Eco* RI marker

3.2 Expression of MT1G mRNA

RT-PCR products of the cell EC9706-MT1G yielded two expected fragments of 480 bp and 309 bp, corresponding to RT-PCR products of β-action and MT1G respectively. While RT-PCR products of the cell EC9706-null only yielded one fragment of 480 bp β-action and no target gene fragment of 309 bp(Figure 4).

3.3 Expression of MT1G fusion protein with his-tag

MT1G fusion protein with his-tag was detected in the cells EC9706-MT1G and not in cells EC9706-null(Figure 5). This showed stable transfection of *MT1G* gene in EC9706 cells was successful.

4 Discussion

At first, MTs were recognized to involved metal ion homeostasis and detoxification, protection against DNA damage, oxidative stress[7]. In the postgenomic era, it is becoming increasingly clear that MT fulfils different functions[8]. In recent years, more and more data have showed that MTs are associated with tumour cell proliferation and apoptosis, resistance to radiation or chemotherapy, patient survival and prognosis[9,10]. Although metallothionein expression has been implicated in carcinogenic evolution, current knowledge on the potential biological roles of its different isoforms in the various human cancers remains unclear. So far, researchers only found that different MT isoforms in humans possibly play different functional roles during development or under various physiological conditions[11]. Individual isoforms have unique functions[12]. Therefore, detailed studies focused

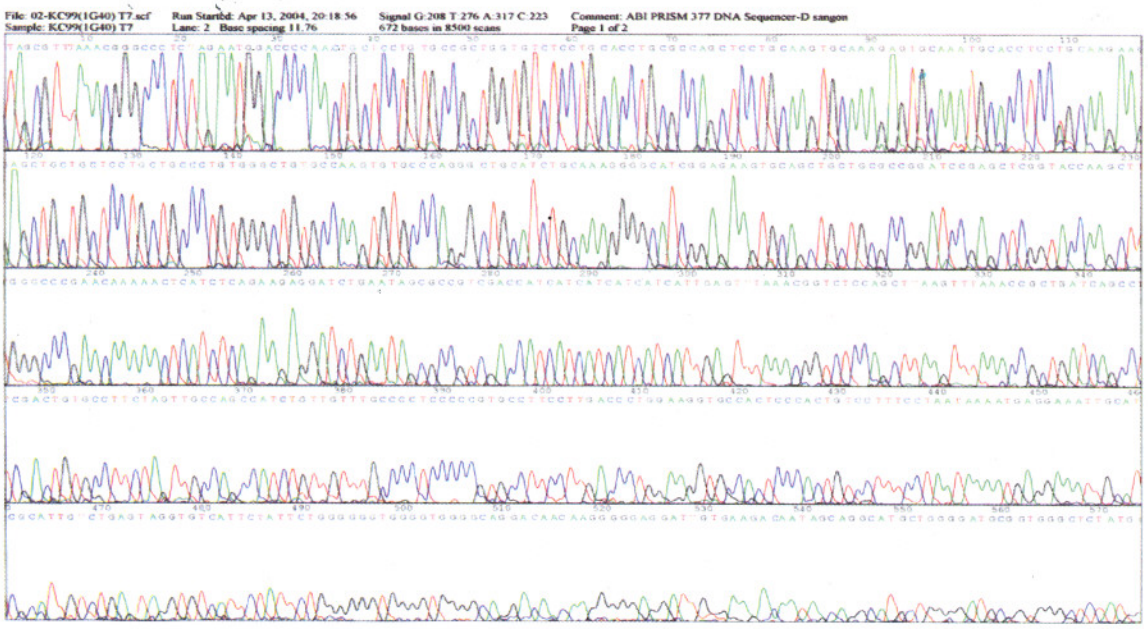

Figure 3. Recombinant eukaryotic expression vector pcDNA3.1(－)-MT1G sequence

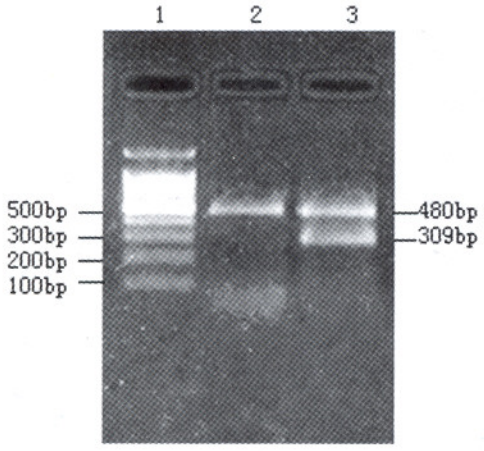

Figure **4**. Expression of MT1G mRNA detected by RT-PCR Lane 1: 100 bp ladder marker; Lane 2: EC9706-null; Lane 3: EC9706-MT1G

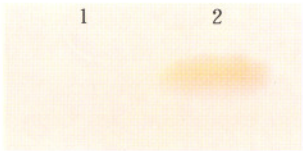

Figure 5. Expression of MT1G fusion protein with His-tag deteced by Western blot. Lane 1: EC9706-null; Lane 2: EC9706-MT1G

on the functional roles of different metallothionein isoforms could elucidate the role of this group of proteins in the carcinogenic process, delineating its possible clinical significance for the management of patients. In this study, we constructed the eukaryotic expression vector of MT1G and expressd it in human esophageal cancer cell EC9706 first.

Due to the high sequence homology of the MT isoforms, the generation of isoform-specific antibodies for MT was hindered[12]. The commercially available E9 antibody, which is used routinely for MT immunohistochemical studies, cannot distinguish different MT isoforms[13]. So, the eukaryotic expression plasmid pcDNA3.1/Myc-His(－) was chosen to encode two tag gene of myc and 6× His. The full MT1G cDNA was inserted into the multi clone site of the eukaryotic expression plasmid pcDNA3.1/Myc-His(－) and located closely at the upstream of two tag gene of myc and 6× Poly-histidines so as to construct recombinant eukaryotic expression vector of MT1G gene: pcDNA3.1/Myc-His(－)-MT1G. Recombinant plasmid was tranfected in esophageal cancer cell EC9706. Then expression of the MT1G fusion protein with 6× His tag was detected with specific anti-6× His antibody which could reflect expression level of MT1G protein indirectly. Although fusion protein was obtained, 6× His tag was very small and stable in physiological pH, folded structure and chemical properties of recombinant protein were not changed and the tag often has little effect on the function of the protein. In addition, pcDNA3.1/Myc-His(－) contains CMV promoter and SV40 ori reproduce

component and provides efficient, high-level expression in a wide range of mammalian cells. Neomycin resistance gene was used to selection of stable transfectants in mammalian cells.

In this study, eukaryotic expression plasmid of MT1G gene was constructed and transfected into human esophageal cancer cells EC9706 successfully. This layed a foundation for further study on the function and mechanism of MT1G in tumorenesis.

Correspondence to:
Qingxia Fan
Department of Oncology
The First Affiliated Hospital
Zhengzhou University
Zhengzhou, Henan 450052, China
Email: fqx2243@sohu.com

References

1. Coyle P, Philcox JC, Carey LC, *et al*. Metallothionein: the multipurpose protein. Cell Mol Life Sci 2002; 59: 627－47.
2. Palmiter RD, Findley SD, Whitmore TE, *et al*. MT-Ⅲ, a brain specific member of the metallothionein gene family. Proc Natl Acad Sci USA 1992; 89: 6333－7.
3. Stennard FA, Holloway AF, Hamilton J, *et al*. Characterization of six additional human metallothionein genes. Biochim Biophys Acta 1994; 218:357－65.
4. Quaife CJ, Findley SD, Erickson JC, *et al*. Induction of a new metallothionein isoform (MT-IV) occurs during differentiation of stratified squamous epithelia. Biochemistry 1994; 33: 7250 －9.
5. Mididoddi S, McGuirt JP, Sens MA, *et al*. Isoform-specific expression of metallothionein mRNA in the developing and adult human kidney. Toxicol Lett 1996; 685: 17 －27.
6. Karin M, Eddy RL, Henry WM, *et al*. Human metallothionein genes are clustered on chromosome 16. Proc Natl Acad Sci USA 1984; 81: 5494－8.
7. Hamer DH. Metallothionein. Annu Rev Biochem 1986; 55:913－51.
8. Vasak M. Advances in metallothionein structure and functions. J Trace Elem Med Biol 2005;19:13－7.
9. Cherian MG, Jayasurya A, Bay BH. Metallothioneins in human tumors and potential roles in carcinogenesis. Mutat Res 2003; 533:201－9.
10. Jasani B, Schmid KW. Significance of metallothionein overexpression in human tumours. Histopathology 1997, 31:211－4.
11. Kagi JHR, Schaffer A. Biochemistry of metallothionein. Biochemistry 1988; 27:8509－15
12. Bylander JE, Li SL, Sens MA, *et al*. Exposure of human proximal tubule cells to cytotoxic levels of CdC12 induces the additional expression of metallothionein 1A mRNA. Toxicol Lett 1995; 76: 209－17.
13. Jasani B, Elmes ME. Immunohistochemical detection of metallothionein. Methods Enzymol 1991; 205:95－107.

Received August 5, 2006

Msp I Polymorphism of the Coagulation Factor Ⅶ Gene in Patients with Ischemic Cerebrovascular Disease in Han Population of Henan, China

Haidong Yu, Hua Qi, Jianhua Lian, Ying He, Hong Zheng

Department of Cell Biology and Medical Genetics, Basic Medical College, Zhengzhou University, Zhengzhou, Henan 450052, China

Abstract: Objective. To determine whether there is any relationship between polymorphisms in gene of coagulation factor Ⅶ and ischemic cerebrovascular disease in Han population of Henan in China. **Methods.** Coagulation factor Ⅶ (R353Q) genotypes were screened in 512 patients with ischemic cerebrovascular disease by PCR and restriction fragment length polymorphisms (PCR-RFLP) assay. **Results.** The R353Q genotypes of factor Ⅶ distribution was in accordance with Hardy-Weinberg equilibrium. The distribution of allele and genotype in R353Q had significant difference between the control group and CVD group. **Conclusion.** The Q allele of the R353Q polymorphism of the factor Ⅶ gene may be a protective genetic factor against ischemic cerebrovascular disease in Han population of Henan, China. [Life Science Journal. 2006;3(4):54-56] (ISSN: 1097-8135).

Keywords: coagulation factor Ⅶ; ischemic cerebrovascular disease; polymorphism; R353Q

Abbreviations: CAD: coronary artery disease; ICVD: ischemic cerebrovascular disease; IHD: ischemic heart disease; FⅦ: coagulation factor Ⅶ

1 Introduction

Coagulation factor Ⅶ (FⅦ) is the initial factor in the extrinsic pathway of the coagulation cascade and FⅦ levels in plasma are usually related to ischemic heart disease (IHD). The updated result of the NPH study showed that FⅦc was strongly related to fatal events of ischemic heart disease[1]. In two Japanese reports, FⅦc was also proposed to be the independent risk factor for coronary artery disease (CAD)[2,3]. Ischemic cerebrovascular disease (ICVD) shares many risk factors related to IHD. ICVD has a complex etiology and pathophysiology generated by the combined effects of genes and the environment. Genetic variation played an important role in the determination of plasma FⅦ levels. In the previous study, the polymorphism at exon 8 of the FⅦ gene (designated R353Q polymorphism) was consistently reported to have a genotype effect on plasma FⅦc levels. Our main purpose was to determine whether there is any relationship between R353Q polymorphism in gene of coagulation FⅦ and ischemic cerebrovascular disease in Han population of Henan, China.

2 Materials and Methods

2.1 Subjects

A total of 512 patients with ischemic cerebrovascular disease were admitted to the First Affiliated Hospital of Zhengzhou University. There were two groups in the study (1) CVD group: 512 subjects (310 males and 202 females, aged 60 ± 10.2 years); (2) control group: 560 subjects (294 males and 266 females, aged 56 ± 9.8 years). The control group were healthy subjects clinically free of vascular disease. All of them were unrelated, and were the Chinese Han population.

2.2 Gene polymorphism

Genomic DNA were extracted from peripheral-blood lymphocytes by the standard phenol-chloroform method. Primers for PCR amplification were made according to the sequence reported by Green *et al*[4], and the conditions of the PCR reaction were 94 ℃ for 5 minutes, followed by 35 cycles of 1 minute at 94 ℃, 1 minute at 56 ℃, 1 minute at 72 ℃, and the final cycle was at 72 ℃ for 5 minutes. PCR reaction mixture of 25 μl contains 100 ng genomic DNA, 10 μmol of the primer, 1.5 mol/L $MgCl_2$, 50 mol/L KCl, 10 mol/L Tris-HCl (PH 8.3), 0.2 mol/L of dNTP each and 2.0 U DNA polymerase. Following amplification, a restriction digestion was performed to detect the FⅦ sequence polymorphism with the enzyme *Msp*I at 37 ℃ for 12 hours. These products and PCR products were separated using electrophoresis through 2% agarose gel and stained with ethidium bromide and visualized under UV light.

2.3 Statistical analysis

The frequencies of the alleles and genotypes were counted and compared by the Chi-square test. Odds Ratios(OR) and their 95% confidence intervals (95%CI) were used to estimate the risk association to the genotype. All statistical procedures were performed with SPSS 10.0 software package. $P<0.05$ was set statistically significant.

3 Results

Three genotypes of R353Q(RR, RQ and QQ) were found in our study (Figure 1). The genotype distribution for both males and females was in accordance with Hardy-Weinberg equilibrium by Chi-square test ($P>0.05$). Due to low number of the subjects homozygous for the Q allele, we concentrated our analysis on the combined group(RQ + QQ). The frequencies of the Q allele and (RQ + QQ) genotype were significantly higher in control group than those in CVD group ($P=0.025$, Odds ratios=0.657, 95%CI, 0.454 − 0.951 for the Q allele and $P=0.016$, Odds ratios=0.625, 95% CI, 0.426 − 0.917). This group of Q carriers had a 35% reduction of the risk of CVD as compared with carrier of R allele (Table 1).

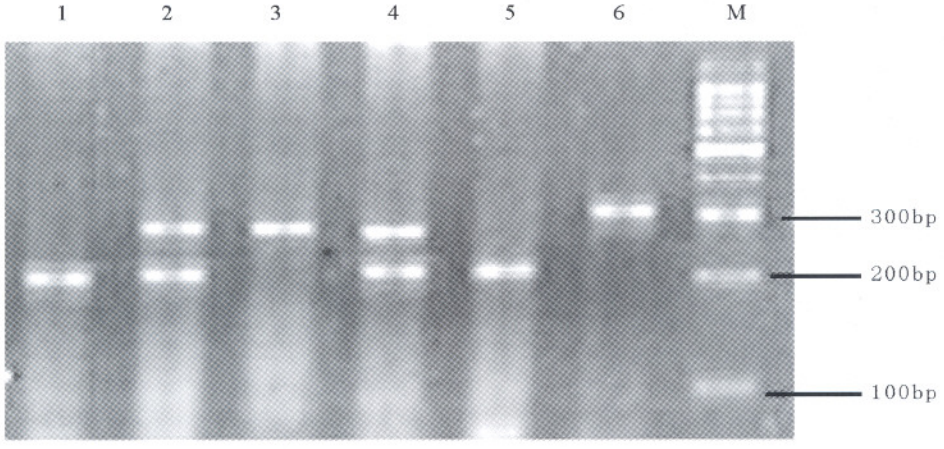

Figure 1. PCR products from amplification of the polymorphic region of the R353Q gene
Lane M: 100 bp DNA Marker; Lanes 1 and 5: RR homozygote with a fragment of 205 bp; Lanes 2 and 4: RQ heterzygote with a fragment of 205 bp and 272 bp; Lane 3: QQ homozygote with fragments of 272 bp; Lane 6: PCR product.

Table 1. Distribution frequency of R353Q genotype and allele in patients with CVD and controls

Genotype	CVD($n=512$)	Control($n=560$)	*P* value	OR(95%CI)
RR	465(90.8)	482(86.4)		1.00
RQ	46(9.0)	76(13.2)	0.018	0.627(0.426 − 0.924)
QQ	1(0.2)	2(0.4)		
RQ + QQ	47(9.2)	78(13.6)	0.016	0.625(0.426 − 0.917)
Alleles				
R	976(95.3)	1042(93.0)		1.00
Q	48(4.7)	78(7.0)	0.025	0.657(0.454 − 0.951)

4 Discussion

FⅦ is a vitamine K-dependent protease and it is the initial factor in the extrinsic pathway of the coagulation cascade. The prospective Northwick Park Heart Study (NPHS) found that raised FⅦ coagulant activity (FⅦc) was an independent risk factor for CAD[1]. Epidemiological evidence suggested that ICVD shared many risk factors with IHD, such as age, hypertension, and smoking, etc. It is also possible that the features of the hemostastic system may influence the development of ICVD, as has been suggested for IHD. Genetic variations play a role in the determination of plasma FⅦ levels. In the previous study, the polymorphism at exon 8 of the FⅦ gene (designated R353Q polymorphism) was consistently reported to have a

genotype effect on plasma FⅦc levels. These polymorphisms arised from a basic substitution of A to G in the second position of the codon 353, leading to substitution of arginine with glutamine (alleles were designated as R and Q, respectively). Green[4] first reported that heterozygous European subjects were 22% lower on FⅦc levels than those in group mean. In some of these studies, the Q allele was also found to be associated with lower FⅦc levels[5,6]. Girelli[7] reported that Q allele had a protective effect against MI. Differences in allelic frequencies had been reported in different ethnic groups. In our study, the frequency of Q allele was 7.0%. The Q allele frequency of the R353Q polymorphism in Chinese was significantly lower than that of the Dravidian Indians (0.29).

It was also lower than frequencies of the Europeans(0.14 – 0.28)[4,6], but higher than that of the Japanese(0.034)[5] and it was similar to that of Korean(0.060)[8], which suggested that the prevalences of gene mutation of R353Q vary with different ethnic groups or geographic regions. The mechanism of R353Q's effect on plasma FⅦ levels is unknown, and several possible explanations have been discussed. Lower plasma levels of the FⅦ protein seen with the Q allele might be due to a conformational change produced by the Arg→Gln substitution that affected the processing of FⅦ in the hepatocytes, resulting in reduced secretion of the protein[9]. In line with this hypothesis, the Q variant was shown *in vitro* to be associated with reduced secretion of FⅦ compared with the R variant, thus accounting for the reduction on plasma FⅦ levels[10]. Our result was similar to the results reported by Girelli[7]. Our study has shown that Q allele of the R353Q polymorphism in the FⅦ gene may play a protective role against ICVD in Han population of Henan, China.

Acknowledgments

The authors express their sincere gratitude to the Henan Key Laboratory of Molecular Medicine, for the financial support of this study.

Correspondence to:
Hong Zheng
Department of Cell Biology and Medical Genetics
Basic Medical College
Zhengzhou University
Zhengzhou, Henan 450052, China
Telephone: 86-371-6665-8161
Email: hzheng@zzu.edu.cn

References

1. Ruddock V, Meade TW. Factor Ⅶ activity and ischaemic heart disease: fatal and non-fatal events. QJM 1994; 87:403 – 6.
2. Shimokata K, Kondo T, Ohno M, *et al*. Effects of coagulation factor Ⅶ polymorphism on the coronary artery disease in Japanese: Factor Ⅶ polymorphism and coronary disease. Thromb Res 2002;105:493 – 8.
3. MasakazuO, Satoshi A, Sadatoshi B, *et al*. R353Q polymorphism, activated factor Ⅶ, and risk of premature myocardial infarction in Japanese men. Circ J 2004; 68:520 – 5.
4. Green F, Kelleher C, Wilkes H, *et al*. A common genetic polymorphism associated with lower coagulation factor Ⅶ levels in healthy individuals. Arteriosclerosis Thromb 1991;11:540 – 6.
5. Takamiya O. Genetic polymorphism (Arg353 < – Gln) in coagulation factor Ⅶ gene and factor Ⅶ levels (coagulant activity, antigen and binding ability to tissue factor) in 101 healthy Japanese. Scand J Clin Lab Invest 1995; 55: 211 – 5.
6. Bernardi F, Marchetti G, Pinotti M, *et al*. Factor Ⅶ gene polymorphisms contribute about one third of the factor Ⅶ level variation in plasma. Arterioscler Thromb Vasc Biol 1996; 16: 72 – 6.
7. Girelli D, Russo C, Ferraresi P, *et al*. Polymorphisms in the factor Ⅶ gene and the risk of myocardial infarction in patients with coronary artery disease. N Engl J Med 2000; 343: 774 – 80.
8. Song J, Yoon YM, Jung HJ, *et al*. Plasminogen activator inhibitor-1 4G/5G promoter polymorphism and coagulation factor Ⅶ Arg353 – >Gln polymorphism in Korean patients with coronary artery disease. J Korean Med Sci 2000;15(2):146 – 52.
9. Humphries SE, Lane A, Green FR, *et al*. Factor Ⅶ coagulant activity and antigen levels in healthy men are determined by interaction between factor-Ⅶ genotype and plasma triglyceride concentration. Arterioscler Thromb 1994;14:193 – 8.
10. Hunault M, Arbini AA, Lopaciuk S, *et al*. The Arg (353)Gln polymorphism reduces the level of coagulation factor Ⅶ-*in vivo* and *in vitro* studies. Arterioscler Thromb Vasc Biol 1997;17: 2825 – 9.

Received June 12, 2006

Prevalence of Dental Fluorosis in Children from Fluorosis-endemic Areas

Jingyuan Zhu[1], Li Fang[2], Yue Ba[1], Xuemin Cheng[1], Liuxin Cui[1]

1. Department of Environmental Health, College of Public Health, Zhengzhou University, Zhengzhou, Henan 450052, China

2. Zhengzhou University Hospital, Zhengzhou, Henan 450052, China

Abstract: Objective. To study the prevalence of dental fluorosis in children and its possible relationship with fluoride intake by drinking water. **Methods.** 198 children aged 8 – 12 years old were allocated into 2 groups (A and B) according to the water fluoride levels. Dental fluorosis was examined by Dean's method and CFI was calculated. The children's urinary samples were collected. Ion-selective electrode method was used to determine the fluoride concentration in drinking water and urinary samples. **Results.** The significant differences were found between two groups in children urinary fluoride levels (0.62 mg/L and 1.49 mg/L) and the prevalent incidence of dental fluorosis (13.51% and 43.68%) ($P<0.01$). There were significant correlations between dental fluorosis and fluoride level in drinking water, dental fluorosis and fluoride level in urine respectively ($\chi^2=21.73, P<0.005$). **Conclusion.** For the fluoride level of 1.22 mg/L in drinking water, dental fluorosis should be closely monitored. The urinary fluoride level of children may be an effective index. [Life Science Journal. 2006;3(4):57 – 60] (ISSN: 1097 – 8135).

Keywords: water fluoride; urinary fluoride; dental fluorosis

Abbreviations: CFI: community fluorosis index

1 Introduction

Over fluoride intake during the formative years of a child's enamel development can cause dental fluorosis which is often a condition marked by permanent staining of adult teeth. The discoloration induced by dental fluorosis, particularly in its advanced forms, can cause significant embarrassment and stress to the impacted child, resulting in adverse effects on esteem, emotional health, and career success. In drinking-water type of fluorosis-endemic areas, drinking water is a main exposure pathway contributing to endemic fluorosis. Although the engineer of altering water sources to lower fluoride in drinking water prevents endemic fluorosis effectively, especially for skeletal fluorosis, the fluctuations in the fluoride concentration in the drinking water and its effect on dental fluorosis are still worth concerning[1, 2]. Even with the low fluoride concentration in drinking water of 0.872 mg/L, cases of mild dental fluorosis in 12-year-old children were observed[3]. In present study, two villages were chosen from Neihuang town in Henan province, a fluorosis-endemic area caused by high fluoride concentration in ground water, to investigate the prevalence of dental fluorosis in children and its possible associations with the fluoride concentrations in drinking water and children's urinary.

2 Materials and Methods

2.1 Villages investigated

The geographical condition, climatic condition, economic development, population, variety of crop and custom are similar in two chosen villages marked as group A and group B, respectively. There is no industrial pollution of fluoride in both villages where ground water is the only source of drinking water.

2.2 Fluoride level in water and children's urine

Five water samples from the east, west, south, north, and middle locations of each village were collected representing the water quality of the whole village. Stratified sampling method was used in collecting the spot urine samples of school going children aged 8 – 12 years old. The urine samples were collected in nonreactive plastic containers and brought to the laboratory within 4 hours. A total of 10 water samples and 100 urine samples from two villages were collected and analyzed by iron-selective electrode method. Total ionic strength adjustment buffer made from sodium citrate, acetic acid and sodium chloride, was added to the standard fluoride solutions as well as the samples before measurement of fluoride. The instrument was calibrat-

ed with two standard solutions so that the concentration of one was 10 times of the other and also that the concentration of the unknown falls between those two standards. Then, the concentration of the unknown was directly read from the digital display of the meter.

2.3 Assessment of dental fluorosis

All the children in the two villages were assessed for dental fluorosis according to Dean's classification. All the examiners were trained. Normal is the station that the enamel represents the usual translucent semivitriform type of structure. The surface is smooth, glossy, and usually pale creamy white color. Questionable means that the enamel discloses slight aberrations from the translucency of normal enamel, ranging from a few white flecks to occasional white spots. This classification is utilized in those instances where a definite diagnosis of the mildest form of fluorosis is not warranted and a classification of "normal" is not justified. Very mild is small opaque, paper white areas scattered irregularly over the tooth but not involving as much as 25% of the tooth surface. Frequently included in this classification are teeth showing no more than about 1 – 2 mm of white opacity at the tip of the summit of the cusps of the bicuspids or second molars. Mild is the station that the white opaque areas in the enamel of the teeth are more extensive but do not involve as much as 50% of the tooth. Moderate means that all enamel surfaces of the teeth are affected, and the surfaces subject to attrition show wear. Brown stain is frequently a disfiguring feature. Severe includes teeth formerly classified as "moderately severe and severe." All enamel surfaces are affected and hypoplasia is so marked that the general form of the tooth may be affected. The major diagnostic sign of this classification is discrete or confluent pitting. Brown stains are widespread and teeth often present a corroded-like appearance.

The prevalence of dental fluorosis and community fluorosis index (CFI) were calculated. CFI was calculated based on the symptoms classifications of dental fluorosis, viz., normal, questionable, very mild, mild, moderate, moderately severe and severe. The number of children in each category was multiplied by the corresponding numerical weight, the products thus obtained for the various categories were added up and the total sum was divided by the total number of people surveyed, giving the community fluorosis index.

2.4 Statistical analysis

The statistical analysis was performed by t-test and Chi-square tests with a 5% significance level.

3 Rusults

3.1 Level of fluoride in water samples

In the village A, the fluoride distribution of water samples ranged from 0.15 mg/L to 0.13 mg/L. The mean value of fluoride was 0.14 mg/L and the standard deviation was 0.01 mg/L. While in the village B, the fluoride concentration in water samples ranged from 1.81 mg/L to 0.66 mg/L. The mean value of fluoride and the standard deviation were 1.22 mg/L and 0.56 mg/L, respectively.

3.2 Level of fluoride in urine samples

The data on fluoride distribution in urine samples in children have been given in Table 1. The significant difference was found between the two villages children's urinary fluoride levels ($P < 0.01$).

Table 1. The level of fluoride in urine of children (mg/L)

Group	Cases (n)	Fluoride ($\bar{x} \pm s$)
A	50	0.62 ± 0.54
B	50	1.49 ± 0.79

t-test, $t = -6.45$, $P < 0.005$

3.3 Dental fluorosis

The results of percentage incidence of dental fluorosis and CFI obtained for both groups were given in Table 2. There was significant difference in prevalence of dental fluorosis between two villages' children ($P < 0.01$). The predominant category of dental fluorosis in group A and group B was very mild (12.6% and 32.2%), followed by questionable (12.6% and 16.1%), mild (0.9% and 8.0%), moderate (0% and 2.3%), and severe (0% and 1.5%) (Table 3).

Table 2. Percentage of dental fluorosis and Dean's Index in children

Group	Cases(n)	Positive cases(n)	Prevalence(%)	CFI
A	111	15	13.51	0.22
B	87	38	43.68	0.68

Chi-square test, $\chi^2 = 22.46$, $P < 0.005$.

3.4 Correlations of dental fluorosis, fluoride level in drinking water and in urine

Significant correlation was found between stages of dental fluorosis and fluoride levels in drinking water. There was also a significant correlations between dental fluorosis and fluoride level in urine (Table 3).

Table 3. Correlations between dental fluorosis and fluoride in water, fluoride in urine

Group	Fluoride in water (mg/L)	Fluoride in urine (mg/L)	Stage of dental fluorosis (*n*)					
			normal	questionable	very mild	mild	moderate	severe
A	0.14	0.62	82	14	14	1	0	0
B	1.22	1.49	35	14	28	7	2	1

Stage of dental fluorosis *vs*. fluoride level in water, $\chi^2=21.73$, $P<0.005$
Stage of dental fluorosis *vs*. fluoride level in urine, $\chi^2=21.73$, $P<0.005$

4 Discussion

High amounts of fluorides in drinking water is the common reason resulting in dental fluorosis. Positive correlation was found between fluoride concentrations in groundwater and occurrence of dental fluorosis in several studies[4,5]. On the other hand, there are many people in the world such as in US receiving drinking water from municipalities that add fluoride to their water systems to prevent dental carries. Some researches have shown carries reduction of up to 40% after fluoridation[6,7]. Although the efficacy of drinking-water fluoridation is well accepted by the policy makers, the benefits are not without consequence. Children from a fluoridated community in Republic of Ireland showed a prevalence of 36% with dental fluorosis[8]. People have paid more attention on the low fluoride level in drinking water with low caries but prevalence of dental fluorosis in children[9].

Both of the two villages investigated are from endemic fluorosis area where altering water sources to lower the fluoride level has been taken to control the endemic fluorosis for more than 10 years. However, the prevalence of dental fluorosis can be affected by the low fluoride concentration less than 1 mg/L in the drinking water[10]. As shown in Table 2, the prevalence of dental fluorosis was significantly lower in the group of children drinking water with 0.14 mg/L fluoride as compared to the group of children drinking water with 1.22 mg/L fluoride. For the more, the stages of children's dental fluorosis tended to become more severe with the rising of fluoride concentration in drinking water (Table 3).

When the CFI value is higher than 0.6, fluorosis is considered to be a public health problem in that area. Although the CFI in both groups were lower than 1.0 (medium public health significance of fluorosis), there were still 13.5% dental fluorosis (mostly very mild to mild) caused by the drinking water with fluoride level of 0.14 mg/L. As for the drinking water with fluoride level of 1.22 mg/L, slightly above optimum levels of exposure recommended by WHO (1.0 mg/L), the prevalence of dental fluorosis was 43.68% and severe case was observed (Table 3). Therefore, it would be necessary to keep close monitoring of the fluoride concentration in drinking water and dental fluorosis in the children of right age in this area.

Besides fluoride in drinking water, there are other sources of fluoride that contribute to overall fluoride intake and therefore may contribute to dental fluorosis, such as fluoride toothpaste, food grown in soil containing fluoride or other uncertain source[11]. When assessing the levels of fluoride ingestion, it's difficult to determine the fluoride intake from all potential sources. As urine is the main excretion route for ingested fluoride, and when persons have taken fluoride for a long time and have reached a steady state of balance, they ultimately excrete via urine every day an amount of fluoride essentially equivalent to the amount consumed, so fluoride concentration in urine has a direct relation with intake of fluoride iron and can be an index of total exposure. 24-hour urinary fluoride excretion and the fractional urinary fluoride excretion were used to estimate the total fluoride intake in some studies[12, 13]. The 24-hour urinary fluoride excretion and the fractional urinary fluoride excretion are more reliable than spot sample. Although large variations were observed in the individual urinary fluoride levels, which may be the result of different age, eating and drinking habit, urine pH, urine flow rate, kidney status, and other factors, analysis of spot fluoride concentration in urine is a useful way to estimate the overall fluoride intake of population[14]. In this study, it's reported that as the degree of dental fluorosis increased from normal to severe, the level of spot urinary fluoride excretion was increased. It's suggested that spot sample of urinary fluoride excretion can be used as an indicator for monitoring the dental fluorosis risk when it is not feasible to obtain reliable 24-hour urinary samples.

Correspondence to:
Liuxin Cui
Department of Environmental Health
College of Public Health

Zhengzhou University
Zhengzhou, Henan 450052, China
Telephone: 86-371-6778-1796
Email: clx@zzu.edu.cn

References

1. Tan BS, Razak IA, Foo LC. Fluorosis prevalence among schoolchildren in a fluorided community in Malaysia. Community Dent Health 2005; 22(1): 35－9.
2. Ruan JP, Liu ZQ, Song JL, *et al*. Effect of drinking water change upon the dental fluorosis. Chinese Journal of Stomatology 2004; 39(2): 139－41.
3. Wang BB, Zheng BS, Wang HY, *et al*. Relationship between fluorine concentration in drinking water and dental health of residents in fluorine exposure areas in Bazhou City. Chin J Endemiol 2005; 24(1): 70－2.
4. Shomar B, Muller G, Yahya A, *et al*. Fluorides in groundwater, soil and infused black tea and the occurrence of dental fluorosis among school children of the Gaza strip. J Water Health 2004; 2(1): 23－35.
5. Chandrashekar J, Anuradha KP. Prevalence of dental fluorosis in rural areas of Davangere, India Int Dent J 2004; 54(5): 235－9.
6. Zusman SP, Ramon T, Natapov L, *et al*. Dental health of 12-year-olds in Israel-2002. Community Dent Health 2005; 22(3): 175－9.
7. Pieper K, Schulte AG. The decline in dental caries among 12-year-old children in Germany between 1994 and 2000. Community Dent Health 2004; 21(3): 199－206.
8. Whelton H, Crowley E, O'Mullane D, *et al*. Dental caries and enamel fluorosis among the fluoridated population in the Republic of Ireland and non fluoridated population in Northern Ireland in 2002. Community Dent Health 2006; 23(1): 37－43.
9. Acharya S. Dental caries, its surface susceptibility and dental fluorosis in South India. Int Dent J 2005; 55(6): 359－64.
10. Ruan JP, Yang ZQ, Wang ZL, *et al*. Dental fluorosis and dental caries in permanent teeth: rural schoolchildren in high-fluoride areas in the Shanxi Province, China. Acta Odontol Scand 2005; 63(5): 258－65.
11. Conway DJ, MacPherson LM, Stephen KW, *et al*. Prevalence of dental fluorosis in children from non-water-fluoridated Halmstad, Sweden: fluoride toothpaste use in infancy. Acta Odontol Scand 2005; 63(1):56－63.
12. Ketley CE, Cochran JA, Holbrook WP, *et al*. Urinary fluoride excretion by preschool children in six European countries. Community Dent Oral Epidemiol 2004; 32 (Suppl 1): 62－8.
13. Franco AM, Saldarriaga A, Martignon S, *et al*. Fluoride intake and fractional urinary fluoride excretion of Colombian preschool children. Community Dent Health 2005; 22(4): 272－8.
14. Heintze SD, Bastos JRM, Bastos R. Urinary fluoride levels and prevalence of dental fluorosis in three Brazilian cities with different fluoride concentrations in the drinking water. Community Dent Oral Epidemic 1998; 26 (5): 316－23.

Received April 29, 2006

The Composition and Antifungal Properties of the *Erythrophleum Suaveolens* Guill and Perr. (Leguminosae) Seeds and Oil

Adekunle A. Adedotun, Aya E. Linda, Dabiri O. Olusola

Department of Botany and Microbiology University of Lagos, Yaba, Lagos, Nigeria

Abstract: This study investigated the composition of the *Erythrophleum suaveolens* seed and oil, as well as the antifimgal activity of the oil extracted on some dermatophytic fungi were analyzed. The moisture content of the healthy *E. suaveolens* seeds was 7.50 + 0.61%; while the oil yield (quantity of oil) was 36.00 + 0.34%; 17.50 + 1.28% protein and 27.37 + 0.86% crude fiber. The oil extracted from the *E. suaveolens* seed (quality of oil) was edible and non-rancid with free fatty acid value of 2.17 + 0.34%; peroxide value of 2.57 + 0.89 meq/kg; iodine value 3.14 + 0.68%; unsaponsifiable matter of 16.54 + 0.40 g/kg and refractive index of the oil at 40 °C was 1.52 + 0.32. The oil showed significant antifungal activity against the dematophytes tested *Aspergillus flavus*, *A. niger*, *A./vanity*, *Candida albicans* and (*Microsporum gyseum*), above the 10 mm recommended standard for a good inhibition. The antifungal activity of the orthodox antibiotic, Nystatin, was significantly higher than that of oil on the fungi tested. [Life Science Journal. 2006;3(4):61 - 64] (ISSN: 1097 - 8135).

Keywords: antifungal activity; *Erythrophleum suaveolens*; seeds; oil quality; heavy metals

Abbreviations: AAS: atom absorption spectrometer; FFA: free fatty acid; SDA: saboraud dextrose agar

1 Introduction

The tropical rainforest in Africa is endowed with yet fully exploited economic trees. One of such trees is *Erythrophleum suaveolens* Guill and Perr. in the family lequninosae, commonly called sasswood or red water wood. It is called "Ingi" or "orachi" in Igbo and "Emin" or "Obo" in Yoruba[1]. In Nigeria, *E. suavelons* is cultivated in the southeastern states and eaten mainly by Igbos. The seeds of *E. suaveolens* are used as a soup thickener for various dishes. The seed of *E. suaveolens* are relatively cheap to purchase thus used by natives to replace melon "egusi" seeds in preparing the staple vegetable soup in the southeastern Nigeria. In Uganda, the fruit is a favorite food of elephants and they are reported to be responsible for dispersing the seeds[2]. The bark of *E. suaveolens* tree is used as an arrow poison. In large does, the bark extracts occasions a progressive loss or mental reflexes, when applied to animal, that later leads to muscular relaxation, paralysis of the heart and eventual death. Analysis of the bark extracts yields an alkaloid called erytrophleine[3]. *E. suaveolens* bark extracts was claimed to be used in the treatment of heart disease traditionally in Nigeria, though not adopted in modern medicine, but it is said to be of use in the treatment of spasmodic asthma[2].

Seeds are usually one of the sources of the propagation of plants as well as source of food[4]. During harvesting and storage, fungi, bacteria, insects etc attack seeds. Some workers have studied the nutritive value of seeds, which include groundnuts[5], maize[6], palm kernels[7], cocoa beans[8], and melon seeds[9]. These workers have helped evaluate the nutritive value of the seed and seed oil quality. To confirm the identity of most oils and fats, it is normally considered sufficient to determine the iodine value, saponification value, unsaponifiable matter, free fatty acid (FFA) value and peroxide value coupled with qualitative tests for appropriate adulterants[10]. The rancidity of the oil will also indicate the quality of the oil and affect its uses for soap, cream production and edibility.

The FFA and peroxide value can be used to measure rancidity of the oil[11,12]. The composition of the seed, and oil extracted from the seed of *E. suaveolens*, as well as the antifungal activity of the extracted oil have not been reported in literature.

As a continuation of studies in this laboratory on the composition of indigenous African seed plants food, the composition of the *E. suaveolens* seed and its oil is presented here. Also reported are some of the biochemical properties (Saponification value, unsaponifiable matter, peroxide, FFA value and Iodine value), and antifungal properties of the oil extracted from the *E. suavelons* seed. This is

to help access and document the quality of some African foods with respect to *E. suaveolens* seeds.

2 Materials and Methods

2.1 Source of plant materials

The seeds of *E. suaveolens* (1,000 g) were collected from Oyingbo market in Lagos State, Nigeria. The seeds were packed in polythene bags and stored in a refrigerator prior to use. The percentage moisture content of the seeds was determined at 103 °C for 17 hours as described by Agrawal[13].

2.2 Composition of *E. suaveolens* seed

The percentage carbohydrate content of the *E. suaveolens* seed was determined using the methods of Egan *et al*[14]. The methods of Lowry *et al*[15] was used to determine the percentage protein content of *E. suaveolens* seed, while the crude fiber content of the seed was determined using Diamond and Denman methods[16].

2.3 Extraction of oil

The method of extraction of oil is *E. suaveolens* seed was adopted from the oil extraction methods of Egan *et al*[14]. The seeds were ground using a ceramic pestle and mortar before blending in an electric blender. An amount of 20 g of the ground seed was packed into the extraction thimble before covering with a small ball of cotton wool. The thimble was inserted in a quick fit plain body soxhlet extractor. Petroleum either in the quantity of 200 ml (60 – 80 °C) was poured in a 250 ml round-bottom flask of known weight, which was connected to the extractor, and refluxed on an electric thermal heater for 5 hours. The ether was then collected in the plain body extractor and then separated from the flask that contained oil. The flask containing the oil was then heated in an oven at 103 °C for 30 minutes. It was cooled and weighed to get the final weight. The percentage oil content of the sample was calculated using the ratio of the amount of oil produced to the weight of sample used expressed as a percentage. The procedure was repeated until at least 250 ml of essential oil was extracted from the seeds.

2.4 Biochemical properties of the *E. suaveolens* seed oil

The quantity of oil extracted from the seed was determined as a percentage of the oil extracted, expressed over the weight of the seed used as described by Diamond and Denman[16]. The method of Anonymous[17] was used to determine the quality of oil extracted from the seeds, the saponification value, unsaponifiable matter, peroxide value and iodine value. The FFA value was determined according to the method of Egan *et al*[14].

2.5 Heavy metal determination

The method of Solomon[18] was used in the heavy metal determination. An amount of 4.4413 g of the ground seed was weighed into an already made carbon that was charging. This was then put into flurothen furnace at 580 °C for one hour at ash the seed. The ash was dissolved with 10 ml-distilled water in a 100 ml volumetric flask, and 1 ml of HCL was added and gently shaken for proper homogenization. The volume of the solution was made up to 100 ml mark of the flask using distilled water. The solution was then placed in an atom absorption spectrometer (AAS) to aspirate for the presence of elemental metal. Aspiration was done by putting hallow cathode lamp for each metal and the concentration of each heavy metal was measured against a standardized grade[19].

2.6 Antifungal activity of the oil extracted from *E. saveolens*, seeds

A modification of the paper disc diffusion method of Irobi and Daramola[20] was used. Spore or conidia suspension of $10^5 - 10^7$ cells were counted using haemocytometer. About 10 ml Saboraud dextrose agar (SDA) were poured into Petri dishes and allowed to solidify. A micro-pipette was used to introduce 0.1 ml of the spore or conidia suspensions onto the agar plate; spreading was done with a spreading rod under sterile conditions. The fungi, *Aspergillus flavus*, *Aspergillus niger*, *Aspergillus wentii Candida albicans* and *Microsporum gyseum* were obtained from infected skin of a patient at the College of Medicine, University of Lagos, Nigeria. Sterilized paper discs (6 mm, Whatman No, AA 201 7006) were soaked in *E. suaveolens* seed oil for 6 hours. Four of these soaked discs were spread on a fungal inoculum seeded plate with the help of sterile forceps. There were two controls, the first contained the SDA and Fungal inoculum but the discs were soaked in the antibiotics, Nystatin (l00 mg/ml). Three replicates were produced for each Fungus per treatment. All the plates containing the discs were then incubated at 28 – 30 °C. The zone of inhibition was measured after 48 – 72 hours of incubation. The experiment was repeated; the results were statistically analyzed to determine the standard errors[21].

3 Results

The moisture content of *E. suaveolens* seeds used in this study was 7.50 + 0.61%, while the mean oil content (quantity of oil) of the seeds was 36.00 + 0.34%. The FFA content of the *E.*

suaveolens seed oil was 2.17 + 0.14%; peroxide value was 2.57 + 0.8% meq/kg; iodine value was 3.14 + 0.68%; saponiflcation value was 904.81 + 19.18 mg/kg; unsaponiflable matter was 16.54 + 0.40 g/kg and refractive index of the oil at 40 °C was 1.52 + 0.23. Health *E. suaveolens* seeds contain 9.30 + 0.25% carbohydrate and 17.50 + 1 − 28% protein.

The summary of the heavy metal composition of *E. suaveolens* seed is shown in Table 1. The crude fiber content of the seed is 27.37 + 0.86%. The oil extracted from *E. suaveolens* seed showed antifungal activity against the dermatophytes tested, and the zone of inhibition was above 10 mm. The antibiotic, Nystatin, had zone of inhibitions higher than the oil (Table 2).

Table 1. Percentage heavy metal content of *E. suaveolens* seeds

Parameter	Percentage heavy metal content of seeds(%)
Zinc (Zn)	0.003
Iron (Fe)	0.060
Lead (Pb)	N.D*
Copper (Cu)	N.D
Nickel (Ni)	N.D
Sodium (Na)	N.D
Potassium (K)	0.250

* N.D means not detected

Table 2. Antifungal activity of the oil extracted from *E. suaveolens* seeds

Sample	Zone of Inhibition (mean + JS.E mm) Fungi				
	Aspergillus flavus	*Aspergillus niger*	*Aspergillus ventii*	*Candida albicans*	*Microsporum gyseum*
Control	0.00 + 0.00a*	0.00 + 0.00a	0.00 + 0.00a	0.00 + 0.00a	0.00 + 0.00a
Nystatin	26.69 ± 0.246	26.89 ± 0.31b	26.38 + 0.72b	28.00 ± 0.55c	27.89 ± 0.346c
Oil extracted from *E. suaveolens*	11.19 ± 0.89d	10.06 ± 0.10d	14.00 + 0.37e − *	11.00 ± 0.18d	14.05 ± 0.08e

* Zone of inhibition with similar letters show no significant difference at $P = 0.01$
Zone of inhibitions with different letters show significant difference at $P = 0.01$

4 Discussion

This investigations showed that the oil extracted from *E. suaveolens* seed is edible, because the qualitative properties of the oil fits the description of edible oil by Kirk[11] and International Seed Testing Association[22]. *E. suaveolens* seed has a good oil yield of 36.00% and comparable to the oil yield of *Arachis* of 38.50% and *Glycine soja* of 36.40%[10]. The peroxide value of *E. suaveolens* is 2.57 meq/kg. Perl and Krestchemer[23] explained that peroxide value below 10 meq/kg showed that the oil involved is a non-rancid oil. The FFA content of the *E. suaveolens* seed oil is 2.17% and below the 5.00% FFA content recommended for non-rancid oil[24,25], implying that the oil of *E. suaveolens* seed is non-rancid. The high saponification value of the oil indicates that it could be used as a base for soap manufacture. Ekundayo and Idzi[26] explained that saponification value has an inverse relationship with the chain length of the fatty acid in the oil, that is the higher the seed oil saponification value the lower the chain length and *vice versa*.

The oil from *E. suaveolens* seed probably has a broad-spectrum antifungal activity. The zone of inhibition is above the 10 mm mark recommended by Zygadlo and Grosso[27]. Even though the antifungal activity of the *E. suaveolens* seed oil is lower than that of the check antibiotic, Nystatin, it is of significance that the oil has antifungal properties, which provide an indication that probably soup made from *E. suaveolens* seed could be medicinal. The fact that the seed oil was not purified might be responsible for its lower antifungal activity to the nystatin. If the seed's oil active ingredient is isolated and used, it might be more potent than the nystatin at the same concentration.

The heavy metal composition of the seed sample used, had very low heavy metal component below the 0.95% heavy metal value, which is regarded as safe food for human consumption[28]. In some cases a few elements were not detected during the analysis.

These results indicate that the oil *E. suaveolens* seed is edible and non-rancid. It also shows that the oil is non-toxic (does not contain heavy metal) for human consumption, which can also be used as a base for body or hair cream production. Results here suggest that the *E. suaveolens* seed oil is fungi toxic and probably have a broad-spec-

trum antifungal property. The study also provides some evidence that the *E. suaveolens* seed oil is of high nutritional value, a justification for its consumption by the African natives.

Acknowledgement

The authors thank the Director of Federal Institute of Industrial Research, (FIIRO), Oshodi, Lagos, Nigeria, for allowing the use of some equipments during the heavy metal analysis.

Correspondence to:
Adekunle A. Adedotun
Department of Botany and Microbiology
University of Lagos, Yaba, Lagos, Nigeria
Email: aaded@yahoo.com

References

1. Hutchinson L, Dalziel JM. Flora of West Tropical Africa. Crown Agents for Oversea Governments and Administrations, London 1927; 395.
2. Burkill HM. The Useful Plants of West Tropical Africa. Vol 3 Royal Botanic Gardens, Kew 1995; 969.
3. Kokwaro JO. Medicinal Plants of East Africa. East Africa Literature Bureau, Nairobi 1976; 976.
4. Oyeniran JO. Rep. Nigerian Stored Products Research Institute Occasional Paper Series 1980; 2: 1－25.
5. Gray JE. Native Methods of Preparing Palm Oil. A Bulletin of Dept of Agric Nigeria 1922; 2:29－50.
6. Okafor N. Thermophilic micro-organisms from rotting maize. Nature 1996; 210:220－1.
7. Kuku PO. Studies on the ftingal deterioration of Nigerian palm Kernel. MSc Thesis, University of Ibadan 1974; 87.
8. Oyeniran JO. Rep. Nigerian Stored Produ Res Institute, Technical Report 1975; 7:30－5.
9. Adekunle AA, Uma NU. Effect of some fungi on germination and biochemical constituents of Cucumeropsis manni Naud-Holl seeds. International Journal of Plant Disease 1997; 75: 59－73.
10. Hamilton RS, Rossel JB. Analysis of Oils and Fats. Elseiver Applied Science Publishers, New York 1986; 600.
11. Kirk SR. Pearson's Composition and Analysis of Food. Longman Publishers, London 1991; 708.
12. Langanau IEE. The Essential Oil. Vol 2. Krieger Publishing Co, New York 1984; 348.
13. Agrawal RL. Seed Technology. Oxford and IBM Publishing Company, New Delhi 1980; 685.
14. Egan H, Kirk HS, Sawyer R. Pearson's Analysis of Foods. Churchill Living Stone Publishers, London 1981; 596.
15. Lowry OH, Rosebugh NJ, Faw AL, Randall RZ. Protein measurement with the folin phenol reagent. Journal of Biological Chemistry 1951; 193: 265－75.
16. Diamond PS, Denman RF. Laboratory Techniques in Chemistry and Biochemistry. 2nd Edition. Butterworths, London 1973; 522.
17. Anonymous. Methods of Analysis of the Association of Official Analytical Chemists. 14th Edition. Association of Official Analytical Chemists, Washington DC 1990; 1018.
18. Solomon HM. Laboratory Manual of Chemical Methods of Foods and Non-Foods. FIIRO Analytical Services Divisions, Lagos 1982; 200.
19. Lone MI, Aleem SS, Ahmod AKS, Hussain GH. Heavy metal content of vegetable irrigated by sewage/tube will water. Int Journal of Agric and Biology 2003; 4: 533－5.
20. Irobi ON, Daramola SO. Antifungal activities of crude extracts of mitracarpus villosus. Journal of Ethnopharmacology 1993; 40: 137－40.
21. Parker RE. Introductory Statistics for Biology. 2nd Edition EdwarArnold, London 1979; 122.
22. International Seed Testing Association. Seed Science and Technology 1999; 27: 1－333.
23. Perl M, Kretshamer M. Biochemical activities and compounds in seeds: possible tools for seed quality evaluation. Annals of Botany 1988; 62: 61－8.
24. Adekunle AA, Badejo AA. Biochemical properties of essential oil extracted from Cyperus esculentus corm. Tropical Agriculture 2000; 77(1): 1－4.
25. Kuku PO. Fungal deterioration of Nigerian melon seeds (Citrillus vulgar is Schrad). Rep. Nigerian Stored Product Research Institute Technical Report 1980; 27: 63－71.
26. Ekundayo C, Idzi E. Mycoflora and nutritional value of shelled Melon seeds (Citrillus vularis schard) in Nigeria. Plant Foods for Human Nutrition 1990; 42: 215－22.
27. Zygadlo JA, Grosso NR. Comparative study of the antifungal activity of essential oils from Aromatic plants graving wild in the central region of Argentina. Flavour and Fragrance Journal 1995; 10 (2): 113－8.
28. Kansal BD, Singh J. Influence of municipal and soil proterties on accumulation of heavy metals in plants. Journal of Environmental Pollution 1983; 6: 13－6.

Received October 3, 2006

Orthodontic Treatment of 41 Patients with Tooth Size Discrepancy

Aixia Li

Department of Orthodontics, The First Affiliated Hospital of Zhengzhou University, Zhengzhou, Henan 450052, China

Abstract: Objective. To retrospectively study the better orthodontic method for individuals with tooth-size discrepancy through analyzing changes between pre-and post-treatment. **Methods.** 41 orthodontic patients with tooth-size discrepancy were selected. The mesiodistal diameters of teeth were measured with a pair of dividers (accurate to 0.1mm) and Bolton's indices were calculated. The patients were treated with straight wire appliance by extracting teeth, restoring correlated tooth and stripping of enamel, etc. **Results.** After treatment, the patients had normal overjet and overbite in anterior teeth and class I relationship inter-arch. **Conclusions.** It is necessary to be the proper Bolton ratio between inter-arch tooth sizes for the good occlusal relationship. The results suggested that dentists should always keep in mind the general Bolton ratios analysis between maxillary and mandible tooth size during the practice for each patient. [Life Science Journal. 2006;3(4):65-67] (ISSN: 1097-8135).

Keywords: tooth-size discrepancy; Bolton ratios; occlusal relationship

Abbreviations: BR: Bolton ratios; OC: occlusal relationship; TSD: tooth-size discrepancy

1 Introduction

In order to obtain excellent and stable occlusal relationship(OR), it is necessary to be the appropriate Bolton ratios(BR) between upper and lower dentitions. If the tooth-size ratios intermaxillary is disharmony, it is needed to select tooth extraction or decrease the width of related tooth or change the axial inclination degree of anterior tooth, etc.

2 Materials and Methods

2.1 Subjects

41 patients with tooth-size discrepancy(TSD) were selected from those who applied for orthodontic treatment in the First Affiliated Hospital of Zhengzhou University. There were 18 females and 23 males, whose age ranged from 12.5 years old to 21 years old. All were in the permanent dentition stage, with no evidence of attrition or interproximal caries and restorations. Alginate impressions of the dentitions were taken from each subject, and stone casts were prepared. Cephalometric analysis shows that 41 cases were all mild or moderate crowding, class I of bone and average growth direction.

2.2 Measurement of dental models

A pair of dividers with fine tips was used to measure the maximum mesio-distal widths of the teeth on dental casts of pre-post treatment. Using the dividers, the measurements of each dental arch were recorded by punching along a straight line on a card[1]. When punching adjacent measurements, one leg of the dividers was inserted into the previous pinhole so as to reduce the measurement error to a minimum. Anterior arch lengths (canine to canine) and total arch lengths (first molar to first molar) were then measured using a millimetre ruler. Then calculate the Bolton index and crowding. All the work was carried out by the author.

The Bolton anterior ratio (the ratio of the mesio-distal widths of six anterior teeth between upper and lower dentition) and the Bolton overall ratio (the ratio of the mesio-distal widths of the 12 teeth between upper and lower dentition) were calculated[2].

2.3 Classification

All cases included 13 microdontia of upper lateral incisor which showed smaller mesio-distal width of lateral incisor and the larger sizes of the lower anterior teeth, 19 smaller Bolton anterior ratios which showed that the size of lower anterior teeth was smaller than normal(except for deformed crown and congenital loss), 6 larger Bolton anterior ratios which showed the size of lower anterior teeth was more than normality (except for deformed crown and congenital loss), 2 normal anterior Bolton ratios other than disharmony posterior ratios, 1 congenital absence of lower incisor leading to smaller size of lower anterior teeth.

2.4 Orthodontic treatment

Straight wire appliance was used to align and level dentition, then harmonize the relationship intermaxillary. After the fixed appliance was removed, Hawley retainer was worn.

For mild lateral incisor of microdontia, and mild crowding(<2mm) in lower dentition, stripping of enamel of lower incisors was applied to obtain harmony tooth-size. On the contrary, if lower dentition crowding was severe, one lower incisor was extracted. For severe lateral incisor of microtooth and severe or moderate crowding, 4 premolars were extracted, and the deformed tooth was restored after orthodontic treatment. For 13 cases, one lower incisor was extracted from each 6 patients, 4 premolars were extracted from each 4 cases and restored deformed tooth after treatment, and stripping of enamel was used for 3 cases.

In order to obtain harmonious tooth size and excellent OR between upper and lower arch, for mild crowding, stripping of enamel and changing of axial inclination were used. For severe crowding, after extracting 4 premolars and leveling dentition, calculated Bolton index and selected stripping of enamel and changing of axial inclination.

After orthodontic treatment, the incisor was restored for 1 patient with congenital loss of lower incisor in order to obtain normal overjet, overbite and excellent posterior relationship. For disharmony posterior ratio, stripping of enamel was used to obtain good occlusion.

3 Results

There were normal overbite and overjet in anterion teeth and neutral occlusal relationship in posterior teeth. X-ray cephalometrics showed that the SNA, SNB angle and the anterior tooth protrusion degree were normal.

Typical case: Male, 14 years old, Han nationality. The relationship between upper and lower molars was distal cusp to cusp; 2.5 mm upper dentition crowding degree, 7 mm lower crowding, Ⅲ degree deep overbite, Ⅱ degree deep overjet. Upper tooth size was lower because of microdontia of lateral incisor. X-ray cephalometrics showed that (1) average growth pattern, (2) mandible bone retrusion, (3) normal protrusion of upper and lower incisors. Treatment process: lower central incisor was extracted and straight wire appliance was used. See Figure 1 for before and after treatment.

4 Discussion

In 1960s, BR was indicated that appropriate ratio is very important for good occlusion. TSD is the factor of dentition crowding and space, disharmony of inter-arch and other complicated malocclusion. Studies have reported from 20% to 30% of people with significant tooth-size anterior discrepancies and 5% – 14% for overall TSD[3]. A high prevalence of tooth size discrepancies in an orthodontic patient population and the statistically significant correlation of some of these with some dental characteristics suggest that the measurement of inter-arch tooth size ratios might be clinically beneficial for treatment outcomes[4]. For these patients, it is necessary to measure and analyze Bolton anterior and overall ratio. Then the dentist will select relevant methods according to the degree of ratio disharmony.

In this article, 5 kinds of discrepancy were described for they were common in clinical practice. According to cast models analysis, cephalometric analysis and trial of aligning teeth, it wasn't difficult to make treatment planning.

In some cases, the finishing phase is very difficult, requiring the production of complicated biomechanical forces to reach a satisfactory orthodontic solution. A high percentage of these finishing-phase difficulties arise because of tooth size imbalances that could have been detected and considered during initial diagnosis and treatment plan[5]. The correlation between anterior TSD and Angle's Class Ⅰ, Ⅱ, and Ⅲ malocclusions, as well as their prevalence are as follows: (1) Individuals with Angle Class Ⅰ and Class Ⅲ malocclusions show significantly greater prevalence of TSD than do individuals with Class Ⅱ malocclusions; and (2) Mean anterior TSD for Angle Class Ⅲ subjects was significantly greater than for Class Ⅰ and Class Ⅱ subjects[6].

In typical case, upper lateral incisor was not restored because of acceptable shape. After treatment, lower central incisor was consistent to facial midline. If the lateral incisor were restored after 4 second premolars extracted, the restoring process would be complicated and long. The patient and parents wouldn't accept this situation, so previously mentioned method was adopted.

In conclusion, it is necessary to analyze the BR before and during orthodontic treatment.

Left: before treatment Right: after treatment
Figure 1. Intra-oral photographs before and after treatment

Correspondence to:
Aixia Li
Department of Orthodontics
The First Affiliated Hospital
Zhengzhou University
Zhengzhou, Henan 450052, China
Telephone: 86-371-6607-7592
Email: liai73@sina.com.cn

References

1. Baydas B, Oktay H, Metin Daqsuyu I. The effect of heritability on Bolton tooth-size discrepancy. European Journal of Orthodontics 2005; 27(1):98－102.
2. Bolton WA. Clinical application of a tooth-size analysis. Am J Orthod 1962; 48(7):504－29
3. Othman SA, Harradine NW. Tooth-size discrepancy and Bolton's ratios: a literature review. Journal Orthod 2006;33(1):45－51.
4. Akyalcin S, Dogan S, Dincer B, *et al*. Bolton tooth size discrepancies in skeletal Class I individuals presenting with different dental angle classifications. Angle Orthod 2006;76(4):637－43
5. Basaran G, Selek M, Hamamci O, *et al*. Intermaxillary Bolton tooth size discrepancies among different malocclusion groups. Angle Orthod 2006;76(1):26－30.
6. Araujo E, Souki M. Bolton anterior tooth size discrepancies among different malocclusion groups. Angle Orthod 2003; 73(3):307－13.

Received September 12, 2006

Water Quality Assessment of Behta River Using Benthic Macroinvertebrates

Mahendra Pal Sharma, Shailendra Sharma, Vivek Goel, Praveen Sharma, Arun Kumar

Alternate Hydro Energy Centre, Indian Institute of Technology, Roorkee 247667, Uttaranchal

Abstract: Aquatic macroinvertebrates play significant role in responding to a variety of environmental conditions of rivers and streams and therefore may be used as bio-indicators for water quality assessment. In the past, biological communities like plankton, periphyton, microphytobenthos, macrozoobenthos, aquatic macrophytes, fishes etc. have been used for the assessment of water quality of rivers and streams, but now the use of benthic macroinvertebrates as bio-indicators is gaining importance as these can be easily caught and seen with naked eyes and the method is less costlier and less time consuming compared to other methods given above. Behta River of Paonta Sahib in Himachal Pradesh was chosen to assess the suitability of river water for drinking purposes. The present study involved sampling, pre-identification and identification of macroinvertebrates and computing the percent of occurrence of families of various taxonomic groups and conducting physico-chemical analysis of samples from selected location. Macroinvertebrates chosen were identified up to family level, and bio-assessment at various locations has been done using NEPBIOS score system. It was found that out of total 30 genus belonging to 10 families of taxonomical group like *Ephemeroptera*, *Trichoptera*, *Plecoptera*, *Coleoptera*, *Heteroptera*, *Odonata*, *Diptera Mollusca*, *Oligochaetes* etc. have been found in different composition inhabiting the river. The results further show that all the locations assessed for quality using macroinvertebrates and physico-chemical analysis are in the range of water quality class Ⅲ (Moderately Polluted) and the water can not be used for drinking purposes. The measures to reduce point and non-point sources of pollution have been suggested to get the quality suitable for drinking purposes. [Life Science Journal. 2006;3(4):68-74] (ISSN: 1097-8135).

Keywords: benthic macroinvertebrates; indicators; NEPBIOS; NSF water quality index

Abbreviations: NSF: National Sanitation Foundation; NEPBIOS: Nepalese Biotic Score; WQI: water quality index; APHA: American Public Health Association; ASPT: average score per taxon; BOD: biochemical oxygen demand; DO: dissolved oxygen; NTU: nephelometric turbidity unit; U/S: upstream; D/S: downstream

1 Introduction

Aquatic macroinvertebrates play significant role in responding to a variety of environmental conditions of rivers and streams and therefore may be used as bio-indicators for water quality assessment. Benthic macroinvertebrates are the animals that lack a back-bone and generally are visible with the naked eyes. They live in the lower areas of the streams under rocks. They include larval forms of many common insects such as Dragon flies, Damsel flies and Crane flies. Common features of these are as follows:

* Live in water for all or most of their life. Often live for more than one year.
* Stay in the area suitable for their survival.
* Differ in their tolerance to amount and types of pollution.
* Are easy to identify in the laboratory.
* Have limited mobility.

Macro-invertebrate community responses to environmental changes are useful in assessing the impact of municipal, industrial and agricultural waste and impacts from other land uses on surface water. The macroinvertebrates are highly popular as pollution indicators[1].

Benthic organisms are of great significance because they form the food of fishes and their productivity play an important link in the food chain. Benthic organisms are distrivores and form an important link in the food chain, an account of their ability to convert low quality and low energy detritus into better quality food for higher organisms in the food web with the unfolding of the importance of benthos in food chain, benthic productivity has been correlated with fish resources. The qualitative and quantitative changes in the benthic population have also been used as pollution indices[2-4].

Benthic macroinvertebrates are aquatic macrofauna inhibiting the bottom substrate for at least a part of their life cycle. The reason of selecting macroinvertebrates as bio-indicators is that they are visible to unaided eyes and retained on the sieve with a mesh sized of 0.6 mm diameter. They have

sedentary and long life span and sensitive community response to organic loading, thermal impacts, substrate alteration and toxic pollution. Inhabiting the different substratum of river, stream, lake and other water bodies, developed taxonomy and integrated of pollution etc. justifies the reason of selecting them as bio-indicators.

The primary objective of this study was to evaluate the water quality of river Behta for drinking purposes using macroinvertebrates. The other objectives were to describe the importance of using macroinvertebrates as pollution indicator and the bioassessment result validation by physico-chemical analysis using National Sanitation Foundation (NSF) water quality index(WQI). The occurrence of benthic macroinvertebrates community along with the distribution of taxa-group of the river has also been discussed.

2 Materials and Methods

2.1 About Behta River

The Behta River is an important tributary of river Yammuna. It originates in the boulders below the Nahan ridge in the South-Western corner of Himachal Pradesh as the Jalmusa-Ka-Khala (Figure 1). Behta River of Paonta Sahib in Himachal Pradesh was chosen to assess the suitability of river water for drinking purposes.

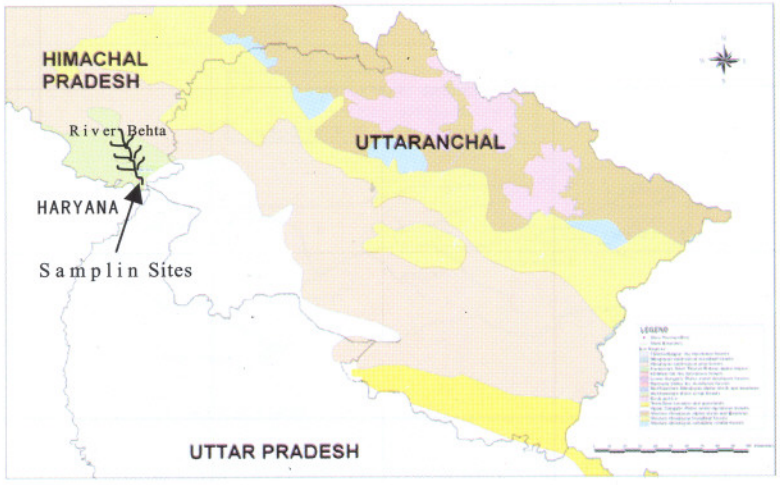

Figure 1. Location map of Himachal Pradesh showing the Behta River

Physico-chemical and biological parameters for two sites on the river Behta at Paonta Sahib were analyzed, and the results revealed that the water quality at the site upstream (U/S) to slaughter house was good which belongs to water quality class Ⅱ, and the water quality at the site downstream (D/S) to slaughter house was moderate which belongs to water quality class Ⅲ. The conclusion of the results is that the water at the D/S to the slaughter house can not be used for the drinking purposes.

This river is mainly fed by the rain water that is cycled as underground water before finally coming up on the surface as a spring. The river flows below the surface for a part of its length in its upper reaches, thereafter the water flows on the surface.

There were two sampling sites selected by us in Paonta Sahib:

i) River Behta at Pownta Sahib U/S to slaughter house (Station-01) at longitude 77.55, lattitude 30.47 and altitude (m) 380.0 (Figure 2).

ii) River Behta at Pownta Sahib 500 m D/S to slaughter house (Station-02) at longitude 77.57, lattitude 30.44 and altitude (m) 369.0 (Figure 2).

The sampling sites are situated within a landscape characterized by cropland, clear cutting, urban sites and industrial activities. 500 m above the sampling site there is a chicken farm. The riverbed is built by meso- and microlithal 60% and 40%, respectively. Filamentous algae and algae tufts are occurring frequently. The average stream width is up to 35 m, mean depth is 40 cm and mean current velocity is 25 cm/s. The water carries foam and is turbid. Mud and stones show reduction phenomena both in lentic and lotic areas.

2.2 Methods

A sample consists of collection of 20 sub-samples each of 0.25×0.25 m^2 taken from all microhabitat types. This procedure (Figure 3) results in sampling of approximately 1.25 m^2 stream bottom

area. Net of mesh size 500 μm is used for collecting the macroinvertebrates. Every large boulder or cobble in the area is picked up if it could be lifted and organisms vigorously washed by hand into the net. Finally, the substrate with smaller boulders should be disturbed by kicking systematically across the area 3 – 4 times such that the invertebrates wash D/S into the net. The organisms are then carefully picked from the net surface and preserved immediately in 80% ethanol or 4% formaldehyde. These samples are returned to the laboratory for processing. Specimen collected are sorted and identified to operational taxonomic unit (at least to family level with the help of regional keys) in the laboratory under a dissecting microscope for identifying the fauna, standard literature was consulted[5-8].

Samples for microbiological examination were collected in non-reactive borosilicate glass bottles that have been cleansed and rinsed carefully, given a final rinse with the distilled water and sterilized in autoclave.

Water samples were collected in plastic container for different physical-chemical parameters. The chemical characteristics were determined by the standard methods suggested of American Public Health Association (APHA)[9] (The results of the analysis are reported in Table 1).

The schematic flow chart of the steps involved in the methodology is given as below (Figure 3).

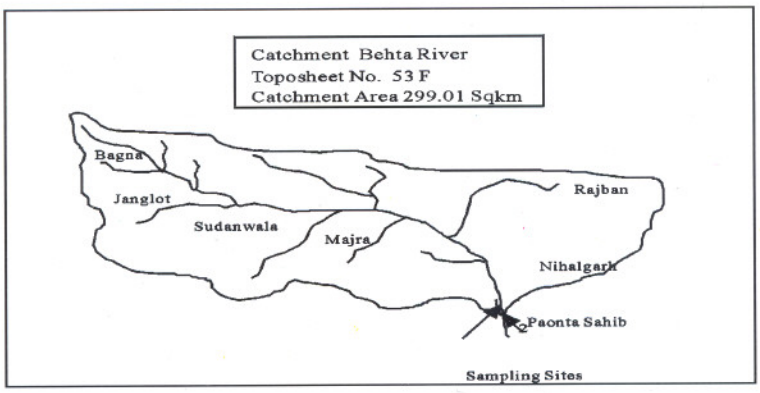

Figure 2. Catchment area of river Behta at Paonta Sahib

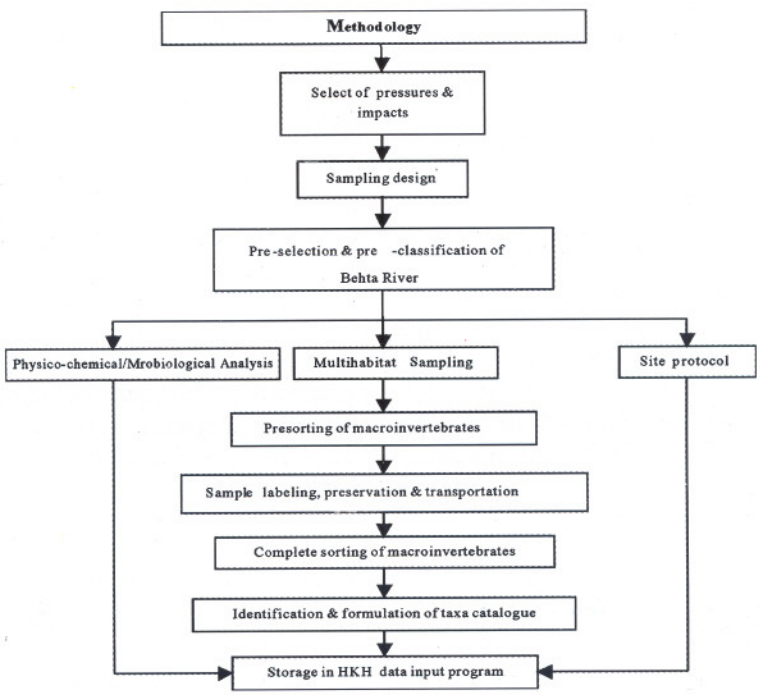

Figure 3. Flow chart of methodology

3 Results and Discussion

3.1 Physical-chemical parameters

Following parameters were analyzed (Table 1).

Table 1. Physicochemical and biological analysis of water samples

Site name	Station-01	Station-02
Pre-classification class	2	3
Estimated discharge [l/s]	510.6	511
Temperature (water) °C	26.5	26.5
Temperature (air) °C	37.0	37
pH	7.84	8.2
Conductivity [μS/cm]	280.0	366
Turbidity NTU	0.84	1.42
Oxygen content [mg/l]	9.54	9.09
% saturation of oxygen	109.4	108.3
Alkalinity [CO_3^{2-}] [mmol/l]	126.0	141
Total hardness [mmol/l]	197.0	201
Chloride [mg/l]	12.2	13.4
Ammonium [mg/l]	0	0
Nitrite [mg/l]	0.001	0.004
Nitrate [mg/l]	0.28	0.3
Ortho-phosphate [μg/l]	98.0	110
Total phosphate [μg/l]	701.0	940
BOD [mg/l]	2.1	3
E. coli [n/100 ml]	500	1600
TDS [ppt]	0.16	0.22
Estimated class using NSF WQI	Ⅱ	Ⅲ
NSF index value	75	69
Water quality index legend	71 – 90	50 – 70

On the basis of these chemical parameters the water quality can be determined using NSF WQI.

NSF WQI: NSF International, founded in 1944 as the NSF, is known for the development of standards, product testing and certification services in the areas of public health, safety and protection of the environment. The index is basically a mathematical means of calculating a single value from multiple test results. The index result represents the level of water quality in a given water basin, such as a lake, river, or stream.

The WQI uses a scale of score from 0 – 100 to rate the quality of the water, with 100 being the highest possible score (Table 2). Once the overall WQI score is known, it can be compared against the following scale to determine how healthy the water is on a given day.

Table 2. WQI quality scale

91 – 100	Excellent water quality
71 – 90	Good water quality
51 – 70	Medium or average water quality
26 – 50	Fair water quality
0 – 25	Poor water quality

Water supplies with ratings falling in the good or excellent range would able to support a high diversity of aquatic life. In addition, the water would also be suitable for all forms of recreation, including those involving direct contact with the water. Water supplies achieving only an average rating generally have less diversity of aquatic organisms and frequently have increased algae growth.

Water supplies falling into the fair range are only able to support a low diversity of aquatic life and are probably experiencing problems with pollution. Water supplies that fall into the poor category may only be able to support a limited number of aquatic life forms, and it is expected that these waters have abundant quality problems. A water supply with a poor quality rating would not normally be considered acceptable for activities involving direct contact with the water, such as swimming.

The range using NSF WQI for the site is 75, which is indicative of good water quality (class Ⅱ).

The range using NSF WQI for the site is 69, which is indicative of moderate water quality (class Ⅲ).

3.2 Biological parameters

The common and dominant families of macroinvertebrates of each group encountered are as follows (Table 3).

The calculation of water quality on the basis of macroinvertebrates families was done on the basis of Nepalese Biotic Score(NEPBIOS) using pre-classification sheet.

NEPBIOS biotic index: A suitable biological method based on indices or score system is possible only when local reference communities are properly scored. Taking this fact into consideration the Nepalese taxa were scored, the average score per taxon (ASPT) calculated and a different biotic score method for Nepal developed with the NEPBIOS (Table 4). The calculation of the water quality on the basis of the presence of the macroinvertebrates families is done on the basis of NEPBIOS using the pre-classification sheet.

Table 3. Occurrence of benthic macroinvertebrates community

Taxonomic group		Family	Behta at Paonta Sahib 10 m U/S to slaughter house(Station-01)		Behta at Paonta Sahib 500 m D/S to slaughter house(Station-02)	
			No. of individual	% of abundance	No. of individual.	% of abundance
Mollusca	1	*Thiaridae*	431	25.11	1951	67.67
	2	*Planorbidae*	–	–	4	0.13
	3	*Lymnaeidae*	2	0.11	4	0.13
	4	*Pisidium*	–	–	1	0.03
	5	*Viviparidae*	4	0.23	–	–
Epheneroptera	1	*Neoephemeridae*	13	0.75	1	0.03
	2	*Baetidae*	617	35.95	324	11.23
	3	*Ephemerilidae*	31	1.80	2	0.06
	4	*Heptageniidae*	52	3.03	10	0.34
	5	*Ephemeridae*	23	1.34	–	–
	6	*Leptophlebiidae*	12	0.69	3	0.10
	7	*Caenidae*	17	0.91	1	0.03
Odaonata	1	*Gomphidae*	11	0.64	76	2.63
	2	*Libellutidae*	3	0.17	1	2.67
Colleptera	1	*Elmidae*	21	1.22	1	0.03
	2	*Hydroptillidae*	8	0.46	3	0.10
	3	*Dryopidae*	29	1.68	–	–
	4	*Psepheniidae*	59	3.43	7	0.24
Trichoptera	1	*Hydropsychidae*	53	3.08	110	3.81
	2	*Glossosomatidae*	63	3.6	6	0.20
	3	*Lepidostomatiodae*	12	0.69	–	–
	4	*Polycentropodiae*	19	1.10	9	0.31
	5	*Hydroptillidae*	32	1.86	4	0.13
	6	*Wenoidae*	17	0.99	–	–
	7	*Leptoceredae*	3	0.17	1	0.03
	8	*Rhyacophillidae*	13	0.75	–	–
	9	*Philopotamidae*	17	0.99	2	0.06
	10	*Goeridae*	34	1.98	–	–
Diptera	1	*Tabanidae*	3	0.17	13	0.45
	2	*Chironomidae*	11	0.64	55	1.90
	3	*Tipulidae*	–	–	9	0.31
	4	*Ephydridae*	3	0.17	13	0.45
	5	*Simulidae*	19	1.10	2	0.06
	6	*Ceratopogonidae*	–	–	1	0.03
Hemiptera	1	*orixidae*	22	1.28	3	0.10
Placoptera	1	*Perlidae*	36	2.01	–	–
Crustacea	1	*Palaemonidae*	23	1.24	176	6.10
Annelida	1	*Oligochaetes*	3	0.17	89	3.08

Three procedures were followed in scoring the taxa.

(1) Numerical procedure: This procedure follows the following formula. Guide Score = SⅠ/STot × 10 + SⅠ－Ⅱ/STot × 8.57 + SⅡ/STot × 7.14 + SⅡ－Ⅲ/STot × 5.71 + SⅢ/STot × 4.28 + SⅢ－Ⅳ/STot × 2.85 + SⅣ/STot ×1.43

Where,

SⅠ, SⅠ－Ⅱ, SⅡ, SⅡ－Ⅲ, SⅢ, SⅢ－Ⅳ, SⅣ are the total number of sites representing the pollutional classes Ⅰ, Ⅰ－Ⅱ, Ⅱ, Ⅱ－Ⅲ, Ⅲ, Ⅲ－Ⅳ, Ⅳ.

STot= SⅠ +SⅠ－Ⅱ +SⅡ +SⅡ－Ⅲ +SⅢ

+ SⅢ − Ⅳ + SⅣ

1.43 is the score interval with 10 as maximum.

(2) Professional judgments:

Step-Ⅰ: Based on the reference made to the scores that has previously been assigned by different authors in their respective country of origin, and the range of pollution class represented by each taxon in the rivers of Nepal.

Step-Ⅱ: Based on the distribution pattern of each taxon (family level) in response to pollution level, the comparison of family (taxon) distribution with the observed water quality classes was carried out to find out if any families with the same ecological distribution were differently scored. If so, whether or not the reasons are matching.

Once NEPBIOS/ASPT is calculated, reference should be made to the below Table 5 for interpretation of the water quality of the particular investigated site.

Table 4. NEPBIOS assigned to the macroinvertebrates

S. No.	Macroinvertebrates	Score
1.	Capniidae, Ephemerellidae (*Drunella* sp.), Epiophlebiidae, Helicopsychidae, Helodidae (Scirtidae), Heptageniidae (*Epeorus rhithralis*), Heptageniidae (*Rhithrogena nepalensis*), Leuctridae, Peltoperlidae, Perlidae (*Acroneuria* spp.), Perlidae (*Calicneuria* spp.), Siphlonuridae, Taeniopterygidae, Uenoidae.	10
2.	Athericidae, Chloroperlidae, Goeridae, Leptophlebiidae (*Habrophlebiodes* sp.), Limnocentropodidae, Neoephemeridae, Perlodidae, Polycentropodidae.	9
3.	Baetidae (*Centroptilumsp.*), Brachycentridae, Chironomidae (Diamesinae), Elmidae, Euphaeidae, Glossosomatidae, Heptageniidae (*Epeorus bispinosus*), Heptageniidae (*Iron psi*), Heptageniidae (*Rhithrogena* spp.), Hydrobiosidae, Lepidostomatidae, Limnephilidae, Nemouridae, Perlidae, Philopotamidae, Psephenidae, Rhyacophilidae, Stenopsychidae.	8
4.	Aphelocheiridae, Baetidae (*Cloedodes* sp.), Baetidae (*Baetiella* spp.), Baetidae (*Baetis* spp.), Baetidae (*Baetiella ausobskyi*), Baetidae (*Baetis* sp. 1), Corydalidae, Ephemerellidae, Ephemerellidae (*Cincticostella* sp.), Ephemeridae, Gammaridae, Gyrinidae, Heptageniidae, Heptageniidae (*Cinygmina* sp.), Heptageniidae (*Notacanthurus cristatus*), Hydraenidae, Leptophlebiidae, Limoniidae, Pleuroceridae, Psychomyiidae, Salifidae (*Barbronia* sp.), Simuliidae, Tipulidae.	7
5.	Aeshnidae, Baetidae (*Baetis* sp.5), Baetidae (*Baetis* sp.4), Caenidae, Ceratopogonidae, Ecnomidae, Ephemerellidae (Torleya nepalica), Heptageniidae (*Electrogena* sp.), Hydrometridae, Hydropsychidae, Hydroptilidae, Potamidae, Scirtidae, Viviparidae.	6
6.	Baetidae (*Baetis* sp.2), Baetidae (*Baetis* sp.3), Bithyniidae, Chlorocyphidae, Coenagrionidae, Corduliidae, Dryopidae, Hydrophilidae, Leptophlebiidae (*Euthraulus* spp.), Lymnaeidae, Odontoceridae, Protoneuridae, Sphaeriidae, Unionidae.	5
7.	Calopterygidae, Chironomidae (*Microtendipes* sp.), Chironomidae (*Polypedilum* sp.), Corbiculidae, Dytiscidae, Gerridae, Glossiphoniidae, Micronectidae, Naucoridae, Nepidae, Palaemonidae, Planorbidae, Ranatridae, Salifidae (*Barbronia weberi*), Thiaridae.	4
8.	Corixidae, Libellulidae, Lumbricidae, Noteridae, Notonectidae, Salifidae	3
9.	Culicidae, Physidae, Tubificidae	2
10.	Chironomidae [Chironomus group riparius (= *thummi*) and group plumosus]	1

On the basis of the NEPBIOS score system, the species present in the samples of the site at Behta River 10 m U/S to the slaughter house shows that water quality of the river belongs to class-Ⅱ.

On the basis of the NEPBIOS score system, the species present in the samples of the site at Behta River 500 m D/S to the slaughter house shows that water quality of the river belongs to class-Ⅲ.

During the investigation at Station-01, it was found that water quality was good with the pH of 7.84 and turbidity of 0.84 Nephelometric Turbidity Unit (NTU). The Biological Oxygen Demand (BOD) is 2.1. Total 34 families of macroinvertebrates belonging to groups *Ephemeroptera*, *Coleoptera*, *Trichoptera*, *Diptera*, *Plecoptera*, *Hemiptera*, *Crustacea*, *Annelida*, *Mollusca*,

Odonata were encountered. The insect population represented 72.98% of total fauna and belonging to orders *Trichoptera*, *Ephemeroptera*, *Coleoptera*, *Diptera*, *Odonata* and *Hemiptera*. The order *Ephemeroptera*, *Trichoptera*, *Coleoptera* and *Placoptera* are dominating in numbers. The results further show that all the locations assessed for quality using macroinvertebrates and physico-chemical analysis are in the range of water quality class Ⅱ (Good) and the water can be used for drinking purposes.

Table 5. Water quality scores based on NEPBIOS

NEPBIOS/ASPT	Water quality
8.00－10.00	Ⅰ
7.00－7.99	Ⅰ－Ⅱ
5.50－6.99	Ⅱ
4.00－5.49	Ⅱ－Ⅲ
2.50－3.99	Ⅲ
1.01－2.49	Ⅲ－Ⅳ
1	Ⅳ

During the investigation at Station-02, it was found that river water was a little alkaline with pH of 8.2 and moderately polluted with turbidity. The study of fresh water macroinvertebrates shows that 30 families belonging to groups *Mollusca*, *Odonata*, *Ephemeroptera*, *Coleoptera*, *Trichoptera*, *Diptera*, *Plecoptera*, *Hemiptera*, *Crustacea* and *Annelida* occurred in the river.

The insect population represented 22.53% of total fauna of Behta River and was belonging to the order *Odonata*, *Ephemeroptera*, *Coeloptera*, *Trichoptera*, *Diptera*, *Placoptera*, *Hemiptera*. Insect have the capability to adapt to varied aquatic habitats due to their extra ordinary structural organization[4,5,7]. The benthic population of aquatic insects was dominated by *Trichoptera* comprising 8 families and diptera comprising 6 families. Most of these families to be tolerant to varied aquatic environment[8,10].

The *Mollusca* fauna of Behta River was represented by 4 families out of which *Thiaridae* family dominated the population. Covers 67.82% of the total population of aquatic fauna. This group has significant positive correlation with the total hardness (201.0 mmol/L), alkalinity (141.0 mmol/L), phosphate (0.94 mg/L) and chloride (13.4 mg/L). The rest of the aquatic invertebrate fauna of Behta River of one family of Crustacea, and a Annilida.

4 Conclusion

Benthic macroinvertebrates community as a whole in the river has been found to have significant positive correlation with the total hardness, total alkalinity, chloride, phosphate and transparency.

The results show that all the locations assessed for quality using macroinvertebrates and physico-chemical analysis are in the range of water quality class Ⅲ (Moderately Polluted) at the Station 02 and the water can not be used for drinking purposes. The measures to reduce point and non-point sources of pollution have been suggested to get the quality suitable for drinking purposes.

Acknowledgement

The authors are thankful to ASSESS-HKH (Project No: 003659) for financial assistance to carry out the work which is a part of program of developing an assessment tool.

Correspondence to:

Mahendra Pal Sharma
Senior Scientific Officer
Alternate Hydro-Energy Centre
Indian Institute of Technology
Roorkee (UA)-247667, India
Email: mpshafah@iitr.ernet.in

References

1. Hallawel JM. Biological Indicator of fresh water pollution and environmental management. Pollution monitoring series. Advisory editor: Kenneth Mellanby, England 1986; 546.
2. Bhutiani R. Limnological status of river Suswa with reference to its mathematical modelling. Ph. D. Thesis, Gurukul Kangdi. Vishwavidyalaya, Haridwar 2004; 325.
3. Sharma S. Biodiversity of litteral benthic organisms and their trophic releationship with shore birds and fishes in Sirpur Lake Indore(M. P.) Devi Ahilya University. Indore 2003; 278.
4. Tyagi P. Occurrence of benthic macroinvertebrates families encountered in river Hindan in Uttar Pradesh(India). J Zool India 2006; 1(9): 209－16.
5. Needham IG, Needham PR. A Guide to the study of fresh-water Biology. Holdden & Day San Francisco 1969; 108.
6. Pennak Robert W. Fresh-water invertebrates of the United States: Protoza to Mollusca. 3rd. ed. John Wiley and Sons, New York, USA 1989; 769.
7. Tonapi GT. Fresh water animals of India-An ecological approach. Oxford and IBH Publishing Co. New Delhi 1980; 341.
8. Merrit RW, Cummins KW, eds. An Introduction to the Aquatic Insects of North America. 3rd ed. Kendall / Hunt Publishing Company, Dubuque 1996; 862.
9. APHA. Standard method for the examination of water and waste water, American Public Health Association, Inc. New York. 20th Ed. 1998; 10－161.
10. Bath KS, Kaur Aquatic insects as bio-indicators at Harike reservoir in Punjab India. Indian Journal of Environmental Sciences 1997; 2:133－8.

Received October 20, 2006

Assessment of *Salmonella* Contamination of Feed Raw Materials and Their Anti-microbial Resistance Profiles in Imo State, Nigeria

Ifeanyi Charles Okoli, Ifeoma C. Ekwueagana, I. Prince Ogbuewu

Tropical Animal Health and Production Research Laboratory, Department of Animal Science and Technology, Federal University of Technology, PMB 1526, Owerri, Nigeria

Abstract: This study was conducted to determine the frequency of isolation of *salmonella* and their microbial resistance profiles, across selected feed raw materials sold in Imo State, Nigeria. Three hundred and sixty (360) bulk samples were collected across different feed raw materials which include animal proteins-foreign fish meal (FFM) and local fish meal (LFM), plant proteins-groundnut cake (GNC) and soybean meal (SBM), fiber sources-palm kernel cake (PKC) and wheat offal (WO), energy grain-maize (MZ) and Minerals-bone meal (BM). The *salmonella* isolated were tested against 14 anti-microbial agent using disc diffusion method. Bacterial load enumeration of the samples indicated a range of >300 to overgrowth of colony forming unit (CFU) at 4 serial dilution. One hundred and twenty (120) samples (33.33%) were positive for *salmonella* isolates with fiber sources and animal protein recording 56.00% and 50.91% prevalence, respectively. Across the individual raw material types, it recorded LFM (90.0%), WO (60.0%), PKC (50.0%), SBM (40.0%) and GNC (28.67%) prevalence while non were isolated from maize and bone meal. Salmonella isolates showed a high rate of resistance to ampicillin (100%), tetracycline and nitrofurantoin (78.6%) and cotrimoxazole (50%), and moderate rate of 42.6%, 35.7%, and 21.4% against cephalexin, streptomycin and ceftriazole, and ciprofloxacin respectively, while low rates of 7.1% were recorded for amoxycillin clavulanate and pefloxacin and 14.39% for oxfloxacin, nalidixic acid and chloramphenicol. The present study showed that feed ingredients sold in Owerri form important vehicles for the introduction of multi-drug resistant *salmonella* organisms into poultry feeds. It is therefore, recommended that feed raw materials should be hygienically processed before inclusion in livestock feeds. [Life Science Journal. 2006;3(4): 75-80] (ISSN: 1097-8135).

Keywords: *salmonella*; feed materials; livestock; antibiotics; drug resistance; Nigeria

Abbreviations: AP: animal protein; BM: bone meal; CFU: colony forming unit; FB: fiber sources; FFM: foreign fish meal; GNC: groundnut cake; ISEPA: Imo State Environment Protection Agency; LFM: local fish meal; MZ: maize; PKC: palm kernel cake; PP: plant protein; SBM: soybean meal; WO: wheat offal

1 Introduction

There is a close relationship between the quality of livestock feed and that of animal products offered for human consumption. This quality is primarily nutritional, but it is also technological, organoleptic and sanitary. Although feed contributes to animal health by preventing dietary deficiencies and optimizing physiological functions, it can also lead to dysfunctions and negatively influence the sanitary quality of animal products when not properly processed[1]. Feeds can serve as important source of food borne diseases in animal food products and has therefore remained an important public health threat worldwide[2]. However, many factors are involved in this public health threat. Kan[3], for example stated that feeds and feed ingredients are possible materials since residues of organochlorine pesticides in poultry and eggs are due to their presence in feedstuffs. Similarly, there is evidence that poultry feeds are important sources of many microbial contaminants including *salmonella* in poultry[4-7]. Prominent among these microbial contaminants are *salmonella* strains, which have been showed to be of critical importance in the Nigerian poultry industry[8,9]. It has been shown that infection in poultry can result from one *salmonella* organism per grams of feed[10] and even one organism per 15 grams of feed[11].

Strict hygienic measures should therefore be applied to the production, processing and distribution of raw materials used as feedstuffs so as to pre-

vent contamination with pathogenic microbes and other undesirables[5]. Hygienic production of animal feeds however involves the processing of feeds under a health hazard free condition[12]. This usually starts from the harvesting, milling, processing, packaging, transportation and eventual marking of the bagged products at the various sales outlets from where the farmer collects to feed his animals[13].

Intensive feeding of poultry in the tropics involves the use of unconventional blending of feed components such as industrial wastes, cereal by-products, poultry waste, animal blood and others containing microbial genera of questionable quantity and quality[14]. Bains and Mackenzie[15] correlated high mortality in infected broiler flocks with increased incidence of *salmonella* in the grain constituents of broiler ration. Vaughn *et al*[16] also found 27% of protein feed ingredient meals collected at mills to carry one or more serotypes of *salmonella*.

A recent study by Okoli *et al*[17] determined that 22.20% of commercial poultry feed samples analyzed in Owerri, Nigeria contained *salmonella* isolates. It is however necessary to understand the major contaminating feed components that of finished feeds in the area in order to restrict sanitization treatment on them. Such information is important a developing economy like Nigeria where it may not be economically feasible to effect whole feed treatment.

The antibiotic resistance among bacterial general is a global problem[5]. The rate at which resistance arise among bacterial populations has been reported to be contingent on the extent of use of a particular antibiotics in a particular environment[18]. Thus *salmonella* and other organisms contributed by the different raw materials used in compounding commercial feeds may harbor resistance factors reflecting antibiotic use in their areas of origin[19]. There is however scarcity of published information about anti-microbial resistance of bacterial isolates form farm animals and farm environments in southeastern Nigeria[19-24]. Furthermore, the fact that avian salmonellosis is a disease of major economic and public health importance demands that its prevalence and anti-microbial resistance profile in different feedstuffs should be understood at any given time in an animal production area.

This study was designed to investigate the prevalence of *salmonella* organism in feed raw materials and their microbial resistance profile in Owerri, Imo State, Nigeria.

2 Materials and Methods

2.1 Study area

The study was carried out in Imo State, Nigeria. The agro-climatic characteristics as well as poultry production systems in the area have been described[5]. The study was carried out during the rainy season months of July to September of 2004. A preliminary field survey was carried out to identify reputable commercial poultry feed sellers in Owerri. These sellers were informed of the nature and purpose of the research and based on the preliminary survey, a list of 8 feed raw materials sold at the outlets which included animal protein-foreign fish meal (FFM) and local fish meal (LFM), minerals-bone meal (BM), fiber sources-wheat offal (WO) and palm kernel cake (PKC), plant protein-soybean meal (SBM) and groundnut cake (GNC) and energy grains-maize (MZ) were purposively selected for the study. The materials were sampled at random across the three months using method described by Okoli[5].

2.2 Sample collection

A total of 360 bulked samples were collected from chosen feed raw materials selling outlets. Each selected sites was visited 3 times corresponding to once every month for sample collection. During the visits, samples were collected as shown in Table 1.

Table 1. Distribution of feed raw material sample types collected for isolation of *salmonella* in Imo State, Nigeria

Visits	FFM	LFM	BM	WO	PKC	SBM	GNC	MZ	Total
July	20	20	10	10	10	20	40	20	160
August	20	20	20	10	20	10	10	10	100
September	10	20	20	10	10	10	20	10	100
Total	50	60	50	30	20	40	70	40	360

Each of the feed raw materials were sampled by carefully opening 3 randomly selected bags that contained the same feedstuff type and collecting about 3 g from each with the aid of sterile universal bottles. These were homogenized to obtain a representative bulk sample of about 12 g of the sample types for analysis. The samples were taken to the laboratory for analysis within two hours of their collection.

2.3 Bacterial load enumeration

These were carried out at Imo State Environment Protection Agency (ISEPA) Microbiology Laboratory. Four-fold serial dilution of the homog-

enized samples as described by Ogbulie and Okpokwasili[25], was prepared for each sample and involved adding 5 g of the sample in 45 ml of sterile deionized water and mixing thoroughly. Thereafter, 0.1 ml of the appropriate dilution was drawn and inoculated onto nutrient agar. After overnight incubation, the bacterial load was enumerated using the colony counter (Suntex^r) to count the colony forming units (CFU).

2.4 Bacterial isolation

Aliquots of the serially diluted samples were enriched in peptone water after overnight incubation at 37 ℃. These were cultured onto then sub selenite broth for selective growth according to method of Cheesbrough[26]. They were subsequently subculture onto MacConkey agar and incubated overnight at 37 ℃. Non-lactose fermenting colonies suggestive of *salmonella* organism were subjected to biochemical test, which included Simmon citrate, indole and urease tests among others to confirm *salmonella* isolation[27].

2.5 Susceptibility testing

The confirmed *salmonella* isolates were screened for anti-microbial resistance profile using the disc diffusion method[28] according to the methods recommended by the National Committee for Clinical Laboratory Standards Guidelines[29]. This was done by streaking the surface of nutrient agar plates uniformly with the organisms. Thereafter, the plates were inverted and left to dry on the bench for 30 minutes before discs (Optun Lab.^{R}) impregnated with known concentrations of anti-microbial substances were placed on the surface with sterile forceps. The plates were then allowed to stand for a pre-diffusion period of about 1 hour before being incubated at 37 ℃ overnight with the lid uppermost. The disc diffusion method is widely recognized to work well with rapidly growing facultatively anaerobic and aerobic organisms such as Enterbacteriaceae[29].

Fourteen anti-microbial drugs were tested against the *salmonella* isolates. They included chloramphenicol (30 μg, CR), ceftriazole (30 μg, CF), nitrofurantoin (200 μg, NI), cotrimoxazole (30 μg, CO), oxfloxacin (10 μg, OF), gentamycin (10 μg, GN), amoxycillin clavulanate (30 μg, AU), nalidixic acid (10 μg, NA), ciprofloxacin (10 μg, CP), streptomycin (10 μg, ST), pefloxacin (10 μg, PF), ampicillin (30 μg, AM), tetracycline (25 μg, TE) and cephalexin (15 μg, CE).

2.6 Statistical analysis

The susceptibility data were recorded qualitatively as resistant or sensitive. The isolates resistant to individual drugs and anti-microbial pattern were computed. The data collected was analyzed using simple descriptive statistics such as percentage and histograms.

3 Results

Results of bacterial load enumeration showed that all of the samples yielded overgrowth or >300 cfu at 4 serial dilution.

3.1 *Salmonella* prevalence

Table 2 showed that 120 (33.33%) of the 360 bulked samples had *salmonella* isolates. Across the feed raw materials groups, fiber sources and animal protein recorded 56.00% and 50.91% prevalence, respectively and was followed by the 32.73% rate obtained in plant proteins, while *salmonella* organism were not isolated from energy grains and mineral groups. Across the individual feed raw materials (Table 3), LFM recorded 90.00% prevalence and was followed by the 60.00%, 50.00% and 40.00% recorded for WO, PKC and SBM, respectively.

Table 2. Frequency of isolation of *salmonella* from the different feed raw material types

Feed type	No. of samples	No. isolated	Percentage
Animal protein	110	56.0	50.91
Plant protein	110	36.0	32.73
Energy grain	40	0.0	0.00
Fiber source	50	28.0	56.00
Mineral	50	0.0	0.00
Total	360	120	33.33

Table 3. Frequency of *salmonella* isolation from various feed raw materials components

Materials	No. of samples	*Salmonella* isolation	% Prevalence
FFM	50	2	4.00
LFM	60	54	90.00
SBM	40	16	40.00
WO	30	18	60.00
GNC	70	20	28.57
BM	50	0.0	0.00
MZ	40	0.0	0.00
PKC	20	10	50.00
Total	360	120	33.33

3.2 Anti-microbial resistance

Figure 1 showed that the *salmonella* isolates recorded high rate of resistance (51 – 100%) to ampicillin, nitrofurantoin and tetracycline, while moderate rate (31 – 50%) were recorded against cotrimoxazole, cephalexin and streptomycin. The

organisms were however lowly resistant to the other antibiotics, with augumentine and pefloxacin recording 7.1% and oxfloxacin, gentamycin, nalidixic acid and chloramphenicol, while ciprofloxacin and ceftriazole returned 21.4%, respectively.

Figure 2 showed a comparison of the anti-microbial resistance of *salmonella* isolates from different poultry feed raw materials groups namely plant protein (PP), animal protein (AP) and fiber sources (FB). Isolates from PP, AP and FB recorded 100% resistance against ampicillin, while PP also singly recorded 100% resistance against nitrofurantoin. Similarly, isolates from AP returned 83.3% resistance to tetracycline and nitrofurantoin, while FB resistance levels were generally low with 0.0% resistance being recorded against oxfloxacin, gentamycin, augumentine and chloramphenicol.

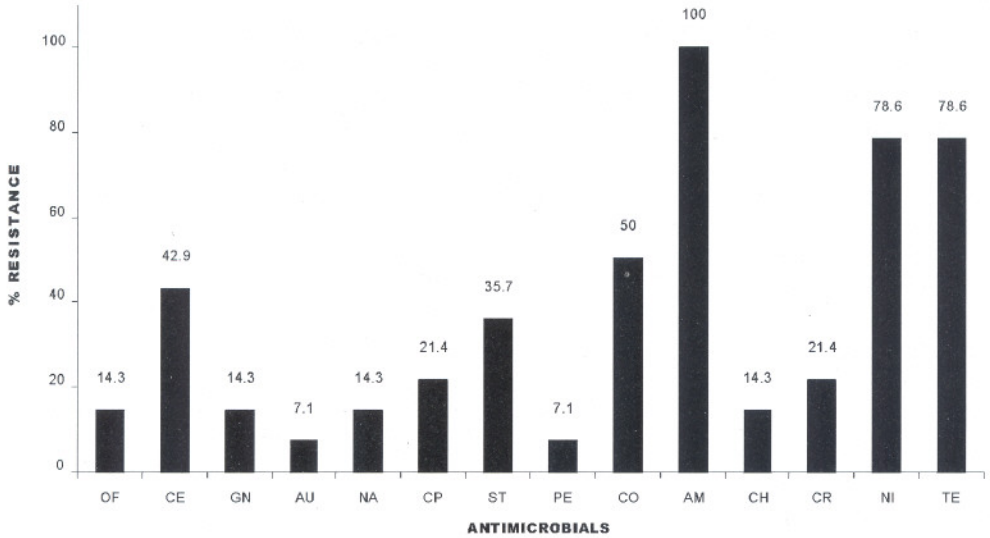

Figure 1. Histogram showing the rate of occurance of antimcrobial resistance patterns of *salmonalla* isolated from poultry feed raw materials in Owerri, Imo State, Nigeria

Key: OF-Oxfloxacin, CE-Cephalexin, GN-Gentamycin, Au-Amoxycillin clavulanate, CP-Ciprofloxacin, ST-Streptomycin, PE-Pefloxacin, CO-Cotrimoxazole, AM-Ampicillin, CH-Chloramphenicol, CR-Ceftriazole, NI-Nitrofurantoin, TE-Tetracycline.

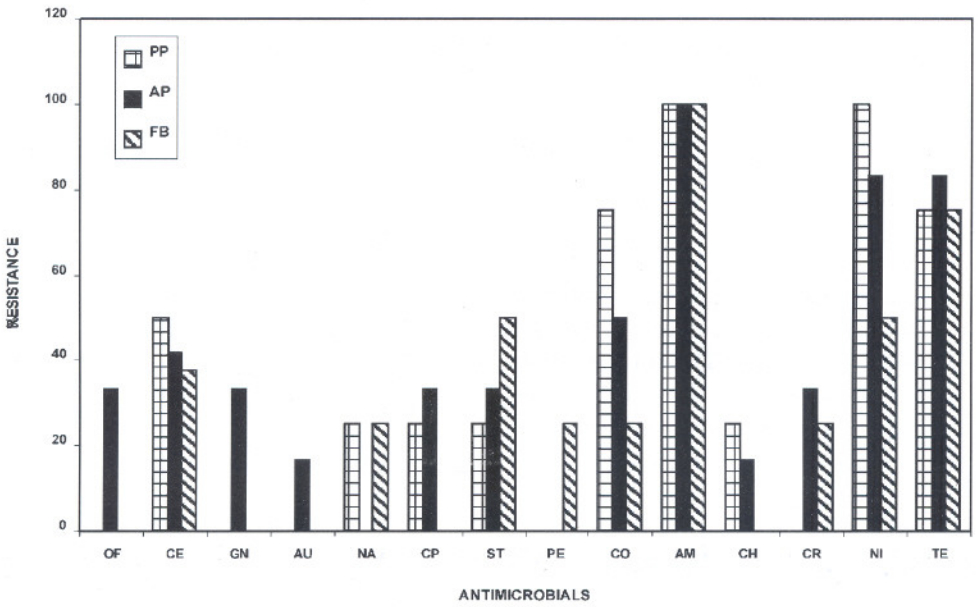

Figure 2. Comparison of antimicrobial resistance rates of *salmonella* isolates from poultryfeed rawmaterials of plant protein, animal protein and fibre sources. Key: As in Figure 1.

4 Disscusion

The high microbial contamination observed in LFM, GNC and PKC is in consonance with[30] which regarded these protein raw materials as "high risk ingredient" readily contaminated by microbes. These high densities of bacterial growth may be due to post-processing handling state of these ingredients. This is in consonance with the report of Butcher and Miles[31], which indicated that high temperatures in ground grains and oil meals encourage moisture migration and condensation inside the storage containers thus promoting bacterial as well as fungal growths. Reports by Bastianelli and Le Bas[1] and Cheesbrough[26] have also shown that tropical countries such as Nigeria are more prone to microbial and fungal contaminations of poultry feed raw materials.

The overall 33.33% prevalence of *salmonella* organism recorded in this study is of economic and public health importance[9,32]. Vaughn *et al*[16], Wilson[30] and MAFF[33] had earlier reported that in UK, 27% of protein feed ingredients carry one or more serotypes of *salmonella*. According to Dupree and Hurner[34], Ogbulie[14] and Ndujihe[35], *salmonella* in commercial feeds may have originated from some of the raw materials used in compounding them. Prevalence rates across the different raw material groups and types were unevenly distributed with local fish meal, recording 90%, while bone meal and maize had none. The observed difference in the prevalence rate of foreign and local fish meals may be attributed to the high level of hygiene employed in processing and handling of the former. The different weather condition experienced during the different seasons in the tropics as well as pre-harvest, harvest and post harvest practices and the bionomics of the organisms are also known to influence pathogenic contamination of local feedstuff[19]. Furthermore, there are program such as those of National Marine fisheries Services (NMFES) that monitors the quality of fish ingredients produced for export[31].

Similarly, considering the level of heat employed the processing of WO and PKC, the high degree of isolation may suggest handling and post-production sources of contamination[20]. The zero prevalence rate observed in BM could be attributed to high temperatures necessary for the ashing techniques employed in preparing the ingredients. The very low moisture content of the finished products may also not be able to support the growth of *salmonella*. While these organisms were not identified to genera level, unpublished field data by Anyanwu[36] and Okoli[32] suggest that *S. enteritidis*, *S. typhimurium* and *S. montevideo* are involved in poultry contamination in this study area.

The present result of anti-microbial resistance of *salmonella* isolated from feed raw materials highlight again the already established multi-drug resistance of bacteria of the Enterbacteriaceae family in Imo State[5,21,19,23]. The 36.7% resistance recorded for streptomycin and 21.4% against ciprofloxacin are again of public health interest since aminoglycosides and fluoroquinolones are currently the drugs of choice in the treatment of both human and animal salmonellosis in the study area. This work again highlighted the high resistance profiles of *salmonella* organism in Imo State against the cheap, readily available first line anti-microbial drugs such as cotrimoxazole, tetracycline, nitrofurantoin and ampicillin among others.

5 Conclusion

The result of the study confirms that feed ingredients are important vehicles for introduction of *salmonella* organisms in finished poultry feeds in Imo state. The high prevalence rate of *salmonella* isolates in this study highlights the need for the institution of *salmonella* monitoring measures programs in the Nigerian feed industry. LFM and fiber sources should be carefully sourced and sanitized before inclusion in animal feeds.

Correspondence to:
Ifeanyi Charles Okoli
Tropical Animal Health and Production Research Laboratory
Department of Animal Science and Technology
Federal University of Technology, P. M. B 1526
Owerri, Nigeria
Email: dr-charleso@yahoo.com

References

1. Hanak E, Boutrif E, Fabre P, *et al*. Food safety management in developing countries: Proceedings of the International Workshop. (scientific editors), CIRAD-FAO, 11 - 13 December, 2000, Montpellier, France. http://www. afssa. fr/ftp/basedoc/Rapport Alimentation animale 2002.
2. Abamuslum G, Murat G, Berna D, *et al*. The microbiological contamination of traditionally processed raw carcasses marketed in Kars, Turkey. International Journal of Food Safety 2002;3:4 - 7.
3. Kan CA. Prevention and control of contaminants of industrial processes and pesticides in the poultry production chain. World's Poultry Journal 2002; 58(2): 159 - 67.
4. Davies RH, Wray C. Distribution of *salmonella* contam-

ination in ten animal feed mills. Veterinary Microbiology 1997; 51: 159 – 69.
5. Okoli IC. Studies on anti-microbial resistance among *E-coli* isolate from feeds and poultry production units, PhD Thesis, Federal University of Technology, Owerri, Nigeria 2004.
6. Maciorowski KG, Jones ET, Pillai SD, *et al*. Incidence, source and control of food borne *Salmonella* spp. in poultry feeds. World's Poultry Science Journal 2004; 60(4): 446 – 58.
7. Nweke CU. An assessment of the mycoflora of some commercial poultry feed brands sold in Owerri, Imo State, Nigeria B Agric Tech Project Report, Federal University of Technology, Owerri, Nigeria. 2005.
8. Halle PD, Umoh JU, Abdu PA. Diseases of poultry in Zaria, Nigeira. A ten-year analysis of clinical records. Nig J Anim Prod 1998; 25 (1): 88 – 92.
9. Bale OO, Sekoni AA, Kwanashie CA. A case study of possible health hazards associated with poultry houses. Nig J Anim Prod 2002; 29: 102 – 11.
10. Gordon RF, Tucker JF. The epizootiology of *Salmonella menston* infection of fowls and the effect of feeding poultry food artifically infected with *salmonella*. Br Poult Sci 1965;6(3):251 – 64.
11. Harry EG, Brown WB. Fumigation with methyl bromide-application in the poultry industrya review. World's Poultry Sci 1974;30:193 – 216.
12. Omede AA. Quality assessment of commercial poultry feeds sold in Nigeria. B Agric Tech Project Reports, Federal University of Technology, Owerri, Nigeria. 2003.
13. Day M. Feed analysis: a plug and play solution. In Focus 2001; 25(2): 17 – 9.
14. Ogbulie JN. Microbial flora of tropical aquaculture systems. PhD Thesis, University of Port Harcourt, Port Harcourt, Nigeria 1995.
15. Bains BS, Mackenzie MA. Transmission of *Salmonella* throughan in tegrated poultry operation. Poult. Sci 1974;53:1114 – 8.
16. Vaughn JB, William LP, LeBlanc RJR, *et al*. *Salmonella* in a modern broiler operation: a longitudinal study. Am J Vet Res 1974;35(5):737 – 41.
17. Okoli IC, Ndujihe GE, Ogbuewu IP. Frequency of isolation of *salmonella* from commercial poultry feeds and their anti-microbial resistance profiles, Imo state, Nigeria. Online Journal of Health and Allied Sciences (In press) 2006.
18. Jacoby GA, Archer GL. New mechanism of bacterial resistance to anti-microbial agents. New England Journal of Medicine 1991; 324: 601 – 12.
19. Okoli IC, Herbert U, Ozoh PTE, Udedibie ABI. Anti-microbial resistance profile of *E. coli* isolates from commercial poultry feeds and feed raw materials. Animal Research International, (Accepted for publication) 2005.
20. Uwaezoke JC, Ogbulie JN, Njoku AJ, Obiajuru IOC, Njoku AJ. Antibiotics sensitivity patterns of bacterial isolates from poultry feed. International Journal Environmental Health Human Development 2000; 1(2): 23 – 8.
21. Chah KF, Bessong WO, Oboegbulam SL. Antibiotic resistance in avian colisepticeamic *E. coli* strain in southeast Nigeria. In Proceeding of the 25th Annual NSAP Conference, Umudike, Nigeria. 19th-23rd March 2000: 303 – 30.
22. Okoli IC, Nwosu CI, Okeudo NJ, *et al*. Management of anti-microbial resistance in avian bacterial pathogens in Nigeria. Environmental Health Human Development 2002; 3(1): 39 – 98.
23. Okoli IC, Chah KF, Herbert U, *et al*. Anti-microbial resistance of non-clinical *E. coli* isolates from a commercial layer poultry farm in Imo State, Nigeria. International Journal of Natural and Applied Sciences 2005; 1 (1): 68 – 77.
24. Okoli IC, Chah KF, Ozoh PTE, Udedibie ABI. Anti-microbial resistance of none clinical *E. coli* isolates from tropical free-range chickens. Online Journal of Health and Allied Sciences, 2005;3(3): http://www.ojhas.org/issue 15/2005-3-3.htm 12/19/2005.
25. Ogbulie JN, Okpokwasili GC. Efficacy of chemotherapeutic agents in controlling bacterial diseases of cultured fish. Journal Aquaculture Tropical 1999; 13: 61 – 72.
26. Cheesbough M. Microbiological test. In: District Laboratory Practice in Tropical Countries. Part 2. Cambridge University Press, Cambridge 2000.
27. Gillies RR, Dodds TC. Bacteriology Illustrated, 4th Ed. Churchill Livingstones, Edinburgh and London 1976.
28. Bauer AW, Kirby WMM, Sherris JC, *et al*. Antibiotic susceptibility testing by a standardized single disk method. American Journal of Clinical Pathology 1966; 36: 493 – 6.
29. NCCLS. Performance standard of anti-microbial disk and dilution susceptibility tests for bacteria isolated from animals. Approval Standards 1999; M31-A, 19(11).
30. Wilson JE. Raw materials: Animal proteins. Proceedings of the society of feed technologist 1990
31. Butcher GD, Miles RD. Veterinary medicine. Large animal clinical science department, Florida Co-operative Extension Service, Institute of Food and Agricultural Sciences, University of Florida. http: //edis.ifas.UN. edu 2004.
32. Okoli IC. *Salmonella* strains Isolated from a turkey farm in Owerri, Nigeria. Unpublished Field Data 2003.
33. MAFF. Reports of the Ministry of Agriculture, Fisheries and Food, (Toby Jug site), Surrey KT6 TNF UK 1990.
34. Dupree HK, Hurner KN. Status of warm water fish farming and progress in fish research. Third report to fish farmers. United State Fishery and Wildlife Services, Washington DC 1984.
35. Ndujihe GE. Frequency of isolation of *salmonella* from commercial poultry fields and their anti-microbial resistance profile. B Agric Tech Project Report, Federal University of Technology, Owerri, Nigeria 2004.
36. Anyanwu BB. Causes of embryo mortalities in breeder turkey eggs in Owerri, Nigeria. Unpublished Field Data 2001.

Received October 4, 2006

Petal Secretory Stucture of *Osmanthus fragrans* Lour.

Meifang Dong, Wangjun Yuan, Yunfeng Ma, Fude Shang

College of Life Science, Henan University, Kaifeng, Henan 475001, China

Abstract: To reveal the features of secretory structure of *Osmanthus fragrans* Lour., the petals of *O. fragrans* were studied thoroughly by paraffin sectioning and electronic scanning microscope. The petal of *O. fragrans* is comprised of epidermis, fundamental tissues and vascular bundles. The petal epidermis consists of one layer of cells with obvious and regular tubercles, plentiful brush-shaped hairs and a small amount of stomas. The fundamental tissue includes many layers of parenchyma cells which contain much prolific oil substances and arrange irregularly. The secretory structure of *O. fragrans* can be named as Osmophores. The aromatic substances are produced, accumulated and stored temporarily in the petal fundamental tissues, and then secreted outside from the petal epidermis. [Life Science Journal. 2006;3(4):81-84] (ISSN: 1097-8135).

Keywords: *Osmanthus fragrans*; petal; secretory structure; Osmophores

1 Introduction

Osmanthus fragrans Lour., Oleaceae, is a kind of traditional and famous flower in China. The Chinese people favour it because of its strong perfume, especial culture, and widely used in food, spice and gardens[1,2]. There are many studies on aroma ingredients of *O. fragrans*[3-8]. The authors also studied secretory structure of other plant species[9-13]. Some papers on the differentiation of flower bud of *O. fragrans* have been published[14-16]. However, there are no reports on the morphology and anatomy of petal and the features of secretory structures of *O. fragrans*. This paper filled these studying gaps, and defined the type of secretory structure of *O. fragrans* firstly.

2 Materials and Methods

2.1 Materials

Petals was from *O. fragrans* "Huangchuanjingui" cultivated in Henan University in October, 2002.

2.2 Methods

Each part of fresh petals of *O. fragrans* and its secretory structure of free-hand sectioning and paraffin sectioning were observed under dissecting microscope. Free-hand section was dyed by Sudan Ⅲ, Sudan Black, dimethyl diaminophenazine chloride and KI-I_2 solution. Paraffin sectioning, which are 10-15 μm thick, were made through FAA fixing petals, then dyed by safranine-fast green, and iron vitriol-hematoxylin, lastly cuffed by Canada gums. Free-hand sectioning and paraffin sectioning were observed and taken photos under an Olympus BH-2.

The petal samples were made as follows: buffer solution flushing fresh petal, air drying, fixation on board, vacuum drying, gold metallic-membrane plating. The samples were observed and taken photos under HITACHI-450 electronic scanning microscope.

3 Results and Analysis

3.1 External shapes of petals

The petals of *O. fragrans* have often four pieces, seldom three, five or even six(variation). The petals were separated from style, stamina and pistils. The bottoms of petals coalesce to a corolla tube that is about 1 mm long. Only petals are scent (stamina lies on the corolla tube). The surfaces of petals are slightly rough and have white spotted tubercles of longitudinal range observed under dissecting microscope(Figure 1). The petals are full and fleshy, which have relation with secretory function. Under electronic scanning microscope were observed large number of protrudent and tidy ridges of longitudinal range on surface of petals(Figure 2) and stomas distribute in it randomly. These stomas can not close and the shapes of guard cells isn't typical(Figure 3). There are pollen grains on the surface of petals(Figure 2).

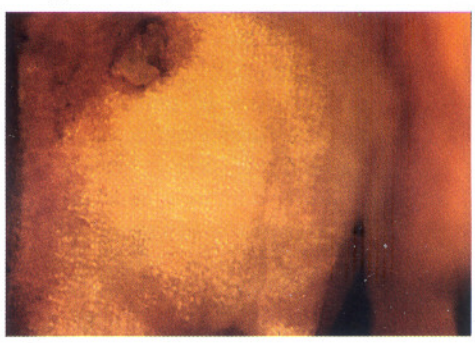

Figure 1. Spotted state tubercles of petal(×30)

Figure 2. Regular tubercles of longitudinal range on surface of petals(×550)

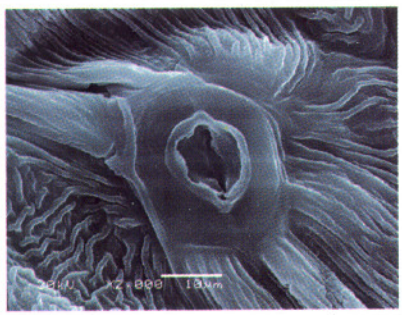

Figure 3. Guard cells of stomas in epiderm(×2000)

3.2 Anatomic structures of petals

Under optical microscope, the petal consists of epidermis, fundamental tissues and vascular bundles. There have plenty of one-layer-cell epidermis and less of two-layer-cell epidermis. The ectotheca of epidermal cell is thin and has rich epidermal trichome, which has no cuticle layer or only has thin cuticle layer. Those trichomes, which are brush-shaped and orgin from the ectotheca of epidermis cell, have the similarity with root hairs, but are straighter. They are denser than root hairs. Epidermal cells are alive and have obvious nucleus and cytoplasm(Figures 4 and 5). Most of epidermal cells own excretion. After dyed by Sudan Ⅲ, cells contain yellow substances(Figure 5); after dyed by Sudan Black, epidermal trichomes are black-grey (Figure 6); after dyed by dimethyl diaminophenazine chloride, cells are brick-red, and the drips in cells are obvious(Figure 4); after dyed by KI-I_2, cells are orange, and the color of drips in cells are deeper(Figure 5).

Fundamental tissues of petals locating under epidermis, are loose parenchyma cells, and have obvious gaps of internal cells. Most of cells are claviform irregularly. The long axis of parenchyma cell is vertical to epidermis(Figures 7, 8 and 9). There is prolific lipid in cells, which was dyed orange by Sudan Ⅲ(Figure 9), and can't be dyed by hematine. Vascular bundles which are simple in structure distribute in fundamental tissues(Figure 7). After stained by KI-I_2 solution, the fundamental tissues didn't become blue(Figures 7 and 8), which illustrated that no starch exists in them. Cells became brick-red after stained by dimethyl diaminophenazine chloride, which was consistent with epidermis.

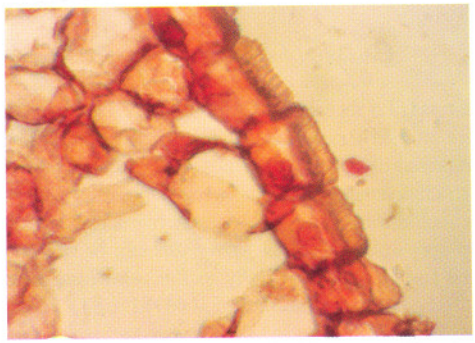

Figure 4. Obvious nucleus and cytoplasm of epidermal cells (×400)

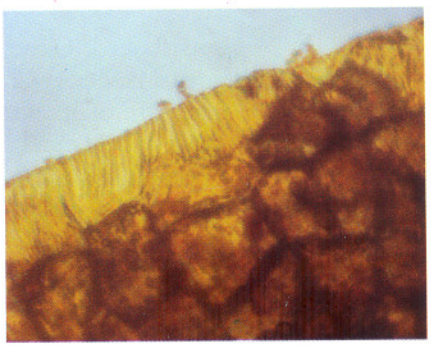

Figure 5. Epidermal cells and the excretion after dyed by KI-I_2(×600)

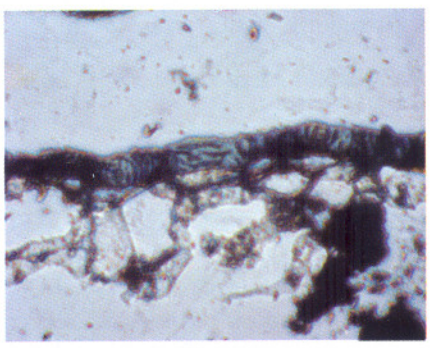

Figure 6. Epidermal cells and the excretion after dyed by Sudan Black(×400)

4 Discussion

According to the opinion of Ding[3], *O. fragrans* "Latifolius Group" has the most fragrant flavor and is the best cultivar group. *O. fragrans* "Thunbergii Group" has the soft and sweet scent and is the better one. *O. fragrans* "Aurantiacus

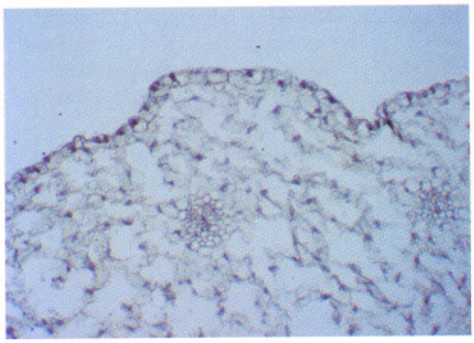

Figure 7. Vascular bundle of petals(×300)

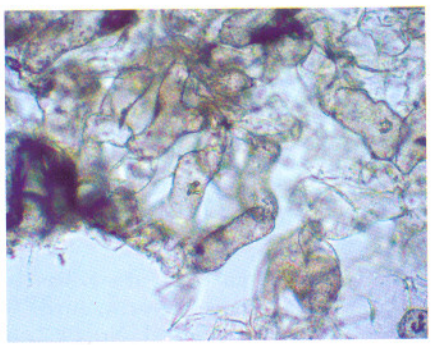

Figure 8. Parenchyma cells of fundamendal tissue of petals which arrange irregularly(×600)

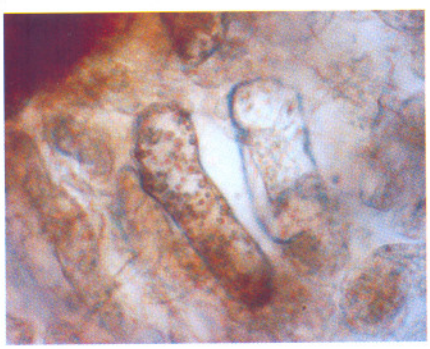

Figure 9. Parenchyma cells of fundamendal tissue of petals and excretion after dyed by Sudan Ⅲ(×800)

Group" has the light scent and is the inferior one. *O. fragrans* "Fragrans Group" is the most inferior one. *O. fragrans* "Huangchuan jingui", one cultivar of *O. fragrans* "Thunbergii Group", was studied by author. The features of secretory structure of *O. fragrans* were found. Scent of *O. fragrans* concentrates in petals, and epidermis of petal has obvious and regular tubercles observed under scanning electronic microscope. Brush structure, among which is overflowed by secretory substance was observed from the cross section of petals, and can be dyed black-grey by Sudan black. Parenchyma cells filled with lipid form fundamental tissue of petals. Vogel[17] held the opinion that scent of some plants came from a kind of special gland named Osmophores, which can be found in Asclepiadanceae, Araceae, Aristolochiaceae and Burmanniaceae. The flowers of those plants can be differentiated according to Osmophores, which can develop to cilium, valve or brush of kernel. For example, spadix of Acreae and some structures inducing insects in plants of Orchidaceae belong to Osmophores, which can be identified through the method of dimethyl diaminophenazine chloride coloration. The gland usually has secretory tissue only comprised of several cells thick, which arrays tightly or loosely. Volatile oil produced by the gland can be given off quickly, however, or stored temporarily in cells, which was studied by Fahn[9]. The author held the views that secretory structure of petal of *O. fragrans* can be named as Osmophores, because it possesses the features of Osmophores. So we can draw the conclusion that total petals of *O. fragrans* are a big Osmophores. Lipid is in epidermis not in fundamental tissues through the dyed Free-hand sectioning of fading petals. Results showed fundamental tissues of petal could produce and temporarily store lipid, then give off through epidermis and its brush-hairs. That can be proved by the fact that the total petal becomes brick-red after dyed by dimethyl diaminophenazine choride. The author firstly answered the reason why *O. fragrans* has strong and enjoyable fragrance.

There are plenty of stomas distributing in petal. A definite conclusion hasn't been drawn on whether those stomas have association with release of aromatic substances.

Acknowledgments

This work was supported by the National Science Foundation of China(30670137) and the Creative Personnel Foundation of Colleges and Universities in Henan Province.

Correspondence to:
Fude Shang
College of Life Science
Henan University
Kaifeng, Henan 475001, China
Email: fudeshang@henu.edu.cn

References

1. Shang FD, Yi YJ, Xiang QB. The culture of sweet osmanthus in China. Journal of Henan University (Social Science) 2003; 43(2): 136－9(in Chinese with English abstract).

2. Yang KM, Zhu WJ. Sweet Osmanthus. Shanghai: Shanghai Science and Techonology Press 2000; 1 – 50(in Chinese).
3. Ding CB, Xiong GT. Study on components of neat oil of osmanthus in Guizhou. Guizhou Science 1993; 11(3): 40 – 5(in Chinese with English abstract).
4. Feng JY, Zhao J, Huang QQ. Study on aroma components of *Osmanthus* by absorption wire gas chromatography/mass spectrometry. Journal of Zhejiang University (Science Edition) 2001; 28(6): 672 – 5(in Chinese with English abstract).
5. Liu H, He ZH, Shen MY. Study on aroma components of *Osmanthus* by supercritical extraction of CO_2. Guangxi Forestry Science 1996; 25(3): 127 – 31(in Chinese with English abstract).
6. Wen GP, Kang ZQ. Study on components of neat oil of *Osmanthus*. Acta Botanica Sinica 1983; 25(5): 468 – 71 (in Chinese with English abstract).
7. Wu HM, Chen X, He XY, Yu Z, Ding JK. The chemical constituents of absolute oils from *Osmanthus fragrans* flowers. Acta Botanica Yunnanica 1997; 19(2): 213 – 6 (in Chinese with English abstract).
8. Zhu ML. Study on components in headspace of various mutants of *Osmanthus*. Acta Botanica Sinica 1985; 27 (4): 412 – 8 (in Chinese with English abstract).
9. Fahn A. Secretory tissue in plant. London: New York Academic Press 1979; 51 – 161
10. Liu WZ, Hu ZH. The secretory structure of *Hypericum perforatum* and its relation to hypericin accumulation. Acta Botanica Sinica 1999; 41(4): 369 – 72(in Chinese with English abstract).
11. Liu WZ. Secretory structures and their relationship to accumulation of camptothecin in *Camptotheca acuminate* (Nyssaceae). Acta Botancica Sinica 2004; 46(10): 1242 – 8.
12. Lu HF, Hu ZH. Comparative anatomy of secretory structures of leaves in *Hypericum* L. Acta Phytotaxonomica Sinica 2001; 39(5): 393 – 404(in Chinese with English abstract).
13. Lu HF, Shen ZG, Li JY, Hu ZH. The patterns of secretory structure and their relation to hypericin content *Hypericum*. Acta Botanica Sinica 2001; 43(10): 1085 – 8.
14. Wan YX. A study on differentiation of floral buds of *Osmanthus fragrans*. Journal of Huazhong Agruicultural University 1988; 7(4): 364 – 6(in Chinese with English abstract).
15. Wang CY, Gao L, P, Lu DF. A study on morphological differentiation of flower bud of *Osmanthus fragrans* "Houban Jingui". Acta Horticulturae Sinica 2002; 29 (1): 52 – 6(in Chinese with English abstract).
16. Yang QJ, Huang YW, Li HP. Studies on formation and development of embryo and endosperm of *Osmanthus fragrans*. Journal of Huazhong Agricultural University 2003; 22(2): 175 – 8 (in Chinese with English abstract).
17. Vogel S. Duftdrüsen im Dienst der Bestaubung. Uber Bau und Funktion der Osmophoren, Arad. Wiss. Lit. Mainz, Abb. Matb. naturwiss. KI. Nr. 1962; 10: 598 – 763.

Received September 21, 2006

Sonosensitization Mechanism of ATX-70 in Sonodynamic Therapy

Chunfeng Ding[1], Junhong Xu[2]

1. Henan Key Laboratory of Laser and Optic-electric Information Technology, Zhengzhou University, Zhengzhou, Henan 450052, China

2. Faculty of Dynamical Engineering, North China University of Water Conservancy and Electric Power, Zhengzhou, Henan 450002, China

Abstract: Sonodynamic therapy (SDT) is an effective method to cure tumors, but the mechanism is not clear up to now. In this work, the mechanism of SDT was analyzed by studying the reactions of gallium-porphyrin analogue (ATX-70). Results showed that the ATX-70 might play two roles in SDT. One was that the high temperature produced in the bubbles at collapse promoted ATX-70 into excited states, and reacted with the dissolved oxygen in liquid and produced oxygen free radicals, which was thought as an effective killer for cancer cells. The other was that ATX-70 played a role as surfactant in the process of cavitations and eased the cavitations, leading to produce more high-energy hydroxide radicals. [Life Science Journal. 2006;3(4):85-89] (ISSN: 1097-8135).

Keywords: sonodynamic therapy; ultrasound; ATX-70; cavitations

Abbreviations: ATX-70: gallium-porphyrin analogue; CL: chemiluminescence; DMSO: dimethylsulfoxide; ICCD: intensified charge coupled device; FCLA: luuoresceinyl cypridina luminescent analog; PDT: photodynamic therapy; SDT: sonodynamic therapy; SL: sonoluminesenece

1 Introduction

Sonodynamic therapy (SDT) is a new method to cure tumors[1-13]. This method, compared to the photodynamic therapy (PDT), has two virtues for clinical application. One is that ultrasound has a deeper penetrability, and the other is that it needn't avoid light in the whole process of treatment. The gallium-porphyrin analogue (ATX-70) is a widely used sonosensitive in SDT[3]. It can selectively gather in the tumors and enhance the effect of therapy. However, the mechanism was unknown[4].

There are different opinions on the mechanism of SDT. Umemura firstly thought the sonoluminescence (SL) excitated the ATX-70 to produce $^1O_2$ which can kill the tumor cells, the same mechanism as PDT[5]. The study of Kessel *et al* pointed that the sonosensitive function of ATX-70 was relative to the cavitation[6]. Miyoshi[3] studied the mechanism thoroughly and found that the oxygen content in the gas bubble was important to the cavitation. 20% O_2 was necessary for sonosensitive process, and the ATX-70 maybe acted as surface activator to strengthen the cavitations. He further indicated that the sonosensitive reaction did not cause from the SL excitated by the sonosensitiver, but has its own mechanism. There are always different viewpoints on whether the $^1O_2$ takes part in the sonosensitive process. The research of Sakusabe *et al*[7] suggested that the sonosensitiver can kill tumor cells by enhancing the yield of $^1O_2$ and other active oxygen in the process of cavitation. Yumita *et al* also thought that the active oxygen produced in the sonosensitive process was crucial in SDT[5]. However, in sonosensitive experiment, Miyoshi[8] *et al* did not find $^1O_2$ by EPR. In addition, it's not sure whether the ATX-70 can be used repeatedly in SDT. At present, there are no detailed reports about these problems.

In this paper, mechanism of the SDT was studied by optical method. In the experiments, the selective probe of active oxygen named fluoresceinyl cypridina luminescent analog (FCLA) and un-selective chemiluminescence (CL) probe named luminal were to detect whether the active oxygen produced in the sonosensitive process timely and directly.

2 Materials and Methods

2.1 Reagent preparation

FCLA (Sigma, USA) was diluted to 50 μmol/L by distilled water. It has been known that FCLA only reacts with $^1O_2$ and O_2^-[14, 15]. Luminol (Sigma, USA) which can react with many

sorts of free radicals and emit photons[16], was diluted to 50 μmol/L by distilled water. ATX-70 (Toyohakka Kogyo, Japan), which was thought as the best sonosensitizer[3], was also diluted to 50 μmol/L by distilled water. SOD (Sigma, USA) selectively consuming O_2^-, was diluted to 10 μmol/L by distilledwater. NaN_3, a sort of medicament to reacting with $^1O_2$ selectively, was prepared with 10 mmol/L[17], and DMSO, reacting with ·OH selectively, was prepared with 10 mmol/L.

When the experiment began, injected some distilled water in the glass firstly, and then added the needed reagents, made the whole volume 2 ml and the concentration of FCLA, luminol, ATX-70, DMSO, SOD and NaN_3 was 1 μmol/L, 1 μmol/L, 2 μmol/L, 2 mmol/L, 1 μmol/L and 2 mmol/L, respectively.

2.2 Apparatus and methods

The experiment setup was shown in Figure 1. The SL or CL was detected by: intensified charge coupled device (ICCD) image system(Princeton Instruments, ICCD-576-S/1, −40 ℃). The ST-130 controller(Princeton Instruments, USA) controlled the ICCD and put the optical signal into computer. The luminescence intensity could be caught by the software of WINVIEW. The ultrasound field made the reagents mixed equably and quickly.

The signal function (AFG320, SONY, Japan) brought sine signal with 500 kHz and fed the signal to power amplifier (ENI CO. Ltd, 2100L, 50-dB). The 50 W signal from the amplifier was used to driver the transducer (diameter: 5 cm, Mingzhu, Guangzhou, China) to emit ultrasound. To avoid the influence of idle photons, the black ink was used as the transmit media of ultrasound, and the temperature was kept 25 ± 1 ℃.

The absorb spectrum of ATX-70 was collected by absorb spectrum system with the split of 10 nm, which usually was used to highly sensitive detection.

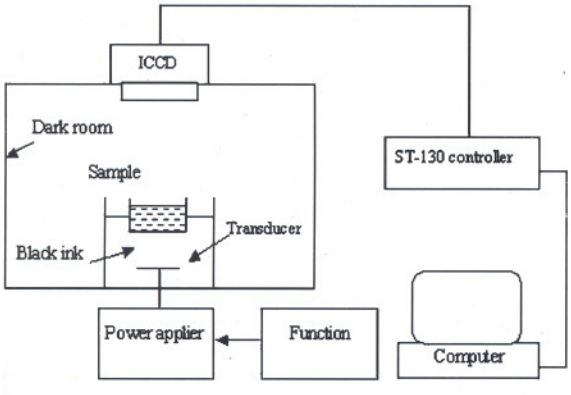

Figure 1. The setup for CL detection

3 Results and Discussion

Figure 2 is the detected curve of CL intensity in different solutions, with the power of ultrasound 50 W, the frequency 500 kHz, and the total time 50 seconds. In the first five seconds, the background intensity of ICCD is about 50 cps, and when the FCLA was added (the second five seconds), the intensity increased to about 450 cps. It can be taken as the experiment background. After that, when the ultrasound began to act on the solution, the CL intensity increased to about 15,000 cps. When ATX-70 was added in, the intensity increased to about 45,000 cps immediately. However, with the SOD was added in, the intensity decreased to about 21,000 cps, and it would decrease ulteriorly to about 2,600 cps when NaN_3 was added in. The experiment was repeated three times, and the standard deviation at each time point was lower than 9%.

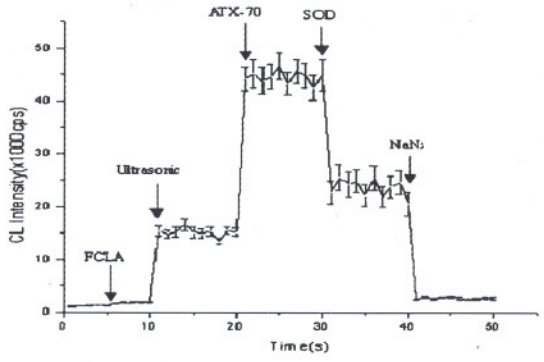

Figure 2. The CL intensity of saturated air liquid in 50 seconds. The data was means ± S.D. (n = 3)

As we know, FCLA can react with active oxygen selectively and emit photons. When the ultrasound appeared, added the ATX-70 to the FCLA solution, and the CL intensity increased obviously. It was believed that it was ATX-70 that accelerates the production of active oxygen radicals. When the SOD was added in the solution, the CL decreased but not disappeared, which indicated that not only O_2^- but also other active oxygen radicals were produced in the process, for the SOD only react with O_2^- and decrease the CL. The CL intensity continuously decreased when the NaN_3 was added in, which further proved that the $^1O_2$ radicals were produced in the ATX-70 solution. The final intensity was 2,600 cps not 450 cps, which indicated that the ATX-70 not only participated in the produce of active oxygen but also promoted the produc-

tion of sonoluminescence directly.

Figure 3 showed the dependence of CL intensity on the gas component in liquid. The left showed the CL intensity under saturated air condition and the right under saturated N_2 condition. The (□) and (■) represent the CL intensity of FCLA and FCLA + ATX-70 solutions, respectively. As shown in Figure 3, the CL intensity of FCLA + ATX-70 solution under N_2 saturated condition was only about 1,000 cps, much lower than that in the air saturated solution, which was reached to about 50,000 cps. It is because that in the air saturated solution, ATX-70 reacted with the dissolved O_2 and produced $^1O_2$ and O_2^-. However, in the N_2 saturated solution, the ATX-70 can't react with O_2, and no active oxygen could be produced. It indicated that, in the cavitations, ATX-70 can't produce the active oxygen free radicals solely, without the dissolved oxygen. Thereby the content of oxygen would affect the CL intensity.

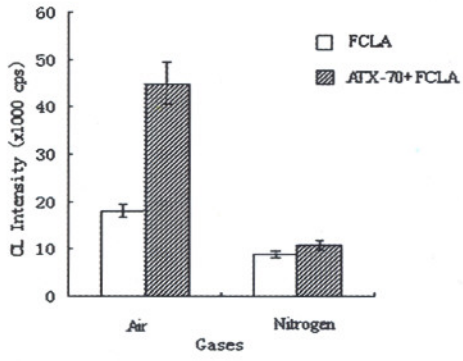

Figure 3. The CL intensities of 1 μM FCLA(□) and FCLA + ATX-70 (■) solutions which were detected in the air saturated (left) and nitrogen saturated conditions (right) respectively. The data was means ± S.D. (n = 3)

Figure 4 showed the absorb spectrums of ATX-70. Curve A represents the spectrum which was detected before the ultrasound and curve B represents the spectrum 20 seconds after the ultrasound. Before and after the ultrasound, the two absorb spectrums of ATX-70 were similar. The peak values of the both spectrums are about 400 nm, and the subordinate values are about 600 nm. The result showed that, in spite of the ATX-70 accelerated the active oxygen produced in cavitations, however, its molecular structure was not destroyed. In Figure 4, the intensity of curve B decreased more slightly than curve A at 400 nm. The reason is that ultrasound makes the ATX-70 redistribute in the solution and leads the scan light of spectrum system not to irradiate them completely.

From the above experiments, it can be concluded that, with the dissolved oxygen, ATX-70 promotes the production of active oxygen radicals in the process of cavitations. To describe how the ATX-70 acts in cavitations, luminal (mainly reacts with ·OH) was added in the following experiments. The sequence of the reagents was shown in Figure 5.

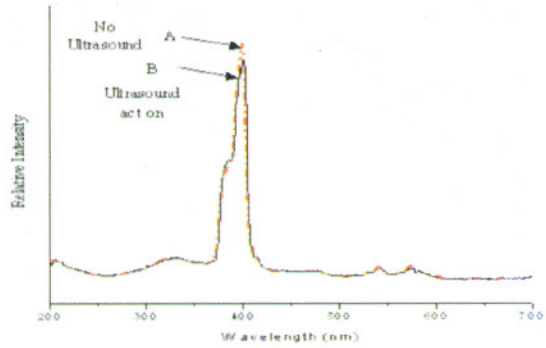

Figure 4. The absorb spectrums of ATX-70 before and after ultrasound act. curve A: spectrum of ATX-70 before ultrasound act; curve B: spectrum of ATX-70 after ultrasound act 20 s

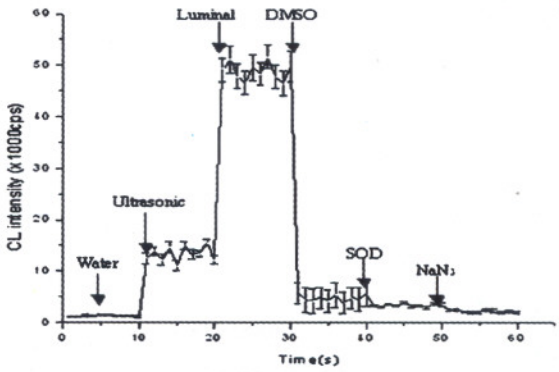

Figure 5. The change of CL intensity in luminal solution for prove the production in cavitation. The data was means ± S.D. (n = 3)

When the luminal was added in the water, with the ultrasound, the CL intensity increased obviously. However, when DMSO was added in, the CL intensity decreased quickly, just above the background. Then, adding the SOD and NaN_3 in order, the CL intensity did not almost change. It indicated that it was ·OH that was mainly produced in the process of cavitations, but the yields of $^1O_2$ and O_2^- were very low. When adding ATX-70 into the luminal solution, as shown in Figure 6 (the experiment was repeated three times), the CL

intensity decreased from about 51,000 cps to about 42,000 cps. Adding FCLA into the mixed solution, however, the CL intensity increased again. It indicated that the ATX-70 can react with the ·OH radicals and decrease the concentration of the ·OH in the cavitation, leading the CL intensity to decrease and more active oxygen to produce.

Based on the above results, the main reaction could be as follows:

$$2H_2O \xrightarrow{caviation} 2\cdot\dot{O}H + 2H + photons \quad (1)$$

$$\dot{O}H + ATX\text{-}70 \rightarrow \cdot OH + A\dot{T}X\text{-}70 \quad (2)$$

$$A\dot{T}X - 70 + 2O_2 \rightarrow {}^1O_2 + O_2^- + ATX\text{-}70 \quad (3)$$

In the experiments, another phenomenon was also found. It is the ATX-70 that can reduce the threshold of sonoluminescence. Experiments showed that when the power was 35 W, sonoluminescence began to appear in the liquid without ATX-70. However, the power decreased to about 28 W when ATX-70 was added. So ATX-70 makes the cavitations become easier. The ATX-70 maybe act as some sort of surface activator to strengthen the cavitations, just like described by Miyoshi[3].

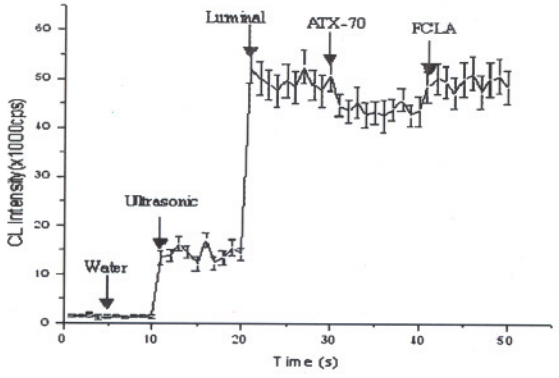

Figure 6. The change of CL intensity for prove the production of active oxygen. The data was means ± S.D. ($n = 3$)

4 Conclusion

In this paper, the main work is to discuss the role of ATX-70 in the process of cavitations. The results showed that the active oxygen, which was used to kill the tumor cells in SDT, was mainly produced by the chemical reaction in the process of cavitations instead of coming from cavitations directly. The main function of ATX-70 in cavitations is to transfer the energy of ·OH to the dissolved oxygen in the liquid, and turn the oxygen into $^1O_2$ and O_2^-. Though ATX-70 increases the yield of active oxygen, its molecular structure does not change, just like some sort of catalyze. The result also showed that ATX-70 is a highly efficient sonosensitizer in SDT.

Acknowledgments

Thanks for the help of Professor Da Xing, who works in South China Normal University, gives me some useful advices for the discussion. Thanks for the help of Yi Zheng, who gives me some advices for the writing.

Correspondence to:
Chunfeng Ding
Henan Key Laboratory of Laser and Optic-electric Information Technology
Zhengzhou University
Zhengzhou, Henan 450052, China
Telephone: 86-371-6776-7625
Email: dingchf@zzu.edu.cn

References

1. Jin Z, Miyoshi N, Ishiguro K, *et al*. Combination effect of photodynamic and sonodynamic therapy on experimental skin squamous cell carcinoma in C3H/HeN mice. J Dermatol 2000; 27 (5): 294 – 306.
2. Kessel D, Lo J, Jeffers R, *et al*. Modes of photodynamic vs. sonodynamic cytotoxicity. J Photochem Photobiol B 1995; 28 (3): 219 – 21.
3. Miyoshi N, Misik V, Riesz P. Sonodynamic toxicity of gallium-porphyrin analogue ATX-70 in human leukemia cells. Radiat Res 1997; 148 (1): 43 – 7.
4. Worthington AE, Thompson J, Rauth AM, *et al*. Mechanism of ultrasound enhanced porphyrin cytotoxicity. Part I: A search for free radical effects, Ultrasound Med Biol 1997; 23 (7): 1095 – 105.
5. Yumita N, Umemura S, Nishigaki R. Ultrasonically induced cell damage enhanced by photofrin Ⅱ: mechanism of sonodynamic activation. In Vivo 2000; 14 (3): 425 – 9.
6. Kessel D, Jeffers R, Fowlkes JB, *et al*. Effects of sonodynamic and photodynamic treatment on cellular thiol levels. J Photochem Photobiol B 1996; 32 (1 – 2): 103 – 6.
7. Sakusabe N, Okada K, Sato K, *et al*. Enhanced sonodynamic antitumor effect of ultrasound in the presence of nonsteroidal anti-inflammatory drugs. Jpn J Cancer Res 1999; 90 (10): 1146 – 51.
8. Miyoshi N, Igarashi T, Riesz P. Evidence against singlet oxygen formation by sonolysis of aqueous oxygen-saturated solutions of Hematoporphyrin and rose bengal. The mechanism of sonodynamic therapy. Ultrason Sonochem 2000; 7 (3): 121 – 4.
9. Hristov PK, Petrov LA, Russanov EM. Lipid peroxidation induced by ultrasonication in Ehrlich ascitic tumor cells. Cancer Lett 1997; 121 (1): 7 – 10.
10. Misik V, Riesz P. Free radical intermediates in sonodynamic therapy. Ann NY Acad Sci 2000; 899: 335 – 48.
11. Misik V, Miyoshi N, Riesz P. EPR spin trapping study of the decomposition of azo compounds in aqueous solutions by ultrasound: potential for use as sonodynamic sensitizers for cell killing. Free Radic Res 1996; 25 (1): 13 – 22.

12. Misik V, Riesz P. Peroxyl radical formation in aqueous solutions of N, N-dimethylformamide, N-methylformamide, and dimethyl-sulfoxide by ultrasound: implications for sonosensitized cell killing. Free Radic Biol Med 1996; 20 (1): 129 – 38.
13. Miyoshi N, Misik V, Fukuda M, *et al*. Effect of gallium-porphyrin analogue ATX-70 on nitroxide formation from a cyclic secondary amine by ultrasound: on the mechanism of sonodynamic activation. Radiat Res 1995; 143 (2): 194 – 202.
14. Nakano M. Detection of active oxygen species in biological systems. Cellular and Molecular Neurobiology 1998; 18 (6): 565 – 79.
15. Matsugo S, Konishi T, Matsuo D, *et al*. Reevaluation of superoxide scavenging activity of dihydrolipoic acid and its analogues by chemiluminescent method using 2-methyl-6-(p-methoxyphenyl)-3, 7-dihydroimidazo [1, 2-a] pyrazin-3-one (MCLA) as a superoxide probe. Biochem Biophys Res Comm 1996; 227: 216 – 20.
16. Uehara K, Maruyama N, Huang Ck, *et al*. The first application of a chemiluminescence probe, 2-methyl-6-(p-methoxyphenyl)-3, 7-dihydroimidazo [1, 2-a] pyrazin-3-one (MCLA), for detecting O_2^- production, *in vitro*, from Kuppfer cells stimulated by phorbol myristate acetate. FEBS Letters 1993; 335 (2): 167 – 70.
17. Tianxi Hu. Free Radical Life Science Progress. Atomic Energy Publishing Company 1997; 5: 65 – 77.

Received June 17, 2006

The Elimination of 50 Hz Power Line Interference from ECG Using a Variable Step Size LMS Adaptive Filtering Algorithm

Hong Wan[1,2], Rongshen Fu[1], Li Shi[1]

1. *College of Electric Engineering, Zhengzhou University, Zhengzhou, Henan 450052, China*
2. *The Information Engineering University of PLA, Zhengzhou, Henan 450052, China*

Abstract: This article demonstrates "a new variable step size LMS adaptive filtering algorithm" to eliminate 50 Hz power line interference. This approach can provide faster convergence rate and smaller mean square error (MSE). [Life Science Journal. 2006;3(4):90-93] (ISSN: 1097-8135).

Keywords: adaptive filter; LMS algorithm; 50 Hz power line interference

Abbreviations: ECG: electrocardiogram; LMS: least mean square; MSE: mean square error; SNR: signal to noise ratio; NLMS: normalized least mean square; SVSLMS: S-function variable step least mean square

1 Introduction

ECG signal is always interrupted by mixed interferences, such as 50 Hz power line interference, respiratory and muscle electric interference etc. Specifically, since signal to noise ratio (SNR) of electrocardiogram (ECG) signal is very low, the interfering frequency at 50 Hz may overwhelm the source signal. Methodologically, elimination of 50 Hz interference has been discussed a lot[1,2]. Majority of the approaches suppose the 50 Hz power line interference frequency not to fluctuate. In this short report, we use a variable step size least mean square (LMS) adaptive filtering algorithm to eliminate the 50 Hz power line interference whose frequency has small fluctuation from ECG signal. The LMS algorithm and stochastic gradient algorithm[3,4], introduced by Widrow and Hoff in 1960, is widely used in practice because of its simplicity, computational efficiency, and good performance under a variety of operating conditions. LMS algorithm is based on mathematical method of the steepest decline, which is to define a performance function along the vector in the direction toward negative gradient of the steepest value to get itself recovery. Figure 1 shows the basic of LMS algorithm. The LMS algorithm can be summarized as

$$y(n)=\sum_{i=0}^{L} W_i x(n-1)=W^{\mathrm{T}}X \qquad (1)$$

where $X(k)=[x(k), x(k-1),\cdots,x(k-L+1)]^{\mathrm{T}}$ and filtering coefficient W is defined as $W(k)=[w_0(k), w_1(k),\cdots,w_{L-1}(k)]^{\mathrm{T}}$, L is the number of filtering order; W_i is the filtering coefficient. The optimization can be determined by using LMS algorithm as OP procedures:

$$\mathrm{OP}=\begin{cases} y(n)=w^{\mathrm{T}}(n)*x(n) & (\textit{Filtering}) \\ e(n)=d(n)-y(n) & (\textit{Error formation}) \\ w(n)=w(n-1)+2*u*e(n)*x(n) & (\textit{Confficient updation}) \end{cases}$$

where u is the step-size control parameter.

The adaptation parameter, step size u selected, must be small enough to ensure that the algorithm converges to the optimum point. However, this small step size causes slow convergence. As a matter of fact, the convergence condition can be satisfied by choosing the range $0\leqslant u\leqslant\frac{1}{\mathrm{Tr}[R]}$. Where $\mathrm{Tr}[R]$ denotes the trace of R and R is the auto-correlation of X. The convergence rate is proportional to the variation of parameter u[5]. If u increases, the y will converge faster but increases mean square error (MSE) and decreases the stability margin. In order to resolve this contradiction, we proposed a new algorithm to modify the variable step size LMS adaptive algorithms.

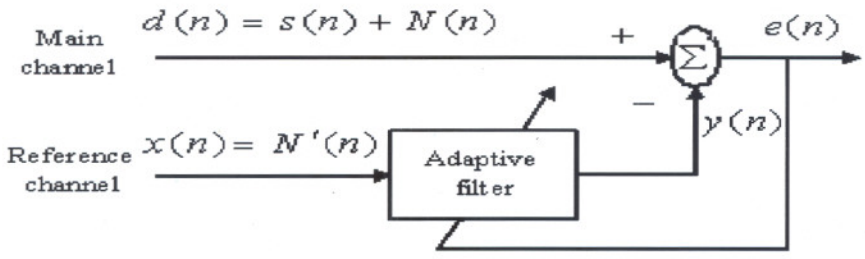

Figure 1. The structure of LMS algorithm

Instead of using numbers, normalized least mean square (NLMS) algorithm[6] modify u by defining variables α and β

$$u(n)=\frac{\alpha}{\beta+x_n^{\mathrm{T}}x_n}=\frac{\alpha}{\beta+r(n)} \qquad (2)$$

where $r(n)=x_n^{\mathrm{T}}x_n$ is defined as the interior product of the input vector $x(n)$.

The value of $u(n)$ has to be put small value to avoid the decreasing stability, therefore, α must be positive number in $0<\alpha<1$ and $\beta\approx 0.0001$. NLMS algorithm can effectively reduce amplifying gradient noise in the process of convergence, and keep the good convergence rate eventually.

In order to improve the performance of the filter, Tan *et al*[7] proposed a new variable step size LMS adaptive algorithm, S-function variable step least mean square (SVSLMS) algorithm, which define $u(n)$ as a Sigmoid function of $e(n)$,

$$u(n)=\beta\left(\frac{1}{1+E(-a^{\|e(n)x(n)\|})}-0.5\right) \qquad (3)$$

The advantage of this algorithm is that the step size is bigger in preliminary stage of unknown system, so having faster convergence rate. When the algorithm has already converged, no matter how big the input interference was, it can keep very small step size to obtain very small MSE.

2 Experiment and Method

To overcome the imperfection of SVSLMS algorithm[8], we use a new variable step size LMS adaptive filtering algorithm.

$$u(n)=\beta(1-e^{(\|e(n)x(n)\|^2)}) \qquad (4)$$

Figure 2 (a) shows the result of using SVSLMS algorithm for analysis. The error function $e(n)$ alternated near zero where the algorithm has steadied or will steady. But $u(n)$ changes too fast. The step size of SVSLMS algorithm varies in phase at adaptive steady state. This is our major concern. When β is in the rang of $0<\beta<2/\lambda_{max}$, in contrary, the proposed algorithm controls the shape of the function, further more $\beta>0$ controls the value range of the function of $u(n)$ if $\alpha>0$. Obviously, we should conclude $0<\mu<1/\lambda_{max}$ and $0<\beta<1/\lambda_{max}$.

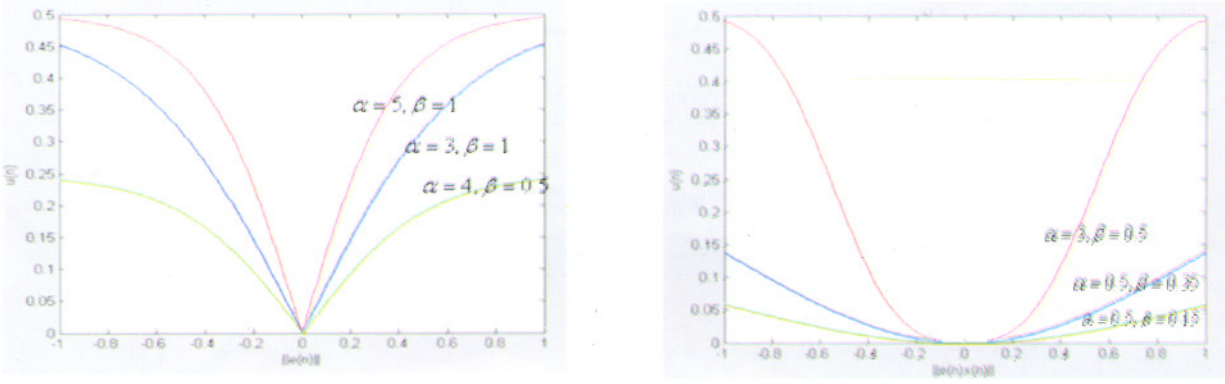

(a) (b)

Figure 2. (a)The graph of $u(n)$ and $\|e(n)\|$ (SVSLMS algorithm) (b)The graph of $u(n)$ and $\|e(n)x(n)\|$ (proposed algorithm)

3 Result and Discussion

In equation (1), $\| e(n)X(n) \|$ is very big and $\mu(n) \approx \beta$ initially as well as obtained the biggest convergence rate. Being close to steady state, $\| e(n)X(n) \|$ will reduce. When it reaches the steady state, both $\| e(n)X(n) \|$ and $u(n)$ becomes very small, and the MSE is also very small. When the input signal is non-stationary random signals, the instantaneous change of input signal causes $\| e(n)X(n) \|$ to change very much. It causes the algorithm automatically in fast convergence condition. The relational graph of $u(n)$ and $\| e(n)X(n) \|$ is shown in Figure 2 (b). From the Figure 2, in order to accelerate convergence rate, α and β should be big. In contrary, make the MSE smaller, α and β should be smaller.

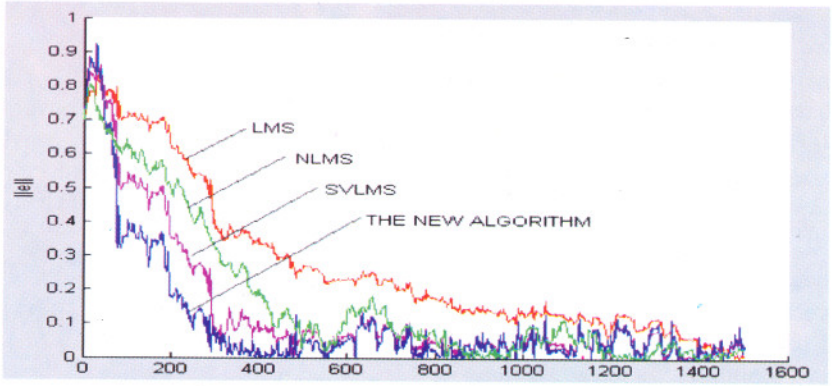

Figure 3. The convergence rate

Figure 3 is the result of examining the convergence performance of algorithms through the computer simulation. It shows the performance of SVSLMS and LMS as well as NLMS. Comparing with the SVSLMS, the convergence rate of the proposed algorithm is faster, and makes the MSE smaller enough.

This report presents new variable step size LMS adaptive filtering algorithm to eliminate the 50 Hz interference from the ECG. The block diagram is shown in Figure 1. Performance of the noise cancellation was tested by using stationary input signal ECG with 50 Hz sine wave added but frequency is undulating between 50 + 1 Hz and 50 − 1 Hz that models the input of main channel. Sine wave whose frequency fluctuates between 50 − 1 Hz and 50 + 1 Hz models the input of reference channel. The result of simulation is shown in Figure 4.

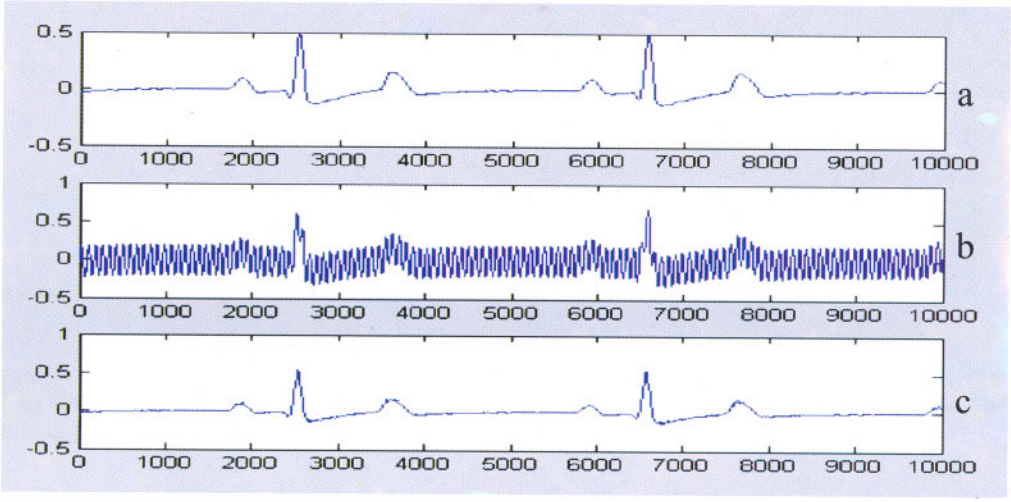

Figure 4. The result of simulation
(a): The ECG signal; (b): The ECG signal with 50 Hz interference; (c) The result of proposed elimination processing

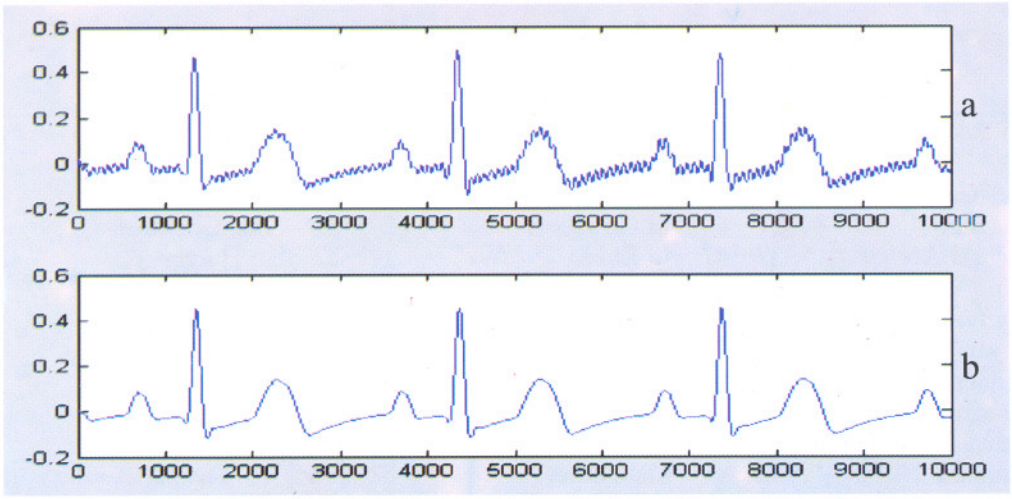

Figure 5. The real ECG signal
(a): The real ECG signal with 50 Hz interference; (b): The result of processing

In practice, we choose the reference channel which contains the 50 Hz interference and its harmonic. The common-mode signal recorded at the right leg reference electrode[9] which is truly correlated with the noise in ECG recording. The result of processing is shown in Figure 5. We see that 50 Hz interference to ECG is violent before processing and restrained after processing.

4 Conclusion

The approach proposed improves the convergence rate to enhance the calculation speed, cause the algorithms being more advantageous to apply in the real-time processing and reduce the MSE so as to improve the quality of eliminating interference. The result obtained by theory and simulation shows that this algorithm, compared with traditional LMS algorithm and other improved LMS algorithm, is much more effective to eliminate the 50 Hz interference from ECG signal.

Correspondence to:
Hong Wan
School of Electric Engineering
Zhengzhou University
Zhengzhou, Henan 450002, China
Telephone: 86-138-3858-0642
Email: wanhong@zzu.edu.cn

References

1. Levkov C, Michov G, Ivanov R, Daskalov IK. Subtraction of 50 Hz interference from the electrocardiogram. Med & Biol, Eng & Comput 1984; 22: 371－3.
2. Christov II, Dotsinsky IA. New approach to the digital elimination of 50 Hz interference from the electrocardiogram. Med & Biol, Eng & Comput 1988; 26: 431－4.
3. Widrow B, Stearns SD. Adaptive Signal Processing. NJ: Englewood Cliffs, Prentice Hall, 1985.
4. Haykin S. Adaptive Filter Theory. Prentice Hall, Englewood Cliffs, NJ 1996.
5. Widrow B, Stearns SD. Adaptive Signal Processing. New York: Prentice-Hall 1985.
6. Haykin S. Adaptive Filter Theory. 3rd Edition. Prentice Hall 2002.
7. Qin JF, Ouyang JZ. A new variable step size adaptive filtering algorithm. Data Gathering and Processing 1997; 12(3): 171－4.
8. Karni S, Zeng G. A new convergence factor for adaptive filters. IEEE Trans. Circuits Syst 1989; 36: 1011－2.
9. Thakor NV, Sheng ZY. Application of adaptive filtering to ECG analysis: noise cancellation and arrhythmia detection. IEEE Trans on Biomedical Engineering 1991; 38 (8): 785－94.

Received June 17, 2006

Author Index

Subject Index

Instructions to Authors

1. General Information

(1) **Goals:** As an international journal published both in print and on internet, *Life Science Journal* is dedicated to the dissemination of fundamental knowledge in all areas of life science. The main purpose of *Life Science Journal* is to enhance our knowledge spreading in the world under the free publication principle. It publishes full-length papers (original contributions), reviews, rapid communications, and any debates and opinions in all the fields of life science.

(2) **Categories of publication:** Research articles, reviews, objective descriptions, research reports, opinions/debates, news, letters to editor, meeting report.

(3) **Cover feature:** The covers of *Life Science Journal* feature illustrations the Editor-in-Chief selects from the articles scheduled for publication in that issue. Authors whose articles are chosen for a cover feature will be asked to provide a high-quality version of the selected illustration as well as a brief legend (four to five sentences) describing the significance of the image. In light of the rapid production schedule for journal covers, authors are expected to provide the requested material within 3 days.

(4) **Publication costs:** US $ 30 per printed page of an article to defray costs of the publication will be paid by the authors when it is accepted. Extra expense for color reproduction of figures will be paid by authors (estimate of cost will be provided by the publisher for the author's approval). For the starting, publication fee will be waived for the current issues and they will be supported by Zhengzhou University.

(5) **Journal copies to authors:** Two hard copies of the journal will be provided free of charge for each author.

(6) **Additional copies bought by authors:** Additional hard copies could be purchased with the price of US $ 4/issue (mailing and handling cost included).

(7) **Distributions:** Web version of the journal is freely opened to the world without payment or registration. The journal will be distributed to the selected libraries and institutions for free. US $ 5/issue hard copy is charged for the subscription of other readers.

(8) **Advertisements:** The price will be calculated as US $ 400/page, i. e. US $ 200/a half page, US $ 100/a quarter page, etc. Any size of the advertisement is welcome.

2. Manuscripts Submission

(1) **Submission methods:** Electronic submission through email is encouraged and hard copies plus an IBM formatted computer diskette would also be accepted.

(2) **Software:** The Microsoft Word file will be preferred.

(3) **Font:** Normal, Times New Roman, 10 pt, single space.

(4) **Indent:** Type 4 spaces in the beginning of each new paragraph.

(5) **Manuscript:** Do not use "Footnote" or "Header and Footer".

(6) **Title:** Use Title Case in the title and subtitles, e. g. **"Debt and Agency Costs".**

(7) **Figures and tables:** Use full word of figure and table, e. g. "**Figure** 1. Annul income of different groups", **Table** 1. Annual increase of investment".

(8) **References:** Number the references in the order of their first mention in the text. References should include all the authors' last names and initials, title, journal, year, volume, issue, and pages etc.

***Reference examples*:**

Journal article: Hacker J, Hentschel U, Dobrindt U. Prokaryotic chromosomes and disease. Science 2003;301(34):790 − 3.

Book: Berkowitz BA, Katzung BG. Basic and clinical evaluation of new drugs. In: Katzung BG, ed. Basic and Clinical Pharmacology. Appleton & Lance Publisher. Norwalk, Connecticut, USA. 1995:60 − 9.

(9) **Submission address:** America: lifesciencej@gmail.com, Marsland Press, P. O. Box 21126, Lansing, Michigan 48909, USA.

China: lifesciencej@zzu. edu. cn, Zhengzhou University, 100 Science Road, Zhengzhou, Henan 450001, China.

(10) **Reviewers:** Authors are encouraged to recommand 2 − 8 competent reviewers with their names and email addresses.

3. Manuscript Preparation

Each manuscript is suggested to include the following components but authors can do their own ways:

(1) Title. Including each author's full name; institution (s) with which each author is affiliated, with city, state/province, zip code, and country.

(2) Abstract. Including Background, Materials and Methods, Results, and Discussion.

(3) Keywords.

(4) Abbreviations. All abbreviations needed are listed here, so that they could be used directly in the article.

(5) Introduction.

(6) Materials and Methods.

(7) Results.

(8) Discussion.

(9) Acknowledgments.

(10) Correspondence. Correspondence author's full name, institution, city, state/province, zip code, country, telephone number, facsimile number (if available), and email address are listed here.

(11) References.

4. Copyright and Permissions

Life Science Journal

Acta Zhengzhou University Overseas Edition
Volume 3 Number 4, December 2006

Published by:
Zhengzhou University
Marsland Press

Sponsor:
North American Branch of Zhengzhou University Alumni

Zhengzhou University
100 Science Road
Zhengzhou, Henan 450001, China
Telephone: 86-371-6778-1272
Email:lifesciencej@zzu.edu.cn
Website:http://life.zzu.edu.cn

Marsland Press
P. O. Box 21126
Lansing, Michigan 48909, USA
Telephone: 517-980-4106
Email: lifesciencej@gmail.com
Website: http://www.sciencepub.org

ISSN 1097-8135
9 771097 813071